UNIVERSITAT POLITÈCNICA DE CATALUNYA BARCELONATECH

Subsurface as a bioreactor: interaction between physical heterogeneity and microbial processes

Núria Perujo Buxeda

Doctoral Thesis

Subsurface as a bioreactor:

Interaction between physical heterogeneity and microbial processes

NÚRIA PERUJO BUXEDA

Universitat Politècnica de Catalunya

Supervisors:

Xavier Sánchez Vila

Universitat Politècnica de Catalunya

Anna M. Romaní Cornet

Universitat de Girona

Doctoral Program in Environmental Engineering, Departament Enginyeria Civil I Ambiental.
Universitat Politècnica de Catalunya

Doctoral Program in Water Science and Technology, Departament Ciències Ambientals.
Universitat de Girona

July, 2018

Thesis presented to obtain the qualification of Doctor from the Universitat Politècnica de Catalunya (UPC) and from the Universitat de Girona.

Agraïments

No és fàcil resumir en unes quantes línies tot el suport que he rebut al llarg d'aquests anys; i quan dic "aquests anys" no em refereixo únicament als anys que ha durat la tesi sinó durant tota la meva formació al llarg de la trajectòria educativa i laboral. I és que sense aquest suport (el qual comença en el moment en que naixem) i tota la gent que m'ha acompanyat al llarg d'aquests anys possiblement el camí triat hauria sigut diferent. No m'agrada posar noms i cognoms, així que la meva intenció en aquests agraïments és que qui s'hagi de sentir al·ludit s'hi senti lliurement sense la necessitat de veure el seu nom escrit en aquestes línies.

Primer de tot vull agrair la companyia i suport de la família, principalment als meus pares. El vostre suport va ser necessari i imprescindible per ajudar-me a no desviar-me del camí. Gràcies per ser-hi sempre, moltes gràcies!

Vull donar gràcies també als professors de l'escola i de l'institut per transmetre les ganes i il·lusió d'aprendre i seguir estudiant, dia rere dia. Així com també als amics d'escola i d'institut gràcies als quals anar a classe era un plus de motivació. Trobar-nos per estudiar i fer els deures ho feia tot molt més amè encara que a vegades estàvem més estona explicant-nos coses que pas fent els deures! Es compten amb una sola mà però estic molt contenta de tenir-vos encara, us estimo! Els amics de la carrera, grans companys de viatge, imprescindibles també durant aquests primers anys d' "independència" personal i majoria d'edat. Igual que els amics d'escola, els amics de la carrera també es poden comptar amb una sola mà, però en tinc més que suficient, us estimo!

Vull fer un petit incís també a les "noies de la meva vida": a les 3 maries, sempre juntes des de petites; a les "noies màster"; a les Bravetes imprescindibles; i com no a la bisbalenca més trempada del món!

I ara ja sí, centrant-nos en la fase doctoral, les primeres persones les quals es mereixen uns agraïments com una casa són els meus directors de tesi, moltes gràcies per fer-ho tant fàcil i per complementar-vos tant bé! Gràcies per donar-me aquesta oportunitat de tastar el que és la recerca; encara que tristament la realitat post-doctoral és bastant crua... no m'arrepenteixo de res.

Vull agrair també a la gent de la *"depu"*, em vau ajudar moltíssim. I no només això, sinó que sense vosaltres els capítols II i III d'aquesta tesi no haurien sigut possibles, mil gràcies!

Gràcies als companys del seminari per compartir el dia a dia, explicar-nos les penes i ajudar-nos mútuament a desconnectar i agafar aire. No n'era gaire conscient, però ara tinc més que clar que us trobaré a faltar, se m'encongeix el cor (de fet mentre estic escrivint això em cauen 4 llagrimetes) quan penso que aviat s'acabaran els cafès de can Paco, els dinars "a fora", les cerveses dels divendres (encara que això últimament ho teníem una mica abandonat), així com tantes altres mil activitats ludicoesportives que fèiem de tant en tant. I gràcies com no, als meus amfitrions per excel·lència a la UPC, sempre he sentit que us tenia aquí pel que fes falta, mil gràcies!

Deixant de banda els agraïments de caire personal i centrant-me en els agraïments de caire més administratiu, vull agrair els projectes que han donat suport a aquesta tesi: el projecte MARSOL de la Unió Europea, el Ministeri d'Economia i Competitivitat [CGL2014-58760-C3-2-R], el projecte ACWAPUR-PCIN-2015-239, l'ERA-NET Cofund Waterworks 2014, i al Departament d'Universitats, Recerca i Societat de la Informació de la Generalitat de Catalunya així com el Fons Social Europeu (Beca FI-DGR).

I acabo amb una frase que m'agrada molt i que crec que va molt bé recordar de tant en tant i és que *"falten escoles de riure i de respirar"* així que no us oblideu mai ni de riure ni de respirar.

Abstract

Infiltration systems are water treatment technologies where water vertically percolates through porous media while several biogeochemical processes occur. Biofilms are the main responsible for those biogeochemical processes due to their ability to colonize sediments as well as due to their role in transformation of organic matter and nutrients in aquatic ecosystems and subsurface environments. However, an excessive biofilm growth in sand filtration systems can significantly reduce their infiltration capacity (bioclogging), thus constraining the processes that occur therein. Sediment grain size distribution influences the performance of these systems since it determines hydrological characteristics in subsurface sediments influencing biofilm growth as well as the process rates of biogeochemical processes in depth. Furthermore, sediment grain size can also influence the occurrence and depth-extension of bioclogging. The main objective of this doctoral thesis is to study the influence of grain size distributions on biogeochemical processes and on bioclogging in depth in sand infiltration systems used as potential tertiary treatments for the removal of organic matter and nutrients in water. To achieve this objective, two infiltration experiments have been carried out: (a) a laboratory-scale columns experiment using 5 sediment grain size distributions used as potential infiltration systems (Chapter I) and (b) an outdoor infiltration experiment in sediment tanks using two sediment grain size distributions (Chapter II and Chapter III).

The results of this thesis show how sediment grain size distribution influences biofilm establishment and growth, biogeochemical rates as well as occurrence of bioclogging in surface sediments and in depth. Accordingly, coarse sediments (*coarse system*) allow higher biomass in depth but they do not have the ability to remove dissolved phosphorous; however, due to high input loads they showed higher process rates. Grain size distribution of coarse sediment in the upper layer and fine sediment in the bottom layer (*coarse-fine system*) promotes the accumulation of biomass at the interface of the two sediment layers which results in a hot-spot of microbial activity. In addition, it promotes nutrient accumulation in sediments (dissolved phosphorous removal) possibly due to the fact that its flow velocities are smaller than those of a coarse system and therefore the contact time between the water and sediment increases by promoting the assimilation and adsorption of nutrients in the porous medium. Biomass establishment in fine

sediments (*fine system*) results in greater bioclogging due to lower initial porosity compared to systems with coarse sediment on the surface. This lower porosity results in less space available to colonize, and due to this, biofilm in the top layer of the monolayer *fine system* could reach the maturity state earlier than the bilayer *coarse-fine system*. That, together with the lower flows in the fine system, favours the detachment of biofilm in the top layer and its transport in depth. EPS accumulation in depth (due to live bacteria release or due to transport from upper sediment layers) is the main factor causing K variations in depth (potential to cause deep-clogging). Results also showed that mixed sediments of fine and coarse sands (*mixture system*) and the *fine-coarse system* achieve similar performance than fine system reaching similar biomasses between them and lower process rates than the other grain size distributions studied.

Resum

Els sistemes d'infiltració són sistemes de tractament d'aigua on aquesta percola verticalment a través d'un medi porós mentre que una sèrie de processos biogeoquímics tenen lloc. Els biofilms són els principals responsables dels processos biogeoquímics que es donen en el medi porós degut a la seva habilitat per colonitzar sediments així com pel seu rol en la transformació de matèria orgànica i nutrients en sistemes aquàtics i ambients subsuperficials. Al mateix temps un creixement excessiu dels biofilms (*bioclogging*) en sistemes d'infiltració de sorres poden reduir significativament la capacitat d'infiltració d'aquestes sistemes limitant per tant els processos que s'hi donen. Un dels paràmetres influents en el funcionament d'aquests sistemes és la distribució granulomètrica del sediment ja que aquest determina els paràmetres hidrològics en sediments subsuperficials influenciant el creixement del biofilm així com les taxes dels processos d'eliminació de nutrients i matèria orgànica en fondària. Al mateix temps, la mida del sediment també pot influir en l'ocurrència i extensió del *bioclogging*. El principal objectiu d'aquesta tesis doctoral és estudiar la influència que tenen diferents distribucions granulomètriques sobre els processos biogeoquímics i sobre el *bioclogging* en fondària en sistemes d'infiltració de sorres utilitzats com a potencials tractaments terciaris per l'eliminació de matèria orgànica i nutrients en l'aigua. Per assolir aquest objectiu s'han dut a terme dos experiments d'infiltració: (a) un experiment de laboratori amb columnes reblertes de sediment creant 5 distribucions granulomètriques diferents i utilitzades com a sistemes d'infiltració (Capítol I) i (b) un experiment a l'aire lliure amb dipòsits omplerts de sediment creant 2 distribucions granulomètriques diferents (Capítol II i Capítol III).

Els resultats d'aquesta tesi mostren com la distribució granulomètrica influencia l'establiment i creixement dels biofilms, les taxes dels processos biogeoquímics així com també el *bioclogging* en superfície i en fondària. D'acord amb això, sediments grollers (*coarse* system) permeten majors biomasses en fondària però no mostren eliminació de fòsfor, tot i que degut a majors càrregues d'entrada les taxes dels processos que s'hi donen són majors. La configuració granulomètrica de sediment groller a la capa superior i sediment fi a la capa inferior (*coarse-fine* system) promou l'acumulació de biomassa a la interfase dels dos sediments fet que resulta amb un *hot-spot* d'activitat microbiana. A més, promou l'acumulació de nutrients tot i estar formada

per sediment groller, possiblement degut al fet que les velocitats del flux en aquest sistema són menors que les d'un sistema groller i per tant el temps de contacte entre l'aigua i el sediment augmenta promovent aquesta assimilació i adsorció de nutrients. L'establiment de biomassa en sediments fins (*fine* system) resulta en major *bioclogging* degut a menor porositat inicial en comparació amb sistemes amb sorra grollera a la superfície. Aquesta menor porositat resulta en menor espai disponible per colonitzar, i degut això el biofilm de la capa superior del sistema monocapa fi (*fine system*) podria assolir l'estat de maduresa abans que el sistema groller-fi (*coarse-fine system*), això juntament amb els menors fluxos en el sistema fi, afavoreix el despreniment del biofilm superficial i el transport d'aquest en fondària. L'acumulació d'EPS en fondària (degut a producció de bacteris vius o a transport des de capes superiors) és el principal causant de les variacions de la K en fondària (potencial de causar *deep-clogging* a la llarga). S'ha vist que sediments mixtes de sorres fines i grolleres (*mixture* system) i sistemes fi-groller (*fine-coarse* system) resulten en un funcionament similar a la del sediments fins assolint biomasses similars entre ells i taxes inferiors a la resta de configuracions granulomètriques estudiades.

Resumen

Los sistemas de infiltración son sistemas de tratamiento de agua en los cuales ésta se infiltra verticalmente a través de un medio poroso mientras que una serie de procesos biogeoquímicos ocurren. Los *biofilms* son los principales responsables de estos procesos biogeoquímicos debido a su habilidad para colonizar sedimentos y debido a su papel fundamental en la transformación de materia orgánica y nutrientes en sistemas acuáticos i ambientes sub-superficiales. Al mismo tiempo, un crecimiento excesivo de estos biofilms (*bioclogging*) en sistemas de filtración con arenas puede reducir significativamente la capacidad de infiltración de estos sistemas limitando por tanto los procesos que tienen lugar. Uno de los parámetros influentes en el funcionamiento de estos sistemas de filtración es la distribución granulométrica del sedimento ya que éste determina los parámetros hidrológicos de sedimentos sub-superficiales influenciando de este modo el crecimiento del *biofilm* así como las tasas de los procesos de eliminación de nutrientes y materia orgánica en profundidad. Al mismo tiempo, la granulometría también puede influir en la ocurrencia y extensión del *bioclogging*. El principal objetivo de esta tesis doctoral es estudiar la influencia que tienen diferentes distribuciones granulométricas sobre los procesos biogeoquímicos y sobre el *bioclogging* en profundidad en sistemas de filtración a través de arenas los cuales se utilizan como potenciales tratamientos terciarios para la eliminación de materia orgánica y nutrientes en el agua. Para lograr este objetivo se han desarrollado dos experimentos de infiltración: (a) un experimento de laboratorio con columnas de sedimento creando 5 distribuciones granulométricas distintas y utilizadas como sistemas de filtración (Capítulo I) y (b) un experimento al aire libre con depósitos de sedimento creando 2 distribuciones granulométricas distintas (Capítulos II y III).

Los resultados de esta tesis muestran como la distribución granulométrica influencia el establecimiento y el crecimiento de los *biofilms*, las tasas de los procesos biogeoquímicos así como también el *bioclogging* tanto en superficie como en profundidad. Teniendo esto en cuenta, los sedimentos más gruesos (*coarse system*) permiten mayores biomasas en profundidad pero no muestran eliminación de fósforo aunque debido a mayores cargas de entrada las tasas alcanzadas también son mayores. La distribución granulométrica de sedimento grueso en la capa superior y sedimento fino en la capa inferior (*coarse-fine system*) promueve la acumulación de biomasa a la interfície entre las dos medidas de sedimento hecho que resulta en la creación de un *hot-spot* de

actividad microbiana en profundidad. Además, el sistema *coarse-fine* promueve la acumulación de nutrientes en el sedimento favoreciendo su eliminación a pesar de presentar sedimento grueso en la capa superior de filtración; esto podría estar relacionado con el hecho que las velocidades del flujo en este sistema son menores que las de un sistema formado únicamente por sedimento grueso y por tanto el tiempo de contacto entre el agua y el sedimento aumenta favoreciendo la asimilación y adsorción de nutrientes en comparación con el sistema *coarse*. La presencia de biomasa en sedimentos finos (*fine system*) resulta en mayor *bioclogging* debido a menor porosidad inicial en comparación con sistemas que presentan arena gruesa a la superficie. Esta menor porosidad resulta en menor espacio disponible para colonizar, lo que podría provocar que el *biofilm* que se forma en la capa superior del sistema de sedimento fino (*fine system*) lograse el estado de madurez antes que el sistema grueso-fino (*coarse-fine system*), esto conjuntamente con menores flujos en el sistema fino, favorecería el desprendimiento del *biofilm* superficial y por tanto el transporte de éste en profundidad. La acumulación de EPS en profundidad (debido a la producción de microorganismos vivos o al transporte de este EPS en profundidad) es la principal causa de las variaciones de la K en profundidad (lo cual está relacionado con el potencial de causar *deep-clogging* a largo plazo). Se ha visto que sedimentos mixtos de arenas finas y gruesas (*mixture system*) y sistemas con sedimentos finos a la capa superior y sedimentos gruesos a la capa inferior (*fine-coarse system*) resultan en un funcionamiento similar que los sistemas con sólo sedimento fino (*fine system*) alcanzando biomasas similares entre ellos y menores tasas que el resto de distribuciones granulométricas estudiadas.

List of publications

List of publications derived from this doctoral thesis:

Perujo, N., Sanchez-Vila, X., Proia, L., & Romaní, A. M. (2017). Interaction between physical heterogeneity and microbial processes in subsurface sediments: a laboratory-scale column experiment. *Environmental Science & Technology*, *51*(11), 6110-6119. DOI: 10.1021/acs.est.6b06506

Perujo, N., Romaní, A. M., & Sanchez-Vila, X. (2018). Bilayer infiltration system combines benefits from both coarse and fine sands promoting nutrient accumulation in sediments and increasing removal rates. *Environmental Science & Technology*. DOI**:** 10.1021/acs.est.8b00771

Table of contents

List of Figures

6 CHAPTER III: Assessing deep clogging in infiltration systems: biofilm depth-dynamics in two grain-size distributions

7 GENERAL DISCUSSION

List of Tables

6 CHAPTER III: Assessing deep clogging in infiltration systems: biofilm depth-dynamics in two grain-size distributions

7 GENERAL DISCUSSION

List of abbreviations and symbols

AWCD: Average Well Color Developed

ANCOVA: Analysis of Covariance

ANOSIM: Analysis of Similarities

ANOVA: Analysis of Variance

BDOC: Biodegradable Dissolved Organic Carbon

BIX: Biological Index

CER: Cation Exchange Resin

CF: Coarse-Fine system

Chl-a: Chlorophyll-a

DO: Dissolved oxygen

DOC: Dissolved Organic Carbon

DNA: Deoxyribonucleic acid

DNRA: Dissimilatory Nitrate Reduction to Ammonium

DOM: Dissolved Organic Matter

DON: Dissolved Organic Nitrogen

DW: Dry Weight

EEAs: Extracellular Enzyme Activities

EPS: Extracellular polymeric substances

F: Fine system

FI: Fluorescence Index

gC: grams of Carbon

GSD: Grain Size Distribution

HMW: High-Molecular Weight

HRT: Hydraulic Retention Time

HZ: Hyporheic zone

K: Hydraulic conductivity

K_0: Initial Hydraulic conductivity

LD ratio: live/dead ratio

Leu: leucine-aminopeptidase extracellular enzyme activity

LMW: Low-Molecular Weight

Milli-Q: a trademark created by Millipore Corporation to describe 'ultrapure' water of "Type 1"

NO_x: Sum of nitrates and nitrites

OM: organic matter

PCA: Principal Component Analysis

P_{tot}: Total Phosphorus in sediments

P_{inorg}: Inorganic Phosphorus in sediments

P_{org}: Organic Phosphorus in sediments

Phos: alkaline phosphatase extracellular enzyme activity

RDA: Redundancy Analysis

RIBS: Rapid Infiltration Basin Systems

SAT: Soil-Aquifer treatment

SR: Slope Ratio

SSFS: Slow Sand Filtration Systems

TDN: Total Dissolved Nitrogen

TDP: Total Dissolved Phosphorus

WWTP: Wastewater Treatment Plant

β-glu: β-glucosidase extracellular enzyme activity

β-xyl: β-xylosidase extracellular enzyme activity

1 General Introduction

1.1 Sediment biofilms

Biofilms are assemblages of autotrophic (algae and cyanobacteria) and heterotrophic microorganisms (bacteria, fungi, archaea and protozoa) embedded in an extracellular polymeric matrix (Lock et al. 1984; Romaní et al. 2004a) also named EPS (extracellular polymeric substances). Biofilms develop in any surface where water exists for extended periods of time (Schnurr and Allen 2015) including surface and subsurface sediments, stones and aquatic plants (Jarvie et al. 2002) as well as man-made structures such as pipes. In this work we will focus on surface and subsurface sediment biofilms. The composition and structure of biofilms will vary according to abiotic and biotic factors within the environment (Schnurr and Allen 2015). Sediment biofilms show a clear gradient in depth (Fig. 1). Biofilm activity and biomass are generally highest near the sediment surface and decrease in depth (Haglund et al. 2003). In the surface sediment (under light conditions), autotrophic algae in the biofilm are a possible source of organic compounds that may be used by biofilm bacteria (Rulík and Spácil 2004) which makes heterotrophic biofilm compartment to depend less on external substrate inputs (Romaní et al. 2004a). In depth (no light conditions), biofilm growth –mainly heterotrophic- is constrained and supported by the availability of substrates supplied in the influent water (Campos et al. 2002). Highly heterotrophic biofilms showed lower extracellular enzymatic activity than did the more autotrophic biofilms (Romaní and Sabater 2000).

In biofilms, EPS is a complex mixture of macromolecules, primarily composed of polysaccharides but also containing various amounts of protein, lipid, DNA and vitamins (Flemming and Wingender 2010), and the matrix formed is usually highly hydrated (Stoodley et al. 2002). Important sources of EPS are bacteria and algae that form biofilms (Malarkey et al. 2015). The presence of EPS maintains the structural stability of biofilms; contributes to the attachment of cells to substrata and protects biofilms against environmental stress, as well as provides nutrition storage (Vu et al. 2009).

Biofilm formation is a process of consecutive steps defined by a spatial and temporal scale including cell attachment (adhesion), colony formation (accumulation), maturation and finally the dispersal of cells (detachment) to form new biofilm (Sabater and Romaní 1996; Jenkinson and Lappin-Scott 2001). Cell death is important for biofilm development and autolysis can promote

biofilm formation because of the release of cell content (Bayles 2007). Collapse and recolonization can occur periodically in biofilms (Romaní et al. 2008).

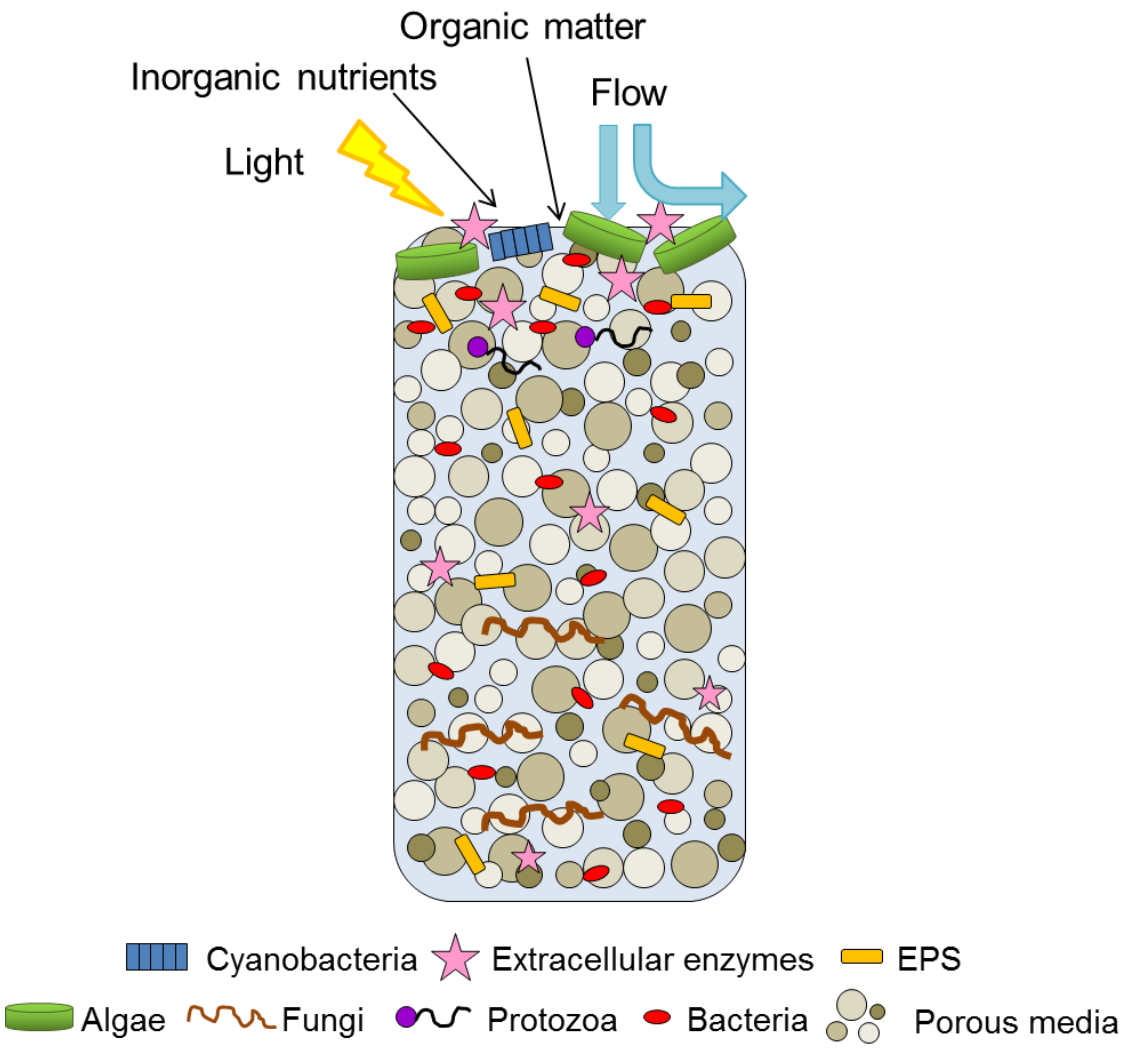

Figure 1 Scheme of a theoretical biofilm structure in sediment depth including environmental factors affecting biofilm structure and function. Modified from Romaní (2010) and Mora-Gómez et al. (2016).

Biofilms are highly efficient and successful ecological communities (Battin et al. 2003) as they play a crucial role in biogeochemical cycles in sediments (Mermillod-Blondin et al. 2005). In fact, they catalyse a number of important processes including mineralization of organic matter (Findlay et al. 2003), assimilation of inorganic nutrients (Findlay and Sinsabaugh 2003), as well as storage and transformation of inorganic and organic nutrients (Pusch et al. 1998).

1.2 Porous media as water treatment technologies

Porous media has been known to be a technology for water treatment since the XIXth Century. The ability of porous media to remove organic matter and nutrients is associated to the presence and development of biofilms. This ability of biofilms for removal/transformation of organic matter and nutrients is widely recognized and used in subsurface environments (Cunningham 1991; Li et al. 2012) to treat municipal sewage and some industrial wastewater improving the quality of water (Duan et al. 2015).

Subsurface infiltration systems are water treatment technologies where water percolates through a bed of porous sand (acting as a sand filter) from the surface to the bottom of the filter (Bekele et al. 2011) (Fig. 2). Properly constructed, sand filters consist of a tank, a bed of sand, a layer of gravel to support the sand and a system of underdrains to collect the filtered water. No chemicals are added to aid the filtration process. Removal mechanisms include biological, chemical and physical processes (Bekele et al. 2011); it is relevant to state that these three groups of processes are not independent.

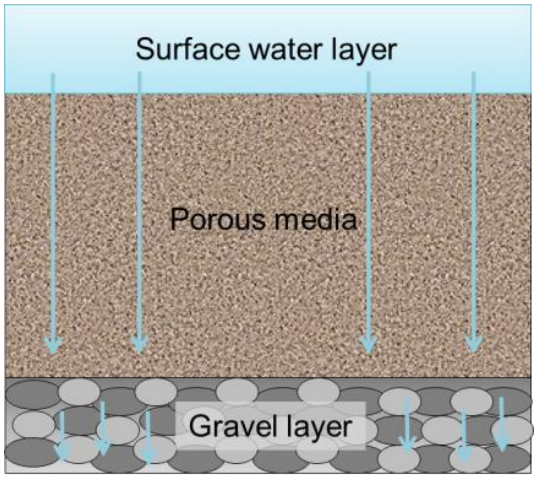

Figure 2 Simplified scheme of the structure of a sand filtration system.

Sand filtration is one of the earliest forms of water treatment. By the early 1800s, slow sand filtration began to be used in Europe, mimicking the treatment observed to be provided by aquifers, mainly to improve water clarity, taste and odour (Dillon et al. 2008). In the mid XIXth Century, the pioneering work of Henry Darcy in Dijon provided the initial way of quantifying infiltration through sand filters. Similarly for wastewater treatment, many engineered treatments

such as lagoons, trickling filters and reed beds were developed (Dillon et al. 2008). Extended literature reports the use of sand filters for nutrient removal indicating its potential to act as a tertiary wastewater treatment (e.g. Wathugala et al. 1987; Arias et al. 2001; Henderson et al. 2007).

In recent years there has been renewed interest in the application of slow sand filters (SSFs) particularly because they are environmentally friendly low-energy methods to operate and achieve high level of treatment (Haig et al. 2014). SSFs have been used for hundreds of years to provide a safe and reliable source of drinking quality water. However, due to a lack of knowledge about the treatment mechanisms – specifically the biological processes involved- SSFs design and operation has not yet been optimised (Haig et al. 2011).

Additional advantages of infiltration systems are simplicity, low capital and low operating costs compared to more sophisticated methods used for tertiary treatment in wastewater treatment plants (WWTPs) (Campos et al. 2002). Related to this, conventional wastewater technologies present severe technical-economic limitations due to their high energy requirements or the investment on chemical compounds (De Godos et al. 2009). Other benefits of applying infiltration systems are the prevention of WWTP effluents to be directly discharged into surface waters of aquatic ecosystems, such as rivers; and in some cases, infiltration of treated water to the aquifer for groundwater recharge (Bardin 2002). On the other hand, infiltration systems have certain limitations such as the large area they need, the temperature-dependency of the wastewater treatment and the clogging of the sand acting as a filter.

Knowledge of porous media used as water treatment technologies can also increase the understanding of natural aquatic systems such as the hyporheic zone (HZ) of the river. HZ can be defined as the interstitial area beneath and adjacent to a river or stream that contains water. In this area many important biogeochemical processes have been shown to occur intensively thus playing a key role in the global metabolism of rivers (Boulton et al. 1998). As stated by Or et al. (2007a) full consideration of the interactions of soil microorganisms with their physical and chemical environments will substantially advance our understanding on microbial ecology.

1.3 Biogeochemical processes in surface and subsurface sediments

Water quality is greatly improved in infiltration systems due to physical and biochemical processes that occur during passage through the porous media (Akhavan et al. 2013). Intense biological and physic-chemical processes may occur in these systems (Goren et al. 2014) related to organic matter (Quanrud et al. 2003; Vanderzalm et al. 2010) and nutrient (Zhang et al. 2005; Zhang et al. 2015) removals.

Microbial processes in subsurface sediments are controlled by the supply of organic matter and oxidised molecules used as electron acceptors (Jones and Holmes 1996). Dissolved oxygen (DO) is energetically the most favourable electron acceptor and strongly influences the succession of biogeochemical processes within the vertical (Baker et al. 2000). As the rate of biogeochemical processes is likely to be limited by either the availability of organic matter and of terminal electron acceptors (Baker and Vervier 2004), microbial active zones are often limited to the top layer of porous media (< 60 cm). According to this, the biologically active microbial community in the top few centimetres of sand in the filter bed is considered to be a major factor contributing to water purification in infiltration systems (Campos et al. 2002).

Organic matter (OM) is removed partially in the initial stage of percolation primarily by biodegradation (Hoppe-Jones et al. 2010; Quanrud et al. 2003). The bulk of organic compounds in aquatic environments is complex and polymeric and cannot be directly incorporated into bacterial cells (Chróst and Rai 1993). Microbes are critical in the process of breaking down and transforming polymeric and macromolecular organic matter into low-molecular-weight molecules which can then cross bacterial cell membranes (Rogers 1961) and be reused by other organisms. The rate of organic matter decomposition is dependent on this enzymatic activity which thus plays a key role in carbon cycling in aquatic environments (Turley and Mackie 1994). The microorganisms within biofilms have the capacity to decompose organic matter by producing extracellular enzyme either located outside the cells or released into the biofilm EPS matrix (Freeman and Lock 1995). Through extracellular enzyme activities (EEAs) microorganisms degrade organic matter to acquire inorganic nitrogen and phosphorous as well as carbon (Sinsabaugh et al. 2008; Clinton et al. 2010, Romaní et al. 2012) (Fig. 3).

Inducible enzymes are synthesized at a low basal rate in the absence of the appropriate substrates, whereas when substrate becomes available in the environment, there is a huge increase in the production rate of the particular enzyme (Chróst 1990). At the same time, extracellular enzyme synthesis is also regulated by catabolic repression. A well-known example is the repression of alkaline phosphatase synthesis when inorganic phosphate is available (Allison and Vitousek 2005). Main extracellular enzyme activities related to C, N and P organic components are glucosidases, phosphatases and peptidases involved in the degradation of polysaccharides, phosphomonoesters and peptides.

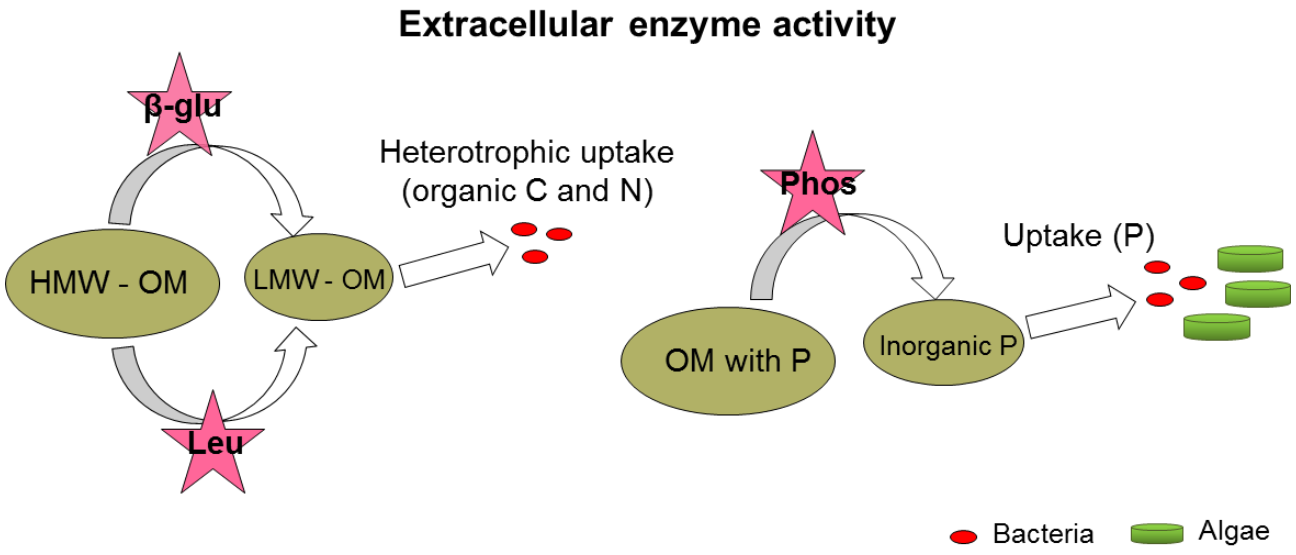

Figure 3 Extracellular enzyme activities (β-glu: β-glucosidase, Leu: leucine-aminopeptidase, Phos: phosphatase) involved in the biodegradation of organic matter. HMW-OM: high-molecular-weight organic matter; LMW-OM: low-molecular-weight organic matter.

In this study we specifically measured β-glucosidase, leucine-aminopeptidase and phosphatase. Whereas bacteria produce β-glucosidases; bacteria, algae and protozoa produce phosphatases (Chróst 1990). β-glucosidase activity has been correlated to the degradation of either organic compounds of algal origin (algal exudates and EPS) or polysaccharidic organic compounds dissolved in flowing water (Jones and Lock 1993). The activity of leucine-aminopeptidase has been positively linked to the activity of photosynthetic primary producers (Francoeur and Wetzel 2003) and to the use of algal-released proteinaceous compounds by microbial heterotrophs (Romaní et al. 2004b). Phosphatase activity indicates the degradation of phosphomonoesters to obtain inorganic phosphorous (Jansson et al. 1988).

Other biogeochemical processes occurring in porous media linked to dissolved organic carbon (DOC), total dissolved nitrogen (TDN) and total dissolved phosphorous (TDP) transformation/removals are summarized in Figure 4. As main C removal processes, significant DOC uptake have been measured for light and dark grown biofilms (Romaní et al. 2004a) as well as carbon respiration of both autotrophic and heterotrophic organisms (Gougoulias et al. 2014) that will release CO_2 to the atmosphere.

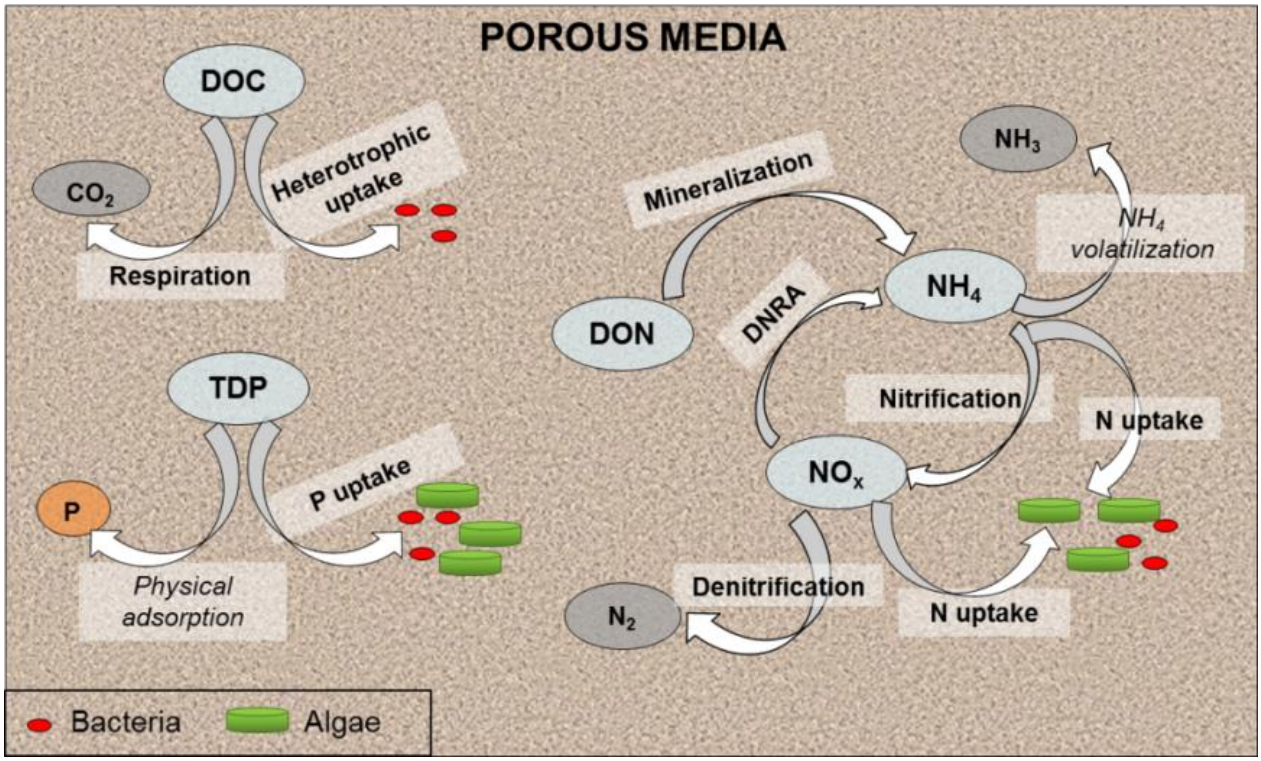

Figure 4 Main biogeochemical processes occurring in porous media. In bold, microbial mediated processes

The removal of nitrogen in infiltration systems is complex and dynamic owing to the many forms of nitrogen and the relative ease of changing from one oxidation state to the next (Mousavinezhad et al. 2015). Nitrogen species in secondary effluent that enters in an infiltration system include NH_4^+, NO_3^-, NO_2^- and organic N. The ammonia fraction can be lost by volatilization and also can be nitrified (in presence of DO) (Kemp and Dodds 2002). However it is important to state that nitrification is not a removal process, it is a conversion process. Further denitrification should occur in depth (anoxic conditions) to effectively remove N from water (Miller et al. 2009; Schmidt et al. 2012). Mineralization of dissolved organic nitrogen (DON) to inorganic forms such as ammonia and nitrate could also happen in infiltration systems (Mousavinezhad et al. 2015). Biofilms are highly metabolic active; for this reason assimilation of N is relevant to meet the

biotic demand of N (Von Schiller et al. 2009). Although many heterotrophic micro-organisms can assimilate nitrate for growth, it appears that in the presence of ammonium, the latter compound is taken up preferentially (Hill 1996). Algae in phototrophic biofilms have also a great potential for N removal through N uptake into the cell (Hoffman 1998).

Sediment has been shown to be the primary factor behind phosphorus retention in freshwater ecosystems (Søndergaard et al. 2003) for this reason phosphorus cycling is especially relevant in sediment biofilms. Phosphorous may be removed either in aerobic or anaerobic environments through proper sorption onto soil media (Chang et al. 2010) as well as through biological uptake (Hu et al. 2005). However, as the sorption sites get filled, the retention capacity for phosphorus will be gradually reduced over time (Hu et al. 2005).

1.4 Variables affecting performance of infiltration systems

Successful treatment in infiltration systems requires a balance between two inter-related issues: hydraulic performance (applying the maximum possible amount of wastewater to the smallest possible land area) and effective improvement of water quality through infiltration (Mousavinezhad et al. 2015).

Ideally an optimal flow velocity should be achieved to allow infiltration from the surface to the subsurface on a practical time scale (Racz et al. 2012); however, rapid movement of water through the soil profile may not allow sufficient time for biogeochemical processes to occur. In fact, contact times between the solid and solution phases influence adsorption and degradation processes (Jardine et al. 2006). On the other hand, biogeochemical processes are limited by availability of organic matter, redox species and inorganic nutrients (Baker et al. 2000; Rusch and Huettel 2000; Hall et al. 2012). In this sense, hydrological parameters (permeability and flow velocity – Hunter et al. 1998-) control the supply rates of solutes in subsurface sediments thus influencing bacterial activity (Claret and Boulton 2008). In fact, low activity rates in deep sediment layers could be either caused by reduced connectivity with the water column or by long interstitial flow paths during which the substances that fuel microbial metabolism are stripped off (Hunter et al. 1998).

It is well known that infiltration systems can clog over time (Baveye et al. 1998). Clogging mechanisms can be classified into three classes: physical, chemical and biological (Vandevivere and Baveye 1992). Even though the causes of clogging are complex, physical blockage and biological clogging are assumed as the main causes (Duan et al. 2015). However, if infiltrated water comes from secondary treated wastewater, the presence of particulate matter in the inlet water is minimized and then biological clogging (also termed bioclogging) is the main cause of system crashes. Bioclogging occurs due to biofilm formation (Rubol et al. 2014) and includes the accumulation of algae and bacteria (Vandevivere and Baveye 1991) as well as the production of EPS (Thullner et al. 2002). Clogging provides a substantial decrease in permeability in infiltration systems (Bouwer 2002; Rubol et al. 2014) implying a reduced water infiltration capacity (Or et al. 2007a) and affecting the pathway of fluid flow in the subsurface (Seifert and Engesgaard 2007). In this sense, clogging may greatly modify DO and electron acceptors distribution in depth (Nogaro et al. 2010).

Although biofilm growth is necessary for effective water treatment performances, its excessive growth also implies deleterious effects in infiltration systems. Accordingly, bioclogging may decrease removal efficiencies (Phanikumar et al. 2005); affect the quality of infiltrated waters (Dechesne et al. 2004) and increase the operating costs (Xia et al. 2014). To alleviate bioclogging and maintain the life of the infiltration system, the sediment top layer has to be scarified periodically (times would vary strongly, depending on the quality of the infiltrated water) (Türkmen et al. 2008).

1.4.1 Influence of grain size heterogeneity on infiltration systems

The sedimentary context (sediment grain size distribution –GSD-) determines hydrological parameters in subsurface sediments influencing the growth of biofilms and the rates of biogeochemical processes (Navel et al. 2012). It also influences the extent of clogging (Hand et al. 2008; Thullner 2010). Table 1 summarizes the particle size class scale defined by Wentworth (1922).

Coarse sands show high hydraulic conductivity (K) and hence high supply of solutes in depth (Battin 2000) but low water contact times. On the other hand, fine sands have high surface-to-volume ratios or colonisable area per sediment volume (Marxsen and Witzel 1990) but biofilm in

depth may be limited by advective mass transfer (Mendoza-Lera et al. 2017). Coarse sands (high porosity media) will allow sufficient oxygen transfer in depth, providing effectively an aerobic environment, while fine sands could foster an anaerobic environment in depth due to low porosity diminishing DO transfer in depth (Rusch and Huettel 2000). Coarser sediments may prevent clogging issues due to lower colonisable surface area, as well as lower adsorption affinities for nitrogen and phosphorous species (Chang et al. 2010) compared to fine sediments. Sediment grain size influences also particle transport in depth which could have implications on the performance of water treatment as biomass from upper layers can be transported downwards, with potential to colonize deep substrates (bioclogging) and also to carry biogeochemical processes in depth. According to Fuchs et al. (2004) distribution and quantity of biomass is determined by nutrient inputs and grain size distribution. Rusch and Huettel (2000) showed that artificial as well as natural particles penetrate deeper into coarse than into fine sands. The idea of grain size affecting transport behaviour of bacteria in porous media was reinforced by Han et al. (2013) and Bai et al. (2016). Furthermore, as heterogeneous porous media has been shown to exhibit much higher net biodegradation than homogeneous flow-through systems, sediment grain size heterogeneity could significantly affect transverse mixing resulting in an enhanced biodegradation (Bauer et al. 2009).

Table 1 Particle size class scale defined by Wentworth (1922)

Diameter (mm)	Wentworth Size Class
> 2 mm	Gravel
1 – 2 mm	Very coarse sand
0.5 – 1 mm	Coarse sand
0.25 – 0.5 mm	Medium sand
0.125 – 0.25 mm	Fine sand
0.0625 – 0.125 mm	Very fine sand
0.0039 – 0.0625 mm	Silt

1.5 Excessive nutrient inputs to ecosystems

Through agricultural practices, urbanization, industrialization and other alterations, humans have increased the input of nutrients into ecosystems thus affecting biochemical cycles especially nitrogen and phosphorus ones (Aslan and Kapdan 2006). Although both, nitrogen and phosphorus

are essential nutrients for organisms and are fundamental to sustaining freshwater ecosystems, excess of nitrogen and phosphorus may have deleterious effects on aquatic ecosystems.

Eutrophication is a global cause of water quality impairment, whereby excess of nutrients modify the structure and function of freshwater ecosystems (Smith 2003). Main effects of eutrophication (Fig. 5) are: increase of algal biomass and productivity (Aslan and Kapdan 2006), modification of physicochemical water characteristics such as colour, odour and turbidity; impairment of biological communities and substitution of sensitive species towards generalist ones (Smith 2003); anoxic waters and fish death (Türkmen et al. 2008) and limitation of using water for recreational purposes (Leaf 2018). Reducing anthropogenic nutrient inputs is a necessary first step to address eutrophication (McCrackin et al. 2017). In fact, eutrophication has been recognised as a significant environmental issue across Europe since the late 1980s, and continues to present a long-term challenge for sustainable nutrient management (Chang 2010).

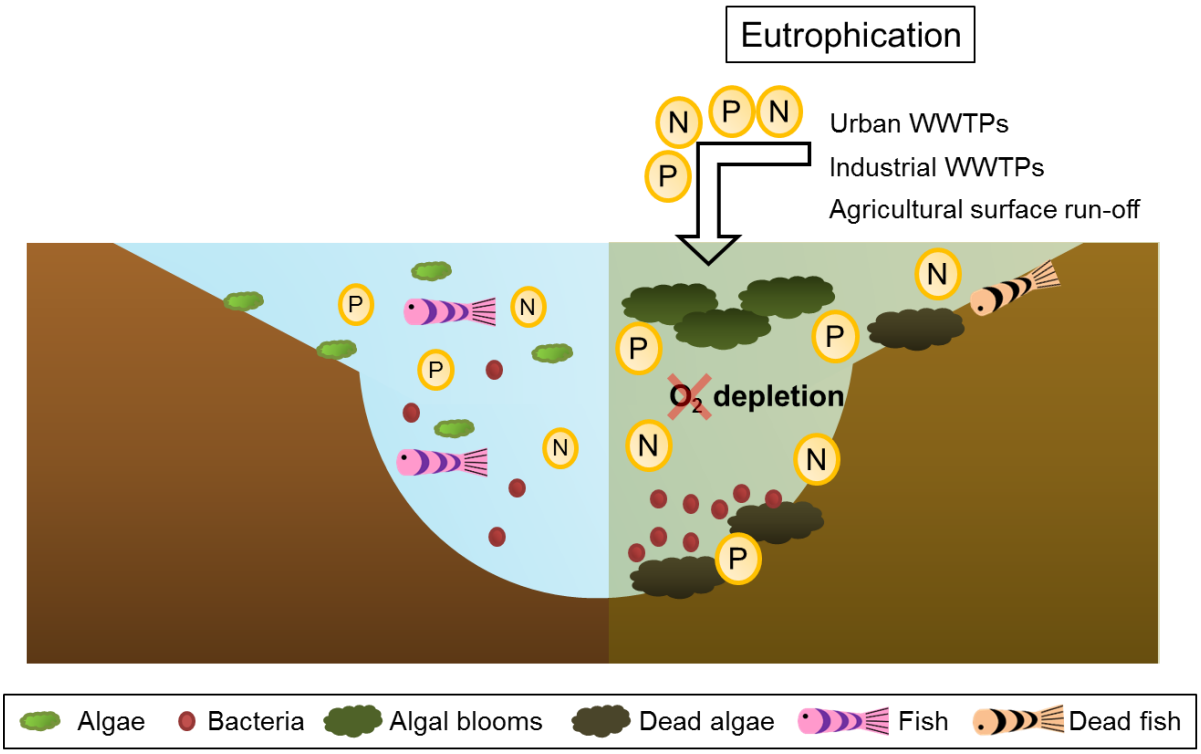

Figure 5 Diagram of the main consequences from eutrophication in freshwater systems

In Mediterranean rivers, the impact of treated wastewater inputs from WWTPs into the river –in terms of nutrient concentrations – can be aggravated, particularly in periods of low river flow. Accordingly, Gücker et al. (2006) stated that the highest impact occurs when treated wastewater is poured into rivers with low dilution capacity thus modifying ecosystem functioning. Wakelin et

al. (2008) affirmed a strong cause-effect between the carbon and nitrogen input loads from WWTPs and the structure and function of freshwater communities. Related to this, Martí et al. (2004) showed an increase of nutrient loadings in river water and low nutrient retention efficiency downstream from a WWTP which reveals that nutrient inputs could have ecological implications not only at local scale but also at regional scale as nutrients can be transported long distances downstream. Also related to the low dilution capacity of freshwater systems, Jarvie et al. (2018) suggested that managing and controlling both P and N inputs to headwater streams will be needed to minimise the risks of degradation of these sensitive headwater environments since headwater streams can be highly vulnerable to water-quality impairment due to their low dilution capacity. Furthermore, by focusing on nutrient mitigation in headwater catchments, there could also be a cumulative downstream improvement in river water quality (Jarvie et al. 2002).

In order to maintain ecosystem integrity, special attention should be paid to WWTP inputs in the more sensitive upper reaches and in receiving bodies with low dilution capacity (Perujo et al. 2016). WWTPs should be designed taking into account the metabolic and functional characteristics of the receiving communities, with the goal of achieving the lowest impact grade. In other words, WWTP inputs should result in the lowest amount of change to the physical and chemical water conditions in order not to exceed the sensitivity threshold values of each receiving biofilm community (Perujo et al. 2016).

A number of policies have been implemented to mitigate the ecological and economic effects of eutrophication and restore aquatic ecosystems by reducing anthropogenic nutrient inputs. In the United States and European Union there has been success in reducing nutrient emissions from agriculture, sewage treatment plants, and fossil fuel combustion (McCrackin et al. 2017). Substantial progress has also been made in upgrading sewage treatment facilities to remove nutrients from the effluent as a result of the EU Urban Wastewater Treatment Directive (Eom et al. 2017). Nevertheless, the costs of mitigating eutrophication are significant (Pretty et al. 2003). Chemical phosphorous precipitation represents a high cost due to the reagents used as well as due to high sludge production and the increase of chlorides and sulphates concentrations in water. With regard to biological elimination either results in very low elimination yields or in complex and expensive processes.

2 Objectives

The main objective of this thesis is to study the influence of sediment grain size distribution (GSD) on biogeochemical processes and on biofilm accumulation in depth in infiltration systems used as water treatment technologies for improving quality of infiltrated water in terms of organic matter and nutrient removals.

The specific objectives are:

- To understand the influence of sediment heterogeneity on physicochemical water parameters and on biofilm biomass and activity in sediment infiltration systems, by specifically studying the relationship between physicochemical and biological parameters and how they influence biogeochemical processes occurring in these systems **(Chapter I)**.
- To compare the performance of a bilayer coarse-fine vertical infiltration system with regard to a monolayer fine sand system; and specifically, to study the distribution of biogeochemical processes in depth, to analyze the importance of nutrient accumulation in sediments with regard to adsorption and assimilation processes, and to link biogeochemical process rates to removal efficiencies at each system in order to decipher whether the bilayer system optimizes the infiltration system performance **(Chapter II)**.
- To deepen our knowledge on bioclogging. Specifically, to analyze the vertical depth-distribution and depth-dynamics of biofilm structural components (algae, EPS, live bacteria and dead bacteria), to determine the potential role of each biofilm component to hydraulic conductivity variations and to study the growth and transport of biofilm structural components in depth linked to sediment grain size distributions and determine their implications on potential deep bioclogging **(Chapter III)**.

3 General Methods

3.1 Sediments

Sediment used for the experimental section was siliceous sand from Adicat tribar (Àrids per a la Indústria i la Depuració, S.L.), rounded shape and free from clays and organic matter. Two sand sizes were used: fine and coarse. D values for the fine sand were d_{10} = 0.08 mm; d_{50} = 0.255 mm and d_{90} = 0.350 mm. D values for the coarse sand were d_{10} = 0.84 mm; d_{50} = 1.0 mm and d_{90} = 1.4 mm. Initial porosity was 0.32 in the fine sand and 0.4 in the coarse sand.

3.2 Hydraulic parameters

Hydraulic conductivity (K, [LT^{-1}]) was calculated using Darcy's law (eq. 1) where, Q is the flow rate [L^3T^{-1}], L_{ab} is the total length of the sediment interval [L], Δh_{ab} (cm) is the piezometric head difference between two sampling depths [L] –Fig. 1- and A is the cross-section area where water infiltrates [L^2]. The residence time within the length of the sediment, also called advection time, was calculated by means of equation 2, where, ϕ is the porosity of the sediment.

$$K_{(a-b)} = \frac{Q \cdot L_{ab}}{\Delta h_{ab} \cdot A} \quad (eq.\,1)$$

$$\text{advection time} = \frac{\phi \cdot L \cdot A}{Q} \quad (eq.\,2)$$

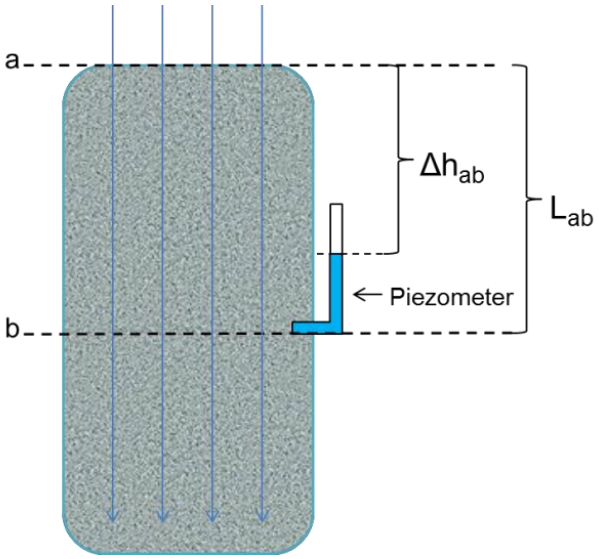

Figure 1 Scheme to identify Δh and L parameters used to calculate K in porous media

3.3 Water parameters

Figure 2 shows a scheme of the methods used for the analysis of water parameters. Samples for dissolved nutrients and dissolved organic carbon (DOC) were filtered in pre-combusted (4h, 450 ºC) filters (GF/F, 0.7 µm, Whatmann). DOC samples (20 mL) were fixed (100 µL sodium azide

2.7 mM), acidified (100 µl HCl 2 N) and kept at 4 ºC until analysis. DOC concentrations (mg $C \cdot L^{-1}$) were determined using a total organic carbon analyser (TOC-V_{CSH} Shimadzu).

For inorganic nutrient determination, samples were filtered again (nylon filters 0.2 µm, Whatmann). Nitrates and nitrites were analysed by ionic chromatography (761 Compact IC 1.1 Metröhm) and a standard of NO_2^- and NO_3^- was prepared to link chromatograph heights to nutrient concentrations. Results are expressed as mg $N\text{-}NO_3^- \cdot L^{-1}$, mg $N\text{-}NO_2^- \cdot L^{-1}$ and mg $N\text{-}NO_x \cdot L^{-1}$ as the sum of NO_2^- and NO_3^-.

Ammonium concentration was determined by the spectrophotometric sodium salicylate protocol (Reardon et al. 1966) which consists of addition of two reagents[1] (1 mL each) to all the samples (10 mL). Samples were kept in the dark for 1 – 12 hours and then absorbance (690 nm) was measured (UV-1800 UV-VIS Shimadzu). To link absorbance values to ammonium concentrations, standard solutions were prepared. Results are expressed as mg $N\text{-}NH_4^+ \cdot L^{-1}$.

Dissolved inorganic P (phosphate) was determined by the molybdenum blue method from Murphy and Riley (1962). The molybdenum blue method consists of addition of a mixed reagent[2] (1 mL) to all the samples (10 mL). Samples were kept in the dark for 1-12 hours and then absorbance (890 nm) was measured (UV-1800 UV-VIS Shimadzu). To link absorbance values to phosphate concentrations, standard solutions were prepared. Results are expressed as mg $P\text{-}PO_4^{3-} \cdot L^{-1}$.

Total dissolved nitrogen (TDN) and total dissolved phosphorous (TDP) samples were digested before analysis. The digestion protocol (adapted from Koroleff 1983) consisted of an oxidation where the reagent prepared in NaOH solution (0.375 M) containing $K_2S_2O_8$ (0.18 M) and H_3BO_3 (0.48 M) was added (2 mL) to filtered samples (20 mL) in tightly capped Pyrex glass tubes. Tubes were closed, shaken and autoclaved (90 min, 115 ºC). For TDN determination, absorbance was measured at 275 and 220 nm (UV-1800 UV-VIS Shimadzu) and a standard was prepared to link absorbance measurements to TDN concentrations, results are expressed as mg $N \cdot L^{-1}$. Dissolved organic nitrogen (DON) was calculated as the difference between TDN and inorganic

[1] Reagent 1: sodium salicylate 0.2 M, citrate trisodium dihydrate 0.14 M and sodium nitroprusside dihydrate 0.001 M. Reagent 2: sodium hydroxide 0.12 M and sodium dichloroisocyanurate dehydrate 0.003M.

[2] Mixed reagent: 20% ammonium paramolybdate tetrahydrate (0.024 M), 50% sulfuric acid (5N), 20% ascorbic acid (0.30 M) and 10 % potassium antimonial tartrate (0.002 M).

nitrogen (DON = TDN – NH_4^+ - NO_x). After digestion, TDP determination followed the molybdenum blue method from Murphy and Riley (1962) and results are expressed as mg $P \cdot L^{-1}$.

Dissolved organic matter (DOM) spectroscopic properties were analysed in a fluorimeter plate reader (Tecan, infinite M200 Pro) to characterize potential changes in DOM quality and included the following parameters: the Slope Ratio (SR) described in Helms et al. (2008) which is inversely correlated to organic matter molecular weight; the Fluorescence Index (FI) described in Cory and McKnight (2005) indicative of the origin of the organic matter; the Biological Index (BIX) described in Huguet et al. (2009) as indicator of recent biological activity and the E_2/E_3 index which is related to photo reactivity (Minero et al. 2007) (Fig. 2).

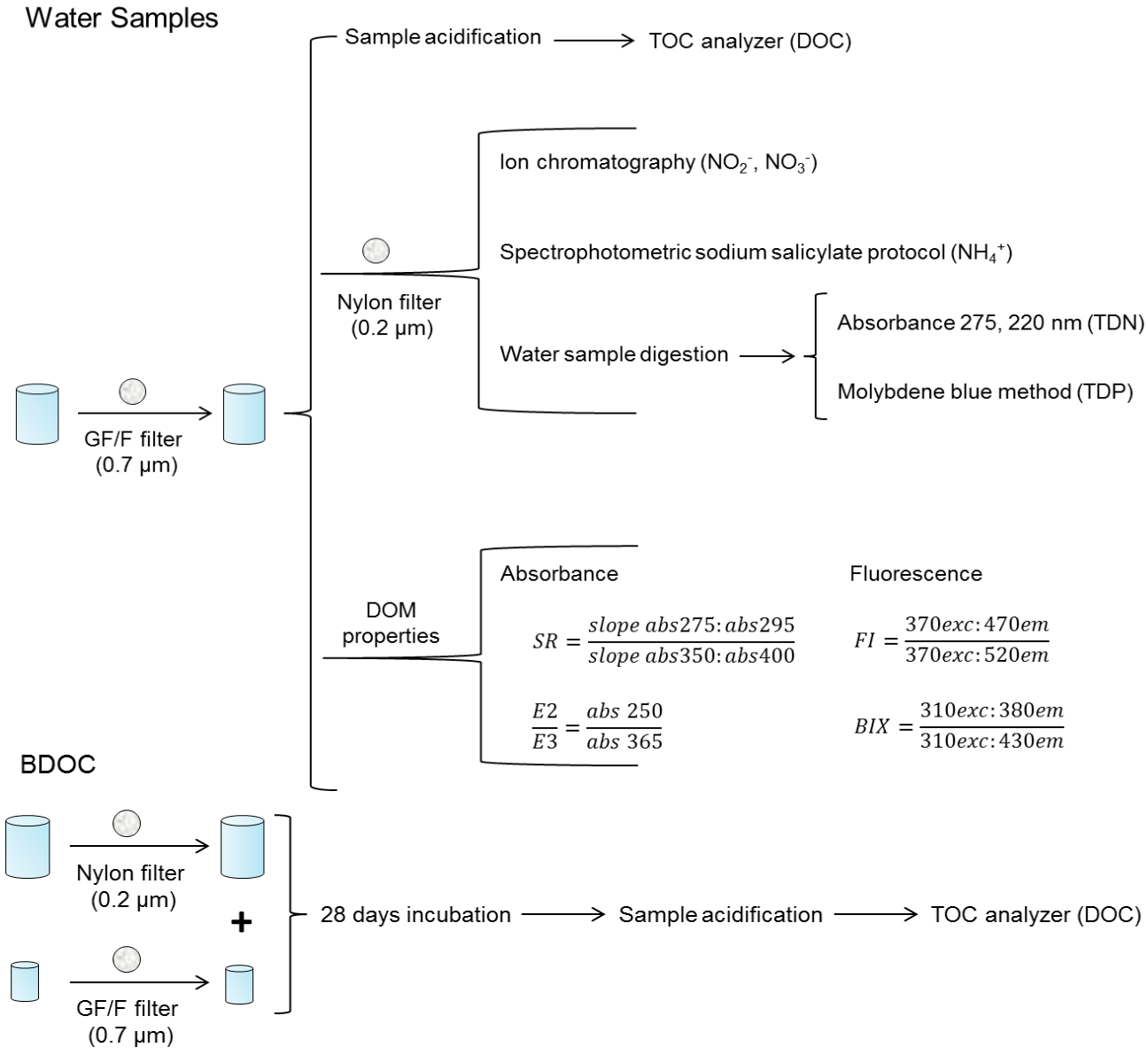

Figure 2 Scheme of the methods used for the analysis of the water samples

Biodegradable dissolved organic carbon (BDOC) was analysed following the protocol described by Servais et al. (1989). Filtered samples (200 mL, nylon filters 0.2 µm) to exclude bacteria were placed on pre-combusted (4 hours, 450 ºC) Pyrex bottles. Another aliquot of filtered sample (2 mL, GF/F 0.7 µm) was added to each Pyrex bottle. Bottles were closed and gently shaken. Initial samples (20 mL) were placed on pre-combusted glass vials (4 hours, 450 ºC), fixed (100 µL sodium azide) and acidified (100 µL HCl 2N). Bottles were incubated for 28 days in dark and constant temperature conditions (18 – 20 ºC). Final samples (2 mL) were placed on pre-combusted glass vials (4 hours, 450 ºC), fixed (100 µL sodium azide) and acidified (100 µL HCl 2N). DOC content of initial and final samples was analysed using a total organic carbon analyser (TOC-V_{CSH} Shimadzu). BDOC content was calculated based on the difference in the DOC content measured in the initial samples minus the DOC content of the final samples, and results are expressed as mg $C_{BDOC} \cdot L^{-1}$.

3.4 Sediment parameters

3.4.1 Carbon, nitrogen and phosphorus content in sediments

For carbon and nitrogen determination in sediments, distilled Milli-Q water (1.5 mL) was added to sediment samples (1 cm^3), then sonicated for 1 minute and shook. Aliquots of the extract (100 µL) were pipetted into pre-weight tin capsules for solids (5 x 8 mm, precleaned, PerkinElmer) and placed in the oven at 60 ºC until drying. The remaining extract was kept at 4 ºC. Pipetting was repeated five times to obtain a final dry weight of ca. 1 - 3 mg in the capsules. Tin cups were closed and weighted and carbon and nitrogen content in sediments were analysed in a CN-analyzer (Carlo Erba). Results are expressed as µg $C \cdot gDW^{-1}$ and µg $N \cdot gDW^{-1}$.

The protocol used for P determination in sediments was adapted from Aspila et al. (1976). Sediment samples (1 cm^3) were dried at 50 ºC, crushed and accurately weighted. Samples for total phosphorous (P_{tot}) determination were transferred into porcelain crucibles, ignited in a muffle furnace (550 ºC for 1h, following Andersen (1976)), and then let to cool for one hour. Samples for total phosphorous and inorganic phosphorous (P_{inorg}) determinations were transferred to 100 mL Erlenmeyer flasks with HCl acid (1.0 M, 25 mL). Mixtures were boiled for 15 minutes on a hot plate, filtered (Whatmann, 2.5 µm) to separate the liquid phase from the sediment, and ten-fold diluted with Milli-Q water. P_{tot} and P_{inorg} were determined by the Molybdenum blue

method (Murphy and Riley 1962, see *section 3.3 Water parameters page 21*). P_{org} was determined by colorimetry, as the difference between P_{tot} and P_{inorg}. Results are expressed as µg $P \cdot gDW^{-1}$. The ratio between P_{inorg}/P_{org} was calculated as an indicator of the proportion of inorganic phosphorous accumulated in sediments versus the organic phosphorous in sediments, where values >1 indicate dominance of inorganic P and values < 1 indicate dominance of organic P. Sediment molar C:N:P ratios were also calculated.

3.4.2 Bacterial Density

Bacterial density was determined by flow cytometry following a protocol adapted from Amalfitano et al. (2009). Sediment samples (1 cm^3) were sonicated for 1 minute, shook for 30 s, and sonicated again for 1 minute to extract the biofilm from sediment grains (Ultrasons, Selecta). A subsample of the obtained extract was pipetted into a glass vial of detaching solution[3] (1:10 v:v). Samples were then shaken for 30 min (150 rpm) at dark and room temperature conditions. Samples were left 10 min at 4 ºC and sonicated with ice during two cycles of 1 minute. After shaking for 1 min, samples were left for 5 min for sedimentation of larger particles and 1 mL of supernatant was transferred in an Eppendorf. Nycodenz (1 mL) was added to the bottom of the Eppendorf and samples were centrifuged (14 000 rpm) for 90 minutes at 4 ºC. Purified extracts were diluted with filtered (nylon filters 0.2 µm, Whatmann) synthetic water[4] to reach a bacterial density around 10^6–10^7 $cells \cdot mL^{-1}$. Purified extract (400 µL) was stained with Syto13 (4 µL Fisher, 5 µM solution) and incubated in the dark for 30 min. Stained samples were counted in a flow cytometer (FACSCalibur, Becton Dickinson). To link fluorescence data to bacterial density, a bead solution (10 µL of 10^6 $beads \cdot ml^{-1}$, Fisher 1.0 µm) was added to the samples in a known concentration. Results are expressed as bacterial $cells \cdot gDW^{-1}$. Bacterial cells are converted to biomass (gC) applying the relation 0.22 $gC \cdot cm^{-3}$ (Bratbak and Dundas 1984) considering a bacterial cell to occupy 0.1 μm^3 of volume (Bratbak 1985).

[3] Detaching solution consists of NaCl (130 mM), Na_2HPO_4 (7 mM), NaH_2PO_4 (3 mM), formaldehyde (37 %), sodium pyrophosphate decahydrate 99 % (0.1 % final concentration), and tween 20 (0.5 % final concentration), and it helps to separate cells avoiding aggregation.

[4] Synthetic water (13 $mg \cdot L^{-1}$ Na_2SO_4, 16.1 $mg \cdot L^{-1}$ Na_2SiO_3, 29.4 $mg \cdot L^{-1}$ $CaCl_2 \cdot H_2O$, 0.6 $mg \cdot L^{-1}$ KCl, 3 $mg \cdot L^{-1}$ $MgSO_4 \cdot 7H_2O$ and 26.5 $mg \cdot L^{-1}$ Na_2CO_3)

3.4.3 Bacterial Viability

Pyrophosphate (5 mL, 50 mM, Quéric et al. 2004) was added to fresh sediment samples (1 cm^3) and they were incubated for 15 minutes at room temperature and soft shaking. Samples were then sonicated for 1 minute with ice to avoid cell disruption (Amalfitano and Fazi 2008). The obtained extract was diluted with filtered (nylon filters 0.2 µm, Whatmann) synthetic water[4] to reach a bacterial density around 10^6–10^7 cells·mL^{-1} and subsamples of the diluted extract (400 µL) were stained with propidium iodide and Syto 9 (8 µL, BacLight Bacterial Viability Kit) (Falcioni et al. 2006). Syto 9 penetrates all bacterial membranes and stains the cells fluorescent green, while propidium iodide only penetrates cells with damaged membranes, and the combination of the two stains produces red fluorescing cells (Boulos et al. 1999). Samples were incubated in the dark for 15 minutes. According to Falcioni et al. (2006) to link fluorescence data to bacterial density, a bead solution (40 µL of 10^6 beads·mL^{-1}, Fisher 1.0 µm) was added to the samples in a known concentration. Bacterial viability was measured by flow cytometry (FACSCalibur, Becton Dickinson). Results are expressed as live cells·gDW^{-1}, dead cells·gDW^{-1} or as the ratio between live and dead bacteria (LD ratio). Live and dead bacteria density units are converted to biomass (gC) applying the relation 0.22 gC·cm^{-3} (Bratbak and Dundas 1984) considering a bacterial cell to occupy 0.1 μm^3 of volume (Bratbak 1985).

3.4.4 Algal biomass (chlorophyll-a concentration)

Chlorophyll-a concentration (chl-a) was determined following the protocol described by Jeffrey and Humphrey (1975). Acetone 90 % (10 mL) was added to each sediment sample (1 cm^3) and samples were kept in the dark for 8-12 h at 4 ºC to extract the chl-a. Samples were sonicated and filtered (GF/C, 1.2 µm, 47 mm). Absorbance was measured at 430, 665 and 750 nm (UV-1800 UV-VIS Shimadzu). Chl-a concentration was calculated as follows (eq. 3):

$$Chl-a\ (\mu g/g\ DW) = \frac{11.4 \cdot (Abs665 - Abs750) \cdot V}{L \cdot S \cdot DW} \quad eq\ (3)$$

Where, V is the acetone volume added to each sample (mL); L is the length of the spectrophotometry cuvette (cm); S is the surface of the sample (cm^2) and DW is the dry weight of the sample (g). To transform chl-a units to biomass, a conversion factor 1 g chl-a = 60 gC is applied (Yacobi and Zohari 2010; Riemann et al. 1989; Lorenzen 1968).

3.4.5 Content of polysaccharides in extracellular polymeric substances (EPS)

EPS were extracted by a cation exchange resin (CER) and the content of polysaccharides was measured spectrophotometrically following the protocol described by Dubois et al. (1956). Previous to EPS determination, CER (Dowex Marathon C sodium form, Sigma-Aldrich) was conditioned with HCl (4 M) and NaOH (1 M) following manufacturer instructions. Sediment samples (1 cm^3) were placed in an Eppendorf with 1 mL of Milli-Q plus 0.3 g of CER. After shaking the Eppendorfs carefully, samples were incubated with ice for 1 h in a shaker (250 rpm) and then centrifuged (11 000 rpm for 15 min at 4 ºC). Supernatant (500 µl) from each sample was pipetted into glass tubes. A phenol solution (12.5 µL, 80 % w/w) was added to the glass tubes. After carefully shaken, 1.25 ml of H_2SO_4 (95.5 %) was added to the samples. Glass tubes were capped. After 10 minutes, samples were carefully shaken and incubated for 20 minutes in a water bath (30 ºC). Absorbance (485 nm) was measured in a spectrophotometer (UV-1800 UV-VIS Shimadzu). To determine content of polysaccharides in EPS, a glucose standard was prepared. Results are expressed as µg glucose-equivalents·gDW^{-1}. To transform polysaccharides units to biomass a conversion factor 1 g glucose = 0.4 gC is applied.

3.4.6 Extracellular Enzyme Activities

Extracellular enzyme activities β-glucosidase (EC 3.2.1.21), β-xylosidase (EC 3.2.1.37), phosphatase (EC 3.1.3.1) and leucine-aminopeptidase (EC 3.4.11.1) were measured using fluorescent-linked artificial substrates (Methylumbelliferyl (MUF)-β-D-glucopyranoside, MUF-β-D-xyloside, MUF-phosphate, and L-leucine-7-amido-4-methylcoumarin hydrochloride (Leu-AMC, Sigma-Aldrich). All enzyme activities were measured under saturating conditions (0.3 mM) (Romaní 2000). Fresh sediment samples (1 cm^3) were placed in falcon tubes with filtered (nylon filters 0.2 µm, Whatmann) synthetic water[5] (4 mL) and artificial substrate (120 µL). A blank for each artificial substrate was prepared with autoclaved Milli-Q water to determine the abiotic hydrolysis of the substrate itself. Samples and blanks were incubated for 1 hour in the dark with agitation. After 1 hour of incubation, glycine buffer (4 mL, pH 10.4) was added to each falcon tube to stop the reaction and maximize MUF and AMC fluorescence. Samples were

[5] Synthetic water (13 mg·L^{-1} Na_2SO_4, 16.1 mg·L^{-1} Na_2SiO_3, 29.4 mg·L^{-1} $CaCl_2·H_2O$, 0.6 mg·L^{-1} KCl, 3 mg·L^{-1} $MgSO_4·7H_2O$ and 26.5 mg·L^{-1} Na_2CO_3)

centrifuged (2000 g) for 2 minutes, and the supernatant (350 µL) of each sample was placed into a 96 wells black plate (Greiner bio-one) for measuring the fluorescence (excitation/emission wavelengths of 365/455 –MUF- and 364/445 –AMC-) in a fluorimeter plate reader (Tecan, infinite M200 Pro). To link fluorescence data and extracellular enzyme activities concentration, MUF and AMC standards were prepared. Results are expressed as nmol MUF·gDW^{-1}·h^{-1} and nmol AMC·gDW^{-1}·h^{-1}.

3.4.7 Functional Diversity

Biolog Ecoplates microplates (AEX Chemunex) were used to determine functional diversity of sediment communities. Each microplate contains three replicate wells of 31 carbon sources and a blank (no substrate). To obtain an extract of the microbial community for the sediment samples a similar procedure to that used for bacteria viability was used. Pyrophosphate (5 mL, 50 mM) was added to the sediment samples which were then incubated for 15 minutes at room temperature and soft shaking. Samples were sonicated for 1 minute with ice. A subsample of the obtained extract (1 mL) was diluted with filtered (nylon filters 0.2 µm, Whatmann) synthetic water[6] (1:50). Microplates were inoculated under sterile conditions with 130 µL of the diluted extract to each well and incubated in dark conditions at 20 ºC for 14 days. Absorbance was measured every 24 hours at 590 nm (Tecan, infinite M200 Pro). The color measured in each well, a measure of the ability of the inoculated community to metabolize the specific substrate was corrected by the color measured in the blank well from each microplate. During the incubation, absorbance measurements increased following a sigmoidal pattern, and after 14 days of incubation the absorbance was saturated. Absorbance data of each substrate, when the average well color developed (AWCD) was 0.5, was used to calculate the sediment biofilm functional diversity by means of the Shannon diversity index (Magurran 1988).

[6] Synthetic water (13 mg·L^{-1} Na_2SO_4, 16.1 mg·L^{-1} Na_2SiO_3, 29.4 mg·L^{-1} $CaCl_2·H_2O$, 0.6 mg·L^{-1} KCl, 3 mg·L^{-1} $MgSO_4·7H_2O$ and 26.5 mg·L^{-1} Na_2CO_3)

4 Chapter I:

Interaction between Physical Heterogeneity and Microbial Processes in Subsurface Sediments: A Laboratory-Scale Column Experiment

4.1 Abstract

Physical heterogeneity determines interstitial fluxes in porous media. Nutrients and organic matter distribution in depth influence physicochemical and microbial processes occurring in subsurface. Columns 50 cm long were filled with sterile silica sand following five grain size distributions combining fine and coarse sands or a mixture of both mimicking potential water treatment barriers. Water was supplied continuously to all columns during 33 days. Hydraulic conductivity, dissolved nutrients and organic matter, as well as biofilm biomass and activity were analysed in order to study the effect of spatial grain size heterogeneity on physicochemical and microbial processes and their mutual interaction. Coarse sediments showed higher biomass and activity in deeper areas compared to the others; however they resulted in incomplete denitrification, large proportion of dead bacteria in depth and low functional diversity. Treatments with fine sediment in the upper 20 cm of the columns showed high phosphorus retention. However, low hydraulic conductivity values reported in these sediments seemed to constrain biofilm activity and biomass. On the other hand, sudden transition from coarse-to-fine grain sizes promoted a hot-spot of organic matter degradation and biomass growth at the interface. Our results reinforce the idea that grain-size distribution in subsurface sandy sediments drives the interstitial fluxes, influencing microbial processes.

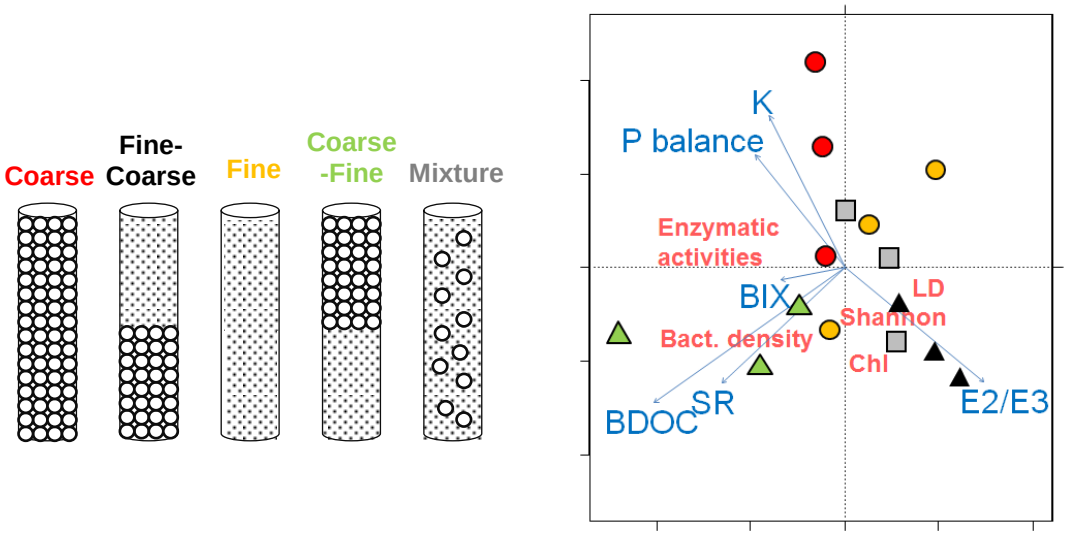

4.2 Introduction

Bacterial communities inhabiting surface and subsurface sediments catalyse a number of ecosystem processes, including uptake, storage, and mineralization of dissolved organic matter, as well as assimilation of inorganic nutrients (Findlay and Sinsabaugh 2003; Romaní et al. 2004a). Processes occurring in subsurface sediments are not only relevant in natural environments (such as in river hyporheic zones), but also in man-made applications for water quality improvement (such as land based wastewater disposal or managed aquifer recharge facilities). Infiltration systems are water treatment systems that rely on water percolation (Bekele et al. 2011) through a porous medium whereby the quality of the effluent improves progressively during the infiltration path as a consequence of the combination of biological, chemical and physical processes (Dillon et al. 2008; Miller et al. 2009) driven by microbial activity (Greskowiak et al. 2005) at the cost of progressively reducing infiltration rates (Pedretti et al. 2012). In this sense, infiltration systems may be advantageous in many aspects; they may increase (by recharge) groundwater supplies, provide further treatment to infiltrated water, and reduce degradation of stream water quality (Türkmen et al. 2008). Infiltration systems may also enable water reuse thereby preserving valuable freshwater resources (Pavelic et al. 2011). Some examples of infiltration systems are Rapid Infiltration Basin Systems (RIBS), Slow Sand Filtration Systems (SSFS), and Soil-Aquifer Treatment (SAT), among others.

Biofilms colonizing subsurface sediments offer the potential for biotransformation of organic compounds, thereby providing an in situ method for treating contaminated groundwater supplies (Cunningham et al. 1991), also relevant for emerging compounds degradation (Rodríguez-Escales and Sanchez-Vila 2016). Processing by extracellular enzymes is the primary mechanism for the microbial degradation of polymeric and macromolecular organic matter into low-molecular-weight molecules which can then cross bacterial cell membranes, becoming available for bacterial growth and nutrient cycles (Romaní et al. 2012). Extracellular enzyme activities (EEAs) are good proxies to determine nutrient demands and decomposition capabilities of microorganisms, as well as to characterize the quantity and quality of available dissolved organic carbon and nutrients in the environment (Romaní et al. 2012).

Heterotrophic bacteria assimilate dissolved organic carbon (DOC) and concomitantly release substantial amounts of carbon in the form of extracellular polymeric substances (EPS) (Sutherland 1985). EPS traps and stores particulates and nutrients for cell metabolism and is generally thought to comprise the major component of bacterial biofilms (Rinck-Pfeiffer et al. 2000). It can also affect the physical characteristics of porous medium through the reduction of available pore spaces for flow and alteration of water retention (Okubo and Matsumoto 1979; Or et al. 2007b), significantly reducing hydraulic conductivity and enhancing dispersion of solutes (Rodríguez-Escales et al. 2016). Microbial processes and biomass accrual in subsurface sediments are determined by the surrounding physical and chemical conditions. The link between physicochemical and biological parameters is complex (Battin and Sengschmitt 1999; Rubol et al. 2014) but the consideration of the interactions of soil microorganisms with their physical and chemical environments is crucial for substantially advance in our understanding of microbial ecology (Rubol et al. 2014; Or et al. 2007a; Wang et al. 2011).

Spatial heterogeneity of particle grain sizes distribution determines the specific physical and chemical conditions in subsurface sediments. Sediment grain size and distribution are key parameters determining interstitial fluxes, which also modulate the distribution of electron donors and acceptors and, consequently, the distribution of microbial processes in subsurface sediments (Malard et al. 2002). Related to this, Higashino (2013) proposed a model where grain diameter plays an important role in determining both hydraulic conductivity and microbial oxygen uptake rate. Low hydraulic conductivity resulted in small dissolved oxygen transfer but large microbial oxygen uptake rate. In coarse sands they stated that even dissolved oxygen transfer rate can be large owing to a large hydraulic conductivity, microbial oxygen uptake rate is small since available surface area for colonization by biofilms is reduced. On the other hand, Essandoh et al. (2013) concluded that the type of soil affects the performance of soil columns; specifically they stated that low hydraulic conductivity results in low microbial growth and low DOC removal. Similarly, Dodds et al. (1996) stated that microbial activity may be greatest with the largest particle size because of increased water exchange through pores, and smallest particle size would promote denitrification.

As the influence of substratum type or grain size on biogeochemical processes and biofilm accumulation is not clear and it remains poorly understood, further investigation is needed to

focus on the interaction between physicochemical and biological parameters in different spatial grain size distributions (GSD). The present work addresses the link between physicochemical and microbial processes in subsurface sediments using laboratory-scale infiltration columns of different sediment GSDs.

The objectives are (1) to understand the influence of subsurface sediment heterogeneity on physicochemical water parameters and on biofilm biomass and activity; as well as (2) to study the relationship between these parameters and how they influence biogeochemical processes occurring in infiltration systems. For this purpose we designed five column setups (mimicking potential sand filter treatments) with different distribution of fine and coarse sands.

We expected that coarse sediment would display higher infiltration rates, which would transfer higher quantity of dissolved oxygen (DO), nutrients, and organic matter during the infiltration process. This will promote biofilm activity and biomass in deeper areas in columns having coarse sands. On the other hand, low hydraulic conductivity in fine sands would promote anaerobic zones potential to denitrification processes, but biofilm activity and biomass in depth will be limited due to reduced transport of nutrients and organic matter in depth. Also we expect high phosphorus retention in fine sediments compared to coarse ones. Mixture of coarse and fine sand would enable the coexistence of slow and rapid zones which would promote aerobic and anaerobic processes at the same layers, as well as enhancing biogeochemical processes and biomass development which could be responsible of stronger bioclogging. Bilayer columns of coarse sediment in the upper layer and fine sediment in the bottom would take advantage of high transfer of DO, nutrients and organic matter in the coarse layer, as well as anaerobic conditions and phosphorus retention in the fine sand.

4.3 Materials and Methods

4.3.1 Experimental design and sampling

The experiment consisted in flow-through columns filled with sediments of different grain sizes. Two grain sizes were used: coarse sand (0.9 – 1.2 mm) and fine sand (0.075 – 0.250 mm), placed in columns 50 cm long and 4.6 cm diameter with different spatial distribution of fine and coarse sands. Five treatments were created (three replicates per treatment for a total of 15 columns) (Fig. 1). Each column was filled with sediment to a height of 40 cm. A layer of 10 cm of water was left above the sediment surface.

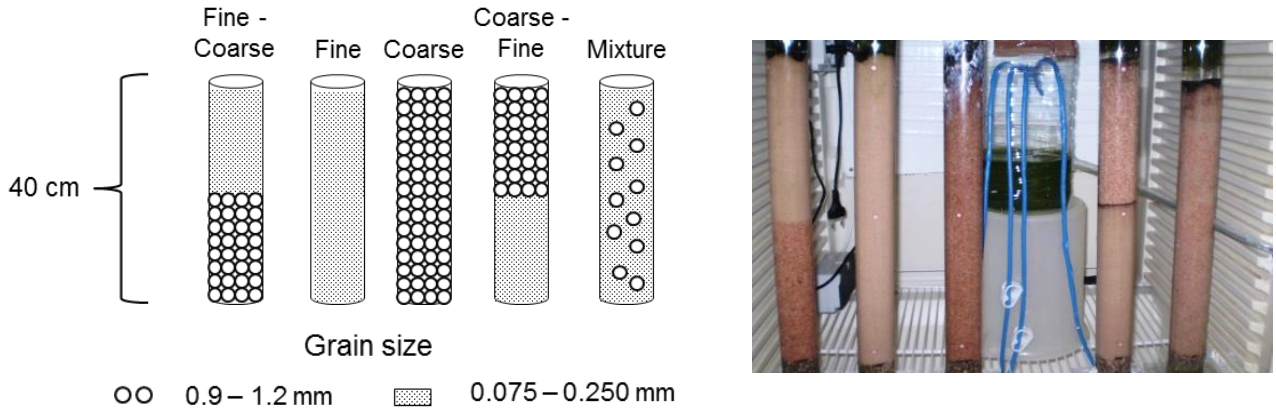

Figure 1 Scheme and photograph of the sediment grain size distributions used in the experiment

Infiltration was performed with synthetic water (13 mg·L^{-1} Na_2SO_4, 16.1 mg·L^{-1} Na_2SiO_3, 29.4 mg·L^{-1} $CaCl_2·H_2O$, 0.6 mg·L^{-1} KCl, 3 mg·L^{-1} $MgSO_4·7H_2O$, 26.5 mg·L^{-1} Na_2CO_3, 0.6 mg·L^{-1} $NH_4H_2PO_4$, 7.3 mg·L^{-1} $(NH_4)(NO_3)$ and 4.27 mg·L^{-1} of humic acids in Milli-Q water) reproducing the chemical signature of a well characterized pristine river (Fuirosos stream, Spain, Ylla et al. 2012). Nutrient and organic matter concentrations were slightly enhanced to facilitate biofilm colonization of the sediment. An inlet water tank (50 L) was placed on top of each group of five columns to produce a flow-through system (Fig. 2). Water tanks were refilled when necessary to ensure continuous infiltration. The experiment was performed at a constant temperature (20 ºC) with a 12:12h light/dark cycle (incident light was 130 – 150 µmol photons·m^{-2}·s^{-1}). The portion of the columns filled with sand was kept in the dark to mimic subsurface conditions by wrapping them with opaque material. Light conditions were allowed in the surface sediment as in real infiltration sand basins. At the start of the experiment, a bacterial inoculum

extracted from natural sediment (from Fuirosos stream) was added to all the columns (700 mL, $1.27 \cdot 10^7$ cel·ml^{-1}).

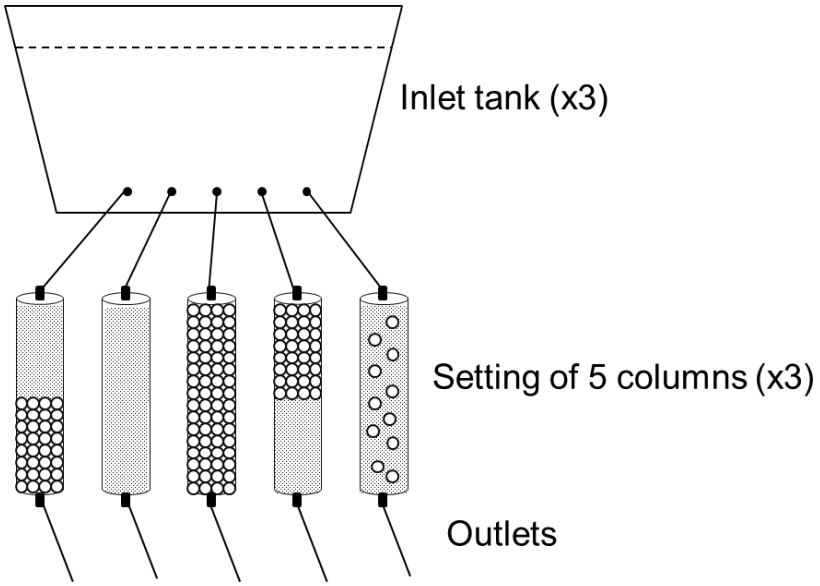

Figure 2 Scheme of the experimental design used in the laboratory-scale column experiment

During the 33 days of the experiment, physical and chemical water characteristics (pH, DO, conductivity and temperature) were measured twice per week with specific probes (HQd Field Case, HACH) in the inlet tanks to ensure homogeneous conditions during all the experiment. Water samples from the inlet tanks and the outlet of each column were taken on days 15, 20, 30 and 33 to measure dissolved nutrients (NO_3^-, NO_2^-, NH_4^+, PO_4^{-3}) and dissolved organic carbon (DOC), as well as several dissolved organic matter (DOM) quality parameters. BDOC was measured once, on day 30. DO in the interstitial water at three different depths were measured weekly with a non-invasive method using an optical fibre (PreSens) (Table 1). Hydraulic conductivity along the columns was measured weekly through the hydraulic head difference between the water in the inlet tank and the outlet of the columns as the system was water saturated (*see 3.2 Hydraulic parameters page 21, and 3.3 Water parameters page 21 in General Methods section for analysis details*).

Table 1 Sampling design description: measured parameters and sampling periodicity

	Parameters	Periodicity
Inlet tank	❖ Physicochemical water parameters (pH, DO, conductivity and temperature)	Twice per week (n = 9 x 3)
Inlet tank and outlets	❖ Dissolved nutrients, DOC, DOM quality and DO	Days 15, 20, 30 and 33 (n = 4 x 3)
Outlets	❖ BDOC	Day 30 (n = 1 x 3)
From the inlet tank to the outlet	❖ Hydraulic conductivity	Weekly (n = 5 x 3)
Column depths: 2, 20 and 38 cm	❖ Interstitial DO	Weekly (n = 5 x 3)
Sediment layers: 0-2, 18-22, 36-38 cm	❖ Bacterial density and viability, chl-a, EPS, EEAs, functional diversity	End of the experiment (n = 1 x 3)

All measurements were performed during the light cycle and at the same time (6 h after the start of the light conditions) to reduce variability between measurements due to day/night cycles. At the end of the experiment, columns were dismantled for sediment biofilm biomass and activity measurements at three different depths (0 – 2 cm, 18 – 22 cm, 36 – 38 cm). Sediment samples were analysed for bacterial density and viability, chlorophyll-a content, EPS, EEAs and functional diversity (*see 3.4 Sediment parameters page 24 in General Methods section for analysis details*). Each layer of sediment was sampled totally and homogenized. Subsamples of 1 cm^3 of sediment were then collected using an uncapped syringe.

4.3.2 Data analysis

Normalized hydraulic conductivity (K/K_0, K being actual hydraulic conductivity and K_0 the initial one at each column) was calculated as a function of time and analysed with ANCOVA analysis. Oxygen balance was calculated from the differences between column outlets and inlets. To study the relationship between oxygen balance and normalized hydraulic conductivity, Pearson's correlation was performed. Nutrient and DOC balances were calculated from the differences between column outlets and inlet tanks and process rates were calculated dividing nutrient balances by advection times. Differences in these parameters were analysed with two factors ANOVA (factor: day and treatment). Differences in DOM properties were also analysed with ANOVA (factor: day and treatment). For better understanding the relationship between physic-

chemical parameters and biological processes occurring in the columns, values of hydraulic conductivity measured the last day of the experiment were analysed through ANOVA (factor: treatment). Biological data from sediment samples and DO from the last sampling day were analysed by a two-way ANOVA (factor: treatment and depth). Whenever significant differences were detected, further Tukey's post-hoc tests were performed. Differences between treatments at each depth were further analysed. To integrate physic-chemical and biological data along the column, a redundancy analysis (RDA) was performed using one matrix with biofilm biomass and activity values, fitted with another matrix containing physic-chemical parameters (nutrient and DO balances, DOM properties and absolute K values) measured the last day of the experiment in each treatment. Since biofilm biomass and activity was measured at three different depths, data was integrated by depth layers to obtain one number per parameter and treatment. Complementarily, ANOSIM analysis was performed to detect differences between treatments. Further, Pearson's correlation was performed. All statistical analyses were carried out with R statistics (vegan package) excepting ANOSIM analysis which was performed using PRIMER v.6 Software. For multivariate analysis, variables were previously scaled using the scale command in R. For ANOVA analysis all variables were logarithmically transformed to bring the variables close to the normal distribution (Shapiro-Wilk normality test). In all the parameters three replicates were used. Table 2 summarizes the statistical analysis of the data.

Table 2 Data analysis description

Parameter	**Analysis**	**Factor**	**Other**
K/K_0 x days	ANCOVA	Factor: treat	Linear adjustment
K/K_0 vs O_2 balance	ANCOVA	Factor: treat	Pearson Correlation
Nutrient balance x days	ANCOVA	Factor: treat	
DOC balance x days	ANCOVA	Factor: treat	
DOM properties x days	ANCOVA	Factor: treat	
Only data from the last day of the experiment:			
Hydraulic conductivity	ANOVA	Factor: treat, depth, treat*depth	Tukey's post-hoc
DO	ANOVA	Factor: treat, depth, treat*depth	Tukey's post-hoc
Biofilm biomass and activity	ANOVA	Factor: treat, depth, treat*depth	Tukey's post-hoc
Integrating physicochemical and biological variables	RDA + ANOSIM	Factor: treat	Pearson Correlation

4.4 Results

4.4.1 Physicochemical parameters

Physicochemical conditions measured at the inlet tanks remained stable throughout the experiment: DO = 8.51 ± 0.26 mg $O_2 \cdot L^{-1}$; pH = 7.7 ± 0.9; conductivity = 131.4 ± 18.65 $\mu S \cdot cm^{-1}$ and temperature = 19.5 ± 0.7 ºC for a total of n = 27 (9 sampling days x 3 inlet tanks).

Flow measured at the start of the experiment was 4.49 $mL \cdot s^{-1}$ in Coarse treatment; 0.65 $mL \cdot s^{-1}$ and 0.36 $mL \cdot s^{-1}$ in Fine-coarse and Fine treatments, respectively; 0.71 $mL \cdot s^{-1}$ in Coarse-fine treatment and 0.34 $mL \cdot s^{-1}$ in Mixture treatment. K_0 values were 8.23 $m \cdot day^{-1}$ in Coarse; 1.22 $m \cdot day^{-1}$ in Fine-coarse; 0.62 $m \cdot day^{-1}$ in Fine; 1.28 $m \cdot day^{-1}$ in Coarse-fine and 0.63 $m \cdot day^{-1}$ in Mixture treatments, respectively (Table 3).

Table 3 Flow and hydraulic conductivity measured at the start of the experiment

Treatment	Initial flow ($mL \cdot s^{-1}$)	K_0 ($m \cdot day^{-1}$)
Coarse	4.49 ± 0.21	8.23 ± 0.31
Fine-coarse	0.65 ± 0.16	1.07 ± 0.27
Fine	0.36 ± 0.17	0.62 ± 0.31
Coarse-fine	0.71 ± 0.04	1.28 ± 0.07
Mixture	0.34 ± 0.21	0.63 ± 0.28

Values are the mean of the replicates (n=3) ± sd.

Hydraulic conductivity displayed a clear decreasing trend with time (Fig. 3). ANCOVA analysis did not show significant differences in normalized K values between treatments although results showed that in the Coarse and Coarse-fine columns K reduction started later as compared to the other treatments which showed a sharp reduction in the first days. All columns showed a negative oxygen balance indicating consumption of oxygen from the column inlet to the outlet. Oxygen consumption increased along the experiment reaching values of -6 mg $O_2 \cdot L^{-1}$ at the end of the experiment. Oxygen consumption was correlated with reduction of hydraulic conductivity (Fig. 4) however at the start of the experiment slightly positive oxygen balance values were reported possibly due to still high instability of the system.

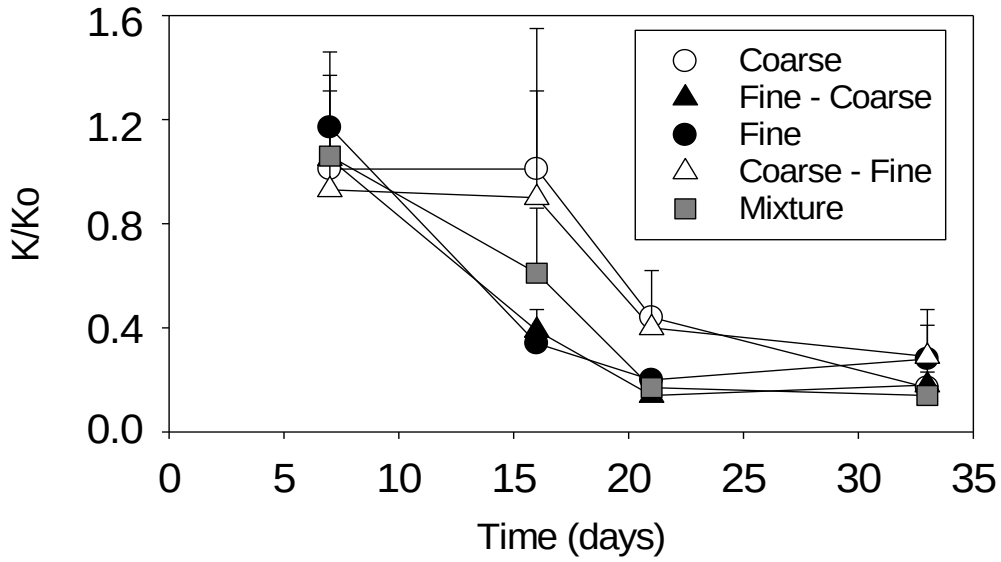

Figure 3 Temporal variation of normalized hydraulic conductivity for each individual treatment (n=12).

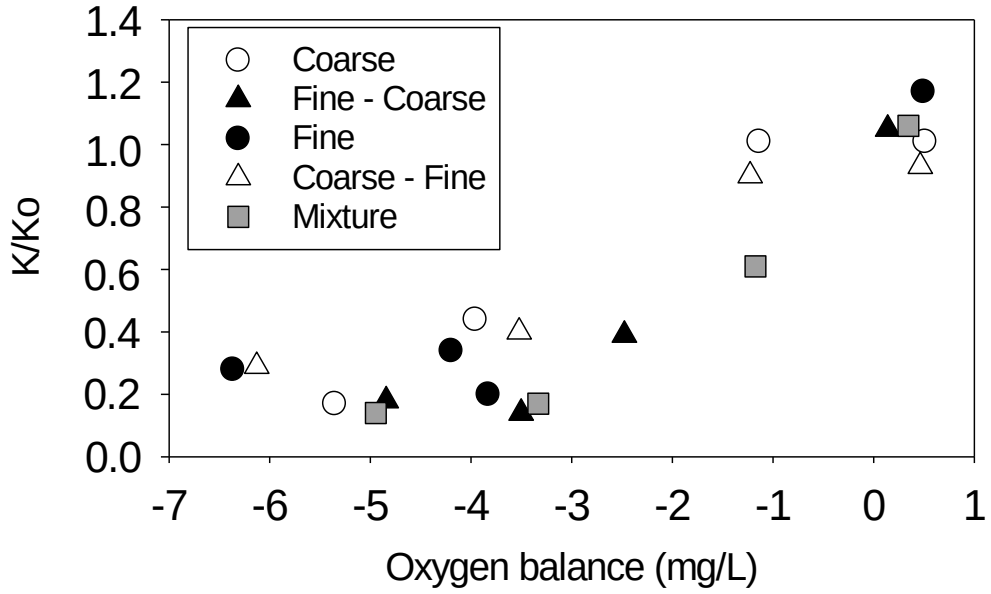

Figure 4 Relationship between oxygen balance and normalized hydraulic conductivity (n=12). Both parameters were positively correlated (Pearson, $r = 0.898$, $p < 0.001$).

On the last day of the experiment, the highest K values were measured in treatments displaying coarse sand at the upper layers (Coarse and Coarse-fine treatments, Table 4). Absolute DO values showed a significant decrease in depth ($p < 0.01$, Table 4). The minimum value reported for DO was 2 $mg \cdot L^{-1}$. No significant differences in DO were detected between treatments at any given depth but slight higher DO concentration was reported at the surface sediment layer especially in Fine-coarse, Fine and Mixture treatment (Table 4). Coarse and Coarse-fine treatments resulted in high DO consumption rate (Table 5). Coarse treatment showed also the shortest advection time

meaning that water passed faster through the sediment. On the other hand, Fine-coarse and Fine treatments showed the longest advection times indicating more time for water to pass through the sediment (Table 5).

Table 4 Hydraulic conductivity and dissolved oxygen measured the last day of the experiment

	K ($m \cdot day^{-1}$)	**O_2 surface ($mg \cdot L^{-1}$)**	**O_2 – 20 cm ($mg \cdot L^{-1}$)**	**O_2 – 40 cm ($mg \cdot L^{-1}$)**
Coarse	**0.31^{b}** ± *0.11*	5.46 ± *0.78*	3.86 ± *0.13*	2.92 ± *0.44*
Fine – coarse	0.10^{a} ± *0.06*	7.75 ± *2.90*	5.43 ± *4.10*	3.44 ± *2.27*
Fine	0.13^{a} ± *0.05*	8.22 ± *3.68*	3.47 ± *0.71*	1.91 ± *0.73*
Coarse – fine	0.19^{ab} ± *0.11*	5.84 ± *0.85*	2.98 ± *0.35*	2.15 ± *0.74*
Mixture	0.11^{a} ± *0.03*	8.66 ± *0.19*	4.86 ± *1.29*	3.33 ± *0.85*

Values are the mean of the replicates (n=3) ± sd. Letters next to the means indicate significant different groups after Tukey's post-hoc analysis ($p < 0.05$).

Table 5 Advection time and process rates for ammonium, nitrates and nitrites (NO_x), phosphate and dissolved oxygen (DO) along the infiltration columns

	Advection time (seconds)	**N-NH_4^+ (µg $N \cdot L^{-1} \cdot s^{-1}$)**	**N-NO_x (µg $N \cdot L^{-1} \cdot s^{-1}$)**	**P-PO_4^{-3} (µg $P \cdot L^{-1} \cdot s^{-1}$)**	**DO (µg $O_2 \cdot L^{-1} \cdot s^{-1}$)**
Day	**p < 0.001**	**p < 0.001**	**p < 0.001**	**p < 0.001**	**p < 0.001**
Treat	**p < 0.001**	**p < 0.001**	**p < 0.001**	**p < 0.001**	**p < 0.001**
Treat*day	Ns	**p < 0.001**	**p < 0.001**	**p < 0.001**	**p < 0.01**
Coarse	736^{a} ± *700*	-1.70^{b} ± *1.17*	2.14^{b} ± *1.61*	0.001^{a} ± *0.04*	-5.05^{c} ± *1.61*
Fine-coarse	3890^{c} ± *2313*	-0.36^{a} ± *0.10*	0.22^{a} ± *0.29*	-0.018^{b} ± *0.02*	-0.82^{a} ± *0.83*
Fine	2500^{bc} ± *1482*	-0.52^{a} ± *0.23*	0.38^{a} ± *0.29*	-0.023^{b} ± *0.03*	-1.53^{ab} ± *1.50*
Coarse-fine	1577^{ab} ± *1160*	-0.75^{a} ± *0.43*	0.63^{a} ± *0.73*	-0.014^{b} ± *0.01*	-2.03^{b} ± *2.00*
Mixture	2029^{ab} ± *1231*	-0.49^{a} ± *0.15*	0.49^{a} ± *0.19*	-0.012^{b} ± *0.01*	-1.01^{ab} ± *1.20*

Values are the mean of the four sampling days (n = 12) ± sd. Positive process rates indicate production while negative process rates mean removal/consumption. Letters next to the means indicate significant differences between treatments (treat) after Tukey's post-hoc analysis.

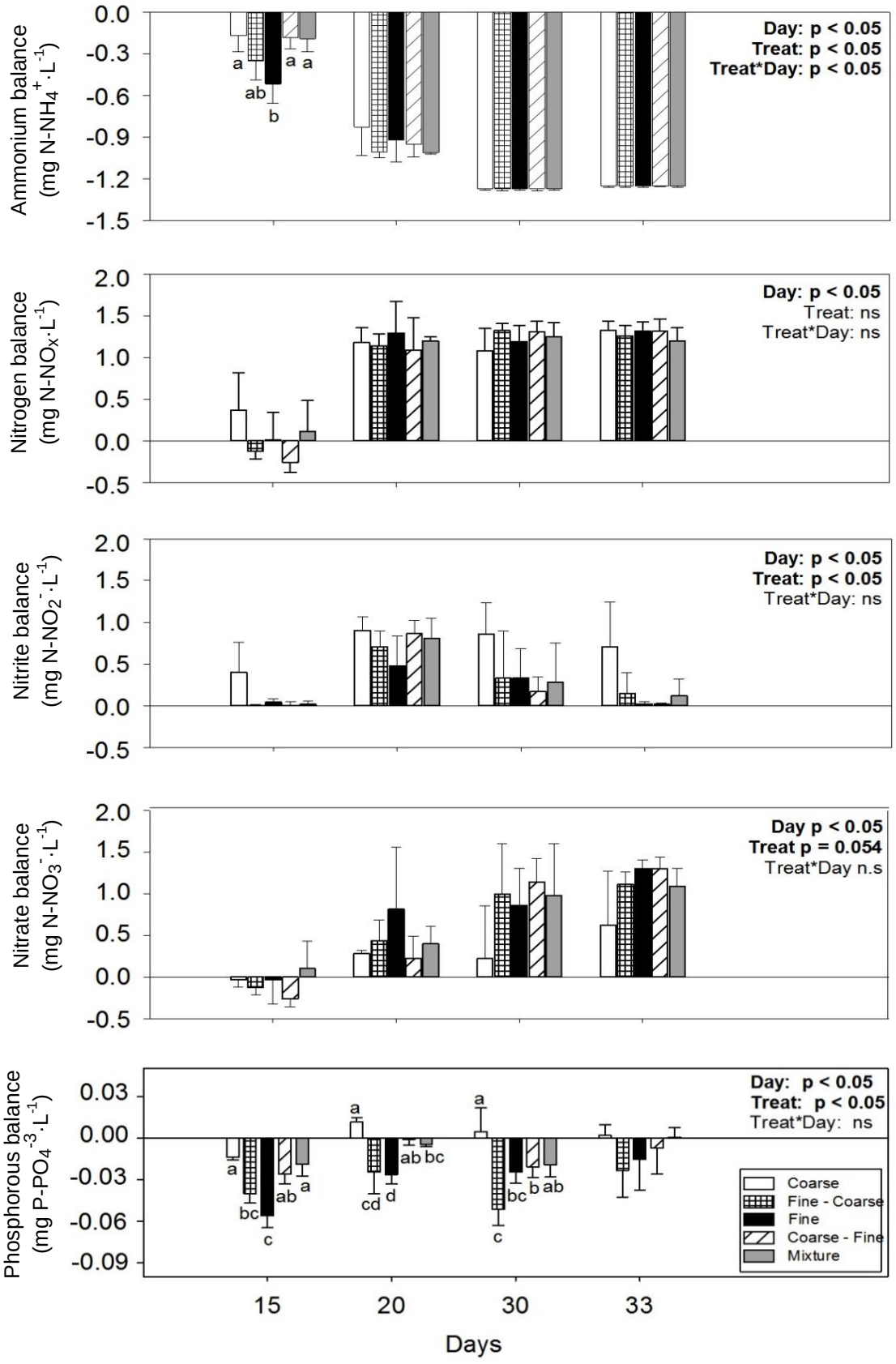

Figure 5 Temporal variation of nutrient balances (outlet minus inlet): (a) ammonium; (b) nitrate and nitrite ($N\text{-}NO_x$); (c) nitrite; (d) nitrate and (e) phosphate. Letters on the bars determine significant differences between treatments (treat) on each day after Tukey's post-hoc analysis ($p < 0.05$).

After 30 days from the start of the experiment all the ammonium supplied at the inlet (1.26 mg N-$NH_4^+ \cdot L^{-1}$) was eventually fully transformed in all treatments (Fig. 5). However, Coarse treatment was showing the highest ammonium consumption rate (Table 5). N-NO_x balance showed mainly positive values indicating nitrate/nitrite production. No significant differences were detected between treatments in N-NO_x balances but when analyzing N-NO_x production rates Coarse treatment resulted in the highest values (Table 5). Phosphorus was mainly retained through all sediment columns and the highest retention was measured for Fine-coarse and Fine treatments (Fig. 5). Mean DOC at the inlet was 1.39 ± 0.38 $mg \cdot L^{-1}$, at the outlet was 1.44 ± 0.28 $mg \cdot L^{-1}$, this results in a very small balance and no differences between treatments were detected. Even though no differences were detected in DOC concentrations differences in DOM properties were reported (Table 6): the Coarse treatment showed the lowest SR and BIX values, while the Coarse-fine one reported the highest BIX values. E_2/E_3 values were highest for the Fine-coarse treatment. The highest BDOC value was observed in the Coarse-fine treatment and the lowest one corresponded to the Fine one.

Table 6 DOM properties measured in each treatment during the experiment

	E_2/E_3	**SR**	**FI**	**BIX**	**BDOC* ($mg \cdot L^{-1}$)**
Day	ns	**p < 0.001**	ns	**p < 0.05**	
Treat	**p < 0.01**	**p < 0.01**	ns	**p < 0.05**	**p < 0.1**
Treat*day	**p < 0.001**	**p < 0.001**	ns	**p < 0.001**	
Coarse	$3.59^{\mathbf{bc}}$ ± *0.8*	$0.57^{\mathbf{a}}$ ± *0.17*	1.56 ± *0.08*	$0.66^{\mathbf{a}}$ ± *0.29*	0.82^{a} ± *0.30*
Fine – Coarse	$3.85^{\mathbf{c}}$ ± *0.4*	$0.74^{\mathbf{b}}$ ± *0.23*	1.60 ± *0.11*	$0.70^{\mathbf{ab}}$ ± *0.51*	0.90^{a} ± *0.35*
Fine	$3.28^{\mathbf{ab}}$ ± *0.5*	$0.87^{\mathbf{b}}$ ± *0.21*	1.56 ± *0.08*	$0.85^{\mathbf{ab}}$ ± *0.31*	0.50^{a} ± *0.33*
Coarse – Fine	$3.40^{\mathbf{ab}}$ ± *0.4*	$0.77^{\mathbf{b}}$ ± *0.21*	1.54 ± *0.11*	$1.00^{\mathbf{b}}$ ± *0.45*	1.32^{b} ± *0.95*
Mixture	$3.01^{\mathbf{a}}$ ± *0.4*	$0.80^{\mathbf{b}}$ ± *0.20*	1.58 ± *0.14*	$0.86^{\mathbf{ab}}$ ± *0.29*	0.63^{a} ± *0.18*

Values are the mean of the four sampling days (n=12) ± sd. Letters next to the means indicate significant differences between treatments (treat) after Tukey's post-hoc analysis. (*BDOC was measured only on day 30 by triplicate).

4.4.2 Sediment biofilm biomass and activity

Bacterial density, chl-a and EPS content in sediments showed a strong vertical gradient in depth with highest values at the surface declining sharply in the top 20 cm (Fig. 6). This pattern in depth was different depending on the treatment. Bacterial density at the surface was not

significantly different between treatments, but a 20 cm depth, the highest values were measured at the Coarse-fine treatment and at 40 cm the highest values were measured at the Coarse treatment. The highest chl-a concentration at the surface was measured at the Fine-coarse and Fine treatments, and at 20 cm depth highest values were found in the Coarse-fine treatment. Mixture treatment showed the lowest EPS concentrations at 20 and 40 cm depth.

LD ratio was below 1 for all treatments and increased in depth except in the Coarse treatment (Fig. 7). Functional diversity decreased in depth (Fig. 7); the lowest value was detected in the Coarse column at 20 and 40 cm depth, and the highest was reported in the Fine-coarse column at 20 cm. Analysing the functional fingerprint, no significant differences were detected between treatments, but that at the surface was different from the ones observed at 20 and 40 cm depth (ANOSIM, r = 0.567, p = 0.0001).

Extracellular enzymatic activities showed a gradient in depth (Table 7). The Coarse-fine treatment showed higher β-glucosidase and β-xylosidase activities in the surface compared to the other treatments. This treatment also showed higher β-xylosidase and phosphatase activities at 20 cm depth. The Coarse treatment showed higher β-glucosidase and leucine-aminopeptidase activities at 40 cm depth.

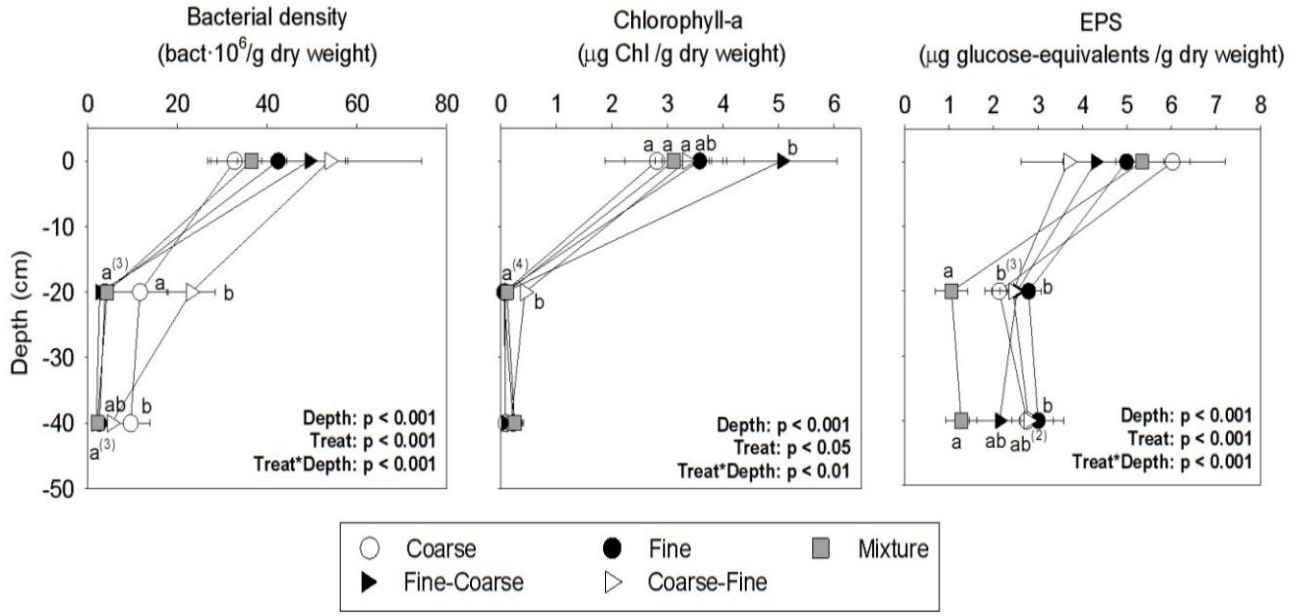

Figure 6 Absolute values of biofilm biomass (bacterial density; chlorophyll-a content and EPS content) measured in sediment at different depths at the end of the experiment. Letters indicate significant differences between treatments (treat) on each depth after Tukey's post-hoc analysis. Superscripts indicate the number of treatments in the same group.

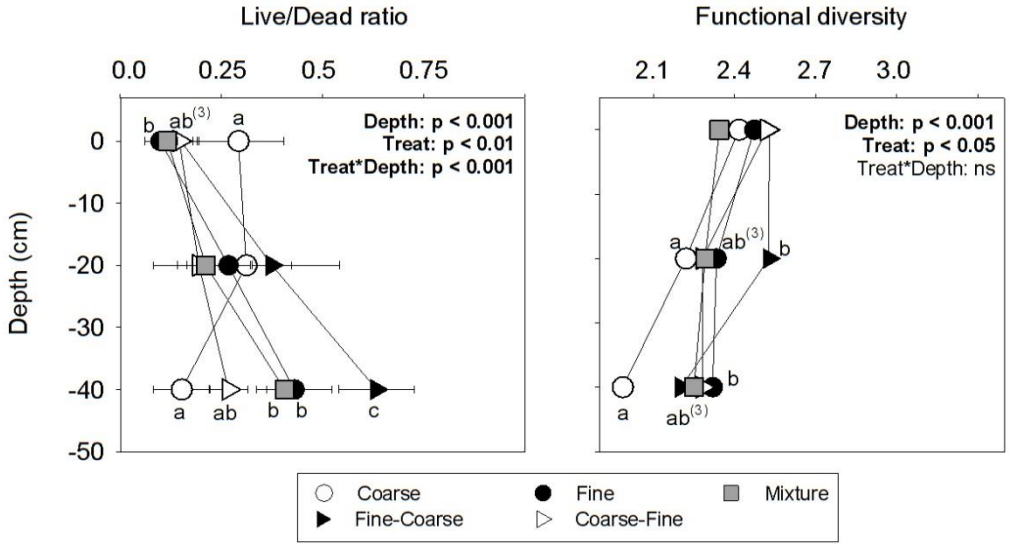

Figure 7 LD ratio values and functional diversity measured as Shannon diversity. Letters indicate significant differences between treatments (Treat) on each depth after Tukey's post-hoc analysis. Superscripts indicate the number of treatments in the same group.

Table 7 Enzymatic activities measured at different depths in each treatment

	Depth (cm)	Coarse	Fine – coarse	Fine	Coarse - fine	Mixture
β-glu						
Depth: p < 0.001	0	3.9^{ab} ± *0.3*	2.30^{a} ± *0.9*	2.39^{a} ± *0.1*	**7.39**^{b} ± *1.5*	3.9^{ab} ± *0.0*
Treat: p < 0.001	20	1.32 ± *0.6*	0.32 ± *0.4*	0.71 ± *0.7*	2.30 ± *1.7*	0.84 ± *0.8*
Treat*depth: ns	40	**1.08**^{b} ± *0.6*	0.15^{a} ± *0.1*	0.48^{a} ± *0.3*	0.42^{a} ± *0.0*	0.38^{a} ± *0.1*
β-xyl						
Depth: p < 0.001	0	1.1^{ab} ± *0.4*	0.61^{a} ± *0.5*	1.1^{ab} ± *0.4*	**1.2**^{b} ± *0.4*	0.66^{a} ± *0.2*
Treat: p < 0.001	20	0.2^{ab} ± *0.1*	0.01^{a} ± *0.0*	0.06^{a} ± *0.1*	**0.90**^{b} ± *0.7*	0.07^{a} ± *0.1*
Treat*depth: ns	40	0.10 ± *0.1*	0.00 ± *0.0*	0.02 ± *0.0*	0.18 ± *0.3*	0.00 ± *0.0*
Phos						
Depth: p < 0.001	0	6.20 ± *0.3*	12.31 ± *3.7*	8.69 ± *2.9*	9.56 ± *1.0*	9.88 ± *2.9*
Treat: p < 0.05	20	3.36^{a} ± *0.6*	2.24^{a} ± *0.3*	3.38^{a} ± *2.4*	**6.06**^{b} ± *1.6*	2.81^{a} ± *0.6*
Treat*depth: ns	40	2.3^{ab} ± *0.7*	1.14^{a} ± *0.3*	2.4^{ab} ± *0.8*	**3.86**^{b} ± *0.9*	2.0^{ab} ± *0.6*
Leu						
Depth: p < 0.001	0	4.10 ± *0.6*	5.84 ± *2.9*	6.40 ± *3.1*	7.43 ± *0.8*	2.58 ± *0.7*
Treat: p < 0.05	20	**4.9**^{b} ± *0.8*	1.96^{a} ± *1.1*	2.5^{ab} ± *1.1*	4.0^{ab} ± *0.9*	3.3^{ab} ± *0.8*
Treat*depth: p < 0.1	40	**4.42**^{b} ± *0.6*	1.18^{a} ± *0.4*	1.73^{a} ± *1.0*	3.4^{ab} ± *1.8*	1.59^{a} ± *1.0*

Values are the mean of the replicates (n=3) ± sd, expressed as nmolMUF·g DW^{-1}·h^{-1} for β-glucosidase (β-glu), β-xylosidase (β-xyl) and phosphatase (Phos); and nmolAMC·g dry $weight^{-1}$·h^{-1} for leucine-aminopeptidase (Leu). Letters next to the means indicate significant differences between treatments (Treat) after Tukey's post-hoc analysis comparing treatments at each depth. Values in bold indicate the highest activity measured at each depth.

4.4.3 Integrating physicochemical and biological responses

Integrating values for each individual column and performing an RDA analysis, data corresponding to biofilm activity, biomass and functional diversity was fitted with the environmental variables (nutrient balances, hydraulic conductivity and DOC properties measured the last day of the experiment) to study the conjunction between biofilm and physical properties (Fig. 8). Treatments displaying coarse sand in the first 20 cm (Coarse and Coarse-fine) are placed on the left of the graph; showing the lowest E_2/E_3 values and the highest β-glu, β-xyl and Leu extracellular enzyme activities. However, differences between the Coarse-fine and the Coarse treatments do exist. The former resulted in higher phosphatase activity, bacterial density, BDOC, BIX, FI, and SR. On the other hand, the coarse treatment was characterized by highest hydraulic conductivity, lowest phosphorus retention, highest NO_x production, and low LD ratio as well as low functional diversity.

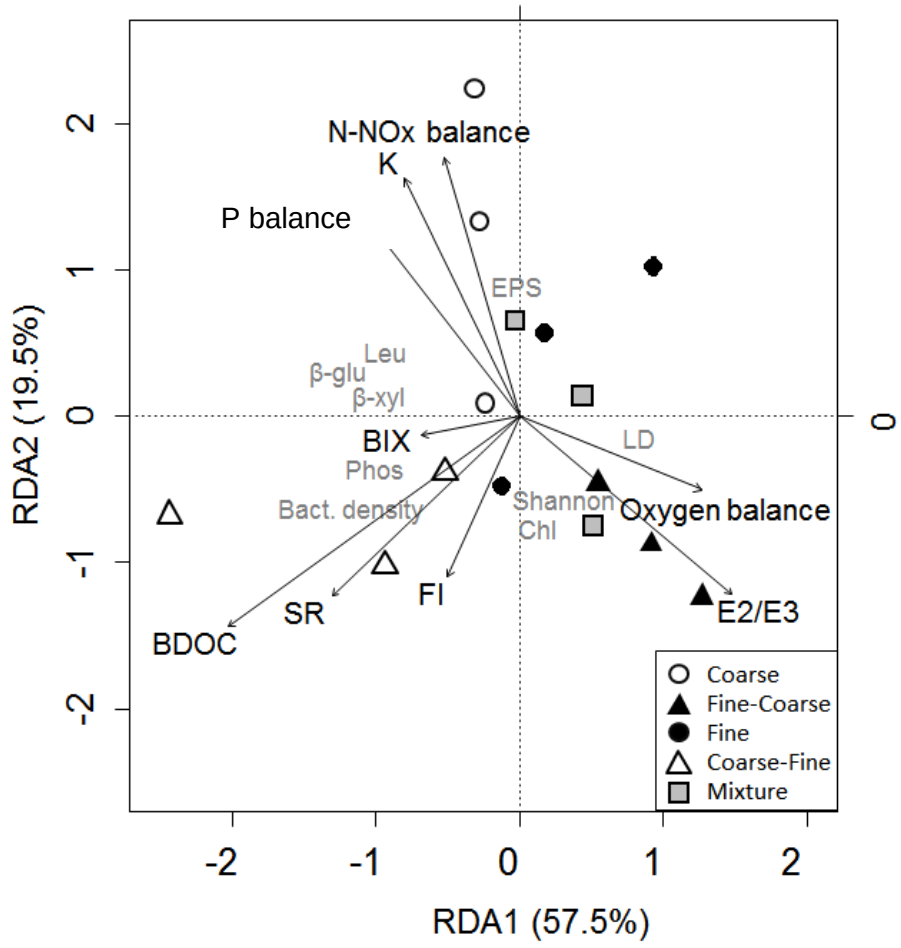

Figure 8 RDA analysis with data from sediment biofilm fitted with physicochemical data from the last day of the experiment. ANOSIM analysis detect differences between treatments (ANOSIM r = 0.604, p = 0.001).

On the right part of the same graph (Fig. 8) we can find the treatments with low hydraulic conductivity (Fine, Fine-coarse, Mixture), all involving fine sand in the upper 20 cm and sharing low values of β-glu, β-xyl and Leu activities, and high E_2/E_3 values and oxygen consumption. However, interpretation of E_2/E_3 index should be done cautiously since its values and the tendencies between treatments vary among time. Significant differences were detected between all treatments (ANOSIM, $r = 0.6$, $p = 0.0001$) except for Fine and Mixture treatment which could not be discriminated. Pearson's correlations were performed for the last day of the experiment with biological and physicochemical parameters. Significant correlations ($r > 0.5$, $p < 0.05$) are described as follows: hydraulic conductivity was positively correlated with positive balances of $N\text{-}NO_x$ and phosphorous indicating production of NO_x and no retention of phosphorus. BDOC was positively correlated to bacterial density. EEAs were positively correlated between them and bacterial density was positive correlated to all of them. Shannon Index was positively correlated to chl-a, LD ratio and E_2/E_3 index. Negative balance of DO was positively correlated to transformation of $N\text{-}NH_4^+$.

4.5 Discussion

4.5.1 Effects of sediment heterogeneity on physicochemical parameters

Saturated hydraulic conductivity (K) is the most relevant parameter driving flow and transport in porous media. As expected, hydraulic conductivity was highest in the Coarse treatment, while the presence of fine sediments in the other treatments resulted in lower hydraulic conductivity values. This coincides with Baveye et al. (1998) and Pavelic et al. (2011) who found higher saturated hydraulic conductivity in coarse-textured materials as compared to fine-textured materials. As expected, high hydraulic conductivity results on high transfer of nutrients, organic matter and DO in depth, which allow for high nitrification rates. Reduction in K as a function of time was mostly associated with biological clogging. However, sharp K reduction at the beginning of the experiment in treatments with fine sediment in the upper layer could be related to sediment compaction (Hoffman et al. 1996). In the columns, reduction of hydraulic conductivity was correlated to oxygen consumption. DO is energetically the most favourable electron acceptor and strongly influences the succession of biogeochemical processes within the subsurface (Baker et al. 2000). Specifically, DO is consumed during the mineralization of organic matter and nitrification of ammonium in the oxic zone. However, decrease of oxygen in subsurface sediments could be also related to slow DO supply resulting from the reduction of K and corresponding water fluxes with time (Martienssen and Schöps 1997). Contrarily to what expected, no denitrification was achieved in any treatment due to the fact that DO concentrations were not low enough. As phosphorus reduction is enhanced by the presence of fine sediment, we expect adsorption to be the main process affecting phosphorus decrease. However, it also could be related to high P uptake by autotrophs (Jarvie et al. 2002), as treatments with fine sediment in the upper part of the columns showed high chl-a concentration at the surface and high phosphorus decrease.

Low SR values reported in the Coarse treatment are indicative of low organic matter degradation (SR values are inversely correlated to organic matter molecular weight, Helms et al. 2008). Oppositely, transition from coarse-to-fine sediment could promote biological activity as indicated by high BIX and SR values.

4.5.2 Linking physicochemical parameters to biofilm biomass and activity

In general, biomass and biofilm activity decreased with depth (e.g. Freixa et al. 2016). This is related to oxygen and nutrients being the limiting factor controlling bacterial growth and metabolic activity (Battin and Sengschmitt 1999) and these resources decreasing in depth (Hall et al. 2012; Nogaro et al. 2013). This work show significant interaction between treatment and depth for most biological parameters, indicating that the sediment grain size distribution was affecting differently the activity and biomass patterns in depth.

Sediments displaying high hydraulic conductivity values are expected to lead to fast transport of organic matter into deeper sediments (Rauch-Williams and Drewes 2006) due to high infiltration rates. This could explain high bacterial biomass concentrations at large depths in coarse sediments. However, the low proportion of live bacteria in depth and the high reduction on functional diversity in these sediments coincide with less degraded organic matter. Also high leucine-aminopeptidase activity achieved in coarse sediments could be an indicator of organic material released because of cell lysis (Ricart et al. 2009).

The coarse-to-fine transition promotes the accumulation and transformation of organic matter at the interface. This is suggested by the highest capacity to degrade polysaccharides as demonstrated by high C-acquiring enzyme activities (β-glu and β-xyl activities). The former is related to cellulose degradation, while the latter is promoted by the presence of hemicellulose (Sabater and Romaní 1996). High phosphatase activity in the transition compared to the other treatments could be related to high chl-a content, since algae are also responsible for this activity but may be also linked to low availability of inorganic phosphorus due to its low retention capacity which may enhance bacterial phosphatase activity. High enzymatic activities in Coarse-fine treatment coincide with biogeochemical aspects explained above (high BIX and SR values) implying that the coarse-to-fine transition promotes the transformation of organic matter into biodegradable low-molecular-weight molecules.

In the treatments displaying low hydraulic conductivity, nutrients and organic matter transport to deeper areas are limited, resulting in low microbial activity and biomass in depth. High E_2/E_3 values measured in such treatments on the last day of the experiment could be indicative of the photodegradability and photoreactivity of DOC (Chow et al. 2013; Macdonald and Minor 2013); however this statement should be interpreted cautiously since results of E_2/E_3 index are not

consistent throughout the sampling days. High chl-a concentration measured in these treatments could be favoured by high advection times which resulted in slow flow and increased the contact time between water, sediment and light in the upper part of the columns. This in turn could be responsible of slight higher values of DO in the upper part of these columns due to release of oxygen from photosynthetic activity. However, as advection times were much shorter (between 12 min and 1 hour) than day/night cycles we expect that the pulses in DO due to algal metabolism will be rapidly dislocated through the columns and then having limited effect on biogeochemical processes. Further work will be necessary to clearly understand specific effects of daily primary production pulses and consequent daily variability on the physicochemical parameters in infiltration systems.

The non-homogeneity of sediment grain size, despite the spatial homogeneity (Mixture treatment) contrarily to what expected, did not favour microbial colonization or extracellular enzymatic activity. Furthermore, it resulted in the lowest values of EPS concentration in depth. Since not many differences were accountable between the Fine and Mixture treatments, we could state that the presence of fine grain size sediments would determine the majority of the biogeochemical processes that take place in the subsurface.

To sum up, sediments composed even partially by coarse sands which display high infiltration rates, transfer high quantity of nutrients and organic matter in depth which promote high bacterial density in deeper areas compared to fine sand sediments. Although not seeing differences in oxygen concentration between treatments; nitrification rates and oxygen consumption rates are greater for coarse sediment. Related to this, higher rates of infiltration may be associated with higher potential process rates. However, low water residence times in coarse sediments result in low functional diversity and a decrease in the proportion of live bacteria in depth. On the other hand, the presence of fine sands limits biofilm activity and biomass in depth due to low infiltration which at the same time reduces nutrient load in depth. According to this, biofilm activity, biomass and process rates could be limited by low nutrient loads. On the other hand, phosphorus retention is enhanced by fine sediment. Transition of coarse to fine grain size sediments promote the accumulation of organic matter in the interface, favouring its decomposition to smaller and more biodegradable compounds and creating hot-spots of bacterial activity and biomass.

4.6 Conclusions

The present work concludes that biological and physicochemical parameters are influenced by the grain size and the GSD of the sediment. In relation to our hypothesis, coarse sediment allows for high biomass in depth and high process rates due to high input loads, while fine sediment promotes accumulation of algae in the upper part of the columns and ameliorates phosphorus retention but biomass in subsurface is constrained by low input loads. However, in contrast to our hypothesis mixture of coarse and fine sediment behaves similarly than only fine sediment. Interestingly, bilayer of coarse sediment in the upper part and fine sediment in the bottom promotes high biomass in the interface between the two layers resulting in high microbial organic matter degradation and nutrient recycling and also allows for phosphorus retention mainly thanks to the fine layer. In short it is important to account for the implications of grain size and spatial transitions between sediment layers in subsurface sediments in order to understand and improve biological and physical knowledge about processes occurring either in natural or in artificial infiltration systems. It is important to take into account that implications of sediment heterogeneity on microbial biomass and activity are not fully characterized by the topsoil few cm, but rather influenced by the grain size spatial distribution of at least the top 40 cm.

5 Chapter II:

Bilayer infiltration system combines benefits from both coarse and fine sands promoting nutrient accumulation in sediments and increasing removal rates

5.1 Abstract

Infiltration systems are treatment technologies based on water percolation through a porous medium where combinations of physical, chemical and biological processes take place. Grain size distribution (GSD) acts as a driver of these processes and their rates and influences nutrient accumulation in sediments. Coarse sands inhibit anaerobic reactions such as denitrification and could constrain nutrient accumulation in sediments due to smaller specific surface area. Alternatively, fine sands provide higher nutrient accumulation but need a larger area available to treat the same volume of water; furthermore they are more susceptible to bioclogging. Combining both sand sizes in a bilayer coarse-fine system would allow infiltrating a greater volume of water and the occurrence of aerobic/anaerobic processes. We studied the performance of a bilayer coarse-fine system compared to a monolayer fine one –by triplicate- in an outdoor infiltration experiment to close the C-N-P cycles simultaneously in terms of mass balances. Our results confirm that the bilayer coarse-fine GSD promotes nutrient removal by physical adsorption and biological assimilation in sediments, and further it enhances biogeochemical process rates (2-fold higher than the monolayer system). Overall, the bilayer coarse-fine system allows treating a larger volume of water per surface unit achieving similar removal efficiencies as the fine system.

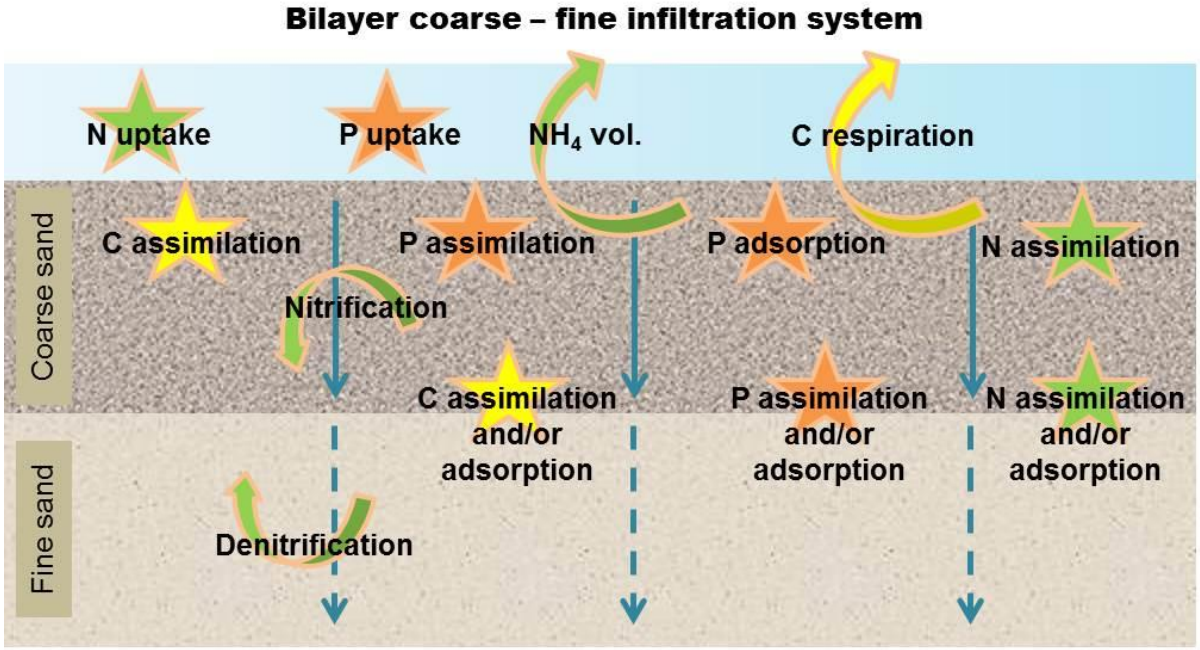

5.2 Introduction

High nutrient loads into freshwater ecosystems worldwide lead to eutrophication, associated harmful algal blooms, and "dead zones" due to hypoxia (Diaz and Rosenberg 2008). In urban areas, the input of nutrients from wastewater treatment plants (WWTPs) into freshwaters might determine eutrophication processes especially in areas characterized by flow intermittency (Martí et al. 2009). However, biogeochemical dynamics are affected by numerous factors which hinder the understanding of physical, chemical and biological dynamics related to the potential nutrient removal of water bodies (Pai et al. 2017). The implementation of infiltration systems in WWTPs before pouring water into streams are considered as a way to decrease nutrient loads inputs to rivers, thus diminishing river eutrophication especially during low flow periods (Fox 2001). Infiltration systems are water treatment technologies that rely on fluid percolation through a porous medium where a combination of biological, chemical and physical processes helps in improving the quality of the influent water during the infiltration path (Dillon et al. 2008).

According to Brix et al. (2001), an important characteristic in infiltration systems is the grain size distribution (GSD) of the porous medium. GSD, mostly linked to the pore size distribution and connectivity, modulates the distribution and transport of terminal electron acceptors, nutrients and organic matter in depth (Boulton et al. 1998; Nogaro et al. 2010), and acts as a driver of the biogeochemical processes and their rates (Baker and Vervier 2004). Also, substrate grain size influences wastewater compounds' adsorption (Ren et al. 2011). On one hand, coarse, well-sorted sediments imply large permeability values that result in high dissolved oxygen (DO) concentrations in depth, promoting aerobic processes such as nitrification (Mueller et al. 2013), but inhibiting anaerobic reactions which are of great importance for the complete total dissolved nitrogen (TDN) removal. Furthermore, coarse sediments enhance high loads of nutrients and organic matter which are associated with high biogeochemical rates but low advection times (Perujo et al. 2017). However, coarse sediments could constrain compounds' adsorption due to smaller specific surface area (Wu et al. 2015). On the other hand, in fine sediments, the low DO supply through infiltration drives anoxic conditions, where bacteria catalyse full denitrification (Dong et al. 2009). It is also known that fine sand has larger specific surface area and high adsorbing capacity (Huang et al. 2013; Meng et al. 2014) but lower permeability which can constrain wastewater treatment (Zhao et al. 2016) since the risk of substrate clogging may

increase (Wu et al. 2015). Considering all this, it is difficult to assess which substrate size is better to use since both grain sizes display benefits and drawbacks. Accordingly, Perujo et al. (2017) carried out an experiment with the aim of deepening in the relationship between physicochemical and biological parameters in different GSDs, and results suggested that a bilayer coarse-fine system may integrate the positive aspects of coarse sands and those of fine sands. Kauppinen et al. 2014 studied the performance of multi-layered sand filters but focusing mainly on pathogens removal and using combinations of 0-8 mm sand, 0-2 mm biotite, and 2-4 mm which showed no different performance between them in terms of nutrients removal. Latrach et al. 2016 used a multisoil-layering system which consisted of a matrix of permeable material (mainly gravel) with soil mixture "boxes" composed of coarse and fine sand, silt, and clay, resulting in a high permeable systems used to treat raw wastewater, but without carrying out a comparison on among system designed with different grain size distributions.

The study of biogeochemical processes in sand filters is relatively complex and several processes are involved in the transformation and removal of carbon, nitrogen and phosphorous compounds (Achak et al. 2009). We are not aware of any work aimed at studying the relevance of a bilayer coarse-fine grain size distribution compared to a monolayer fine sand system to close the C-N-P cycles simultaneously, thus quantifying all the biogeochemical pathways of C, N and P occurring both in the interstitial water and in the sediment surfaces.

The main objective of this research is to compare the performance of a bilayer coarse fine sand system with that of a monolayer fine sand – in triplicate- in an outdoor infiltration experiment and specifically, to study (1) the distribution of biogeochemical processes in the depth profile, (2) the importance of nutrient accumulation in sediments in regards to adsorption and assimilation processes; and (3) the link of biogeochemical process rates to removal efficiencies at each system, in order to decipher whether the bilayer system optimizes the performance of infiltration systems. To achieve these objectives, we move away from qualitative process description, and rely on quantification based on measurements (sampling of interstitial water and sediment and analysis of chemical species in depth from in situ replicated tanks over 104 days) and validated by means of mass balance evaluations in depth as well as the study of C:N:P molar ratios in sediments to further understand nutrient accumulation processes in sediments.

We expected aerobic processes in the upper layer and anaerobic processes in the bottom layer in both systems. We also expected both systems to remove dissolved nutrients through accumulation in sediments but this sediment ability to be linked to the presence of fine sands (which means nutrient accumulation along the vertical profile in the monolayer fine system; and only in the fine sediment layer in the coarse-fine system). Higher process rates are expected in the bilayer system due to higher input loads.

5.3 Materials and Methods

5.3.1 Experimental design and sampling

An outdoor infiltration experiment was performed with secondary treated wastewater (Fig. 1). Two flow-through sand tank systems (3 replicates per system) were created using different GSDs: (1) a bilayer Coarse-fine system (CF) consisting of a 20 cm layer of coarse sand (0.9 – 1.2 mm) placed on top of a 20 cm layer of fine sand (0.075 – 0.250 mm); and (2) a monolayer fine system (F) with 40 cm of fine sand (0.075 – 0.250 mm) (Fig. 2). Sands were purchased from a company dealing (and selling) aggregates (Adicat Tribar, S.L.). They consisted of siliceous sand, rounded shape, free from clays and organic matter and with low metal contents (Al_2O_3 < 0.5% of the sand dry weight, Fe_2O < 0.05%, CaO < 0.05% and K_2O < 0.5%). Both systems consisted of tanks of 0.21 m^3 capacity and 0.46 m^2 of infiltration surface area; in the upper part of each one, a valve was used to ensure a constant water level creating a constant surface water layer. At the bottom of each tank a gravel layer was placed to facilitate drainage of water towards the outlet, to resemble vertical infiltration conditions.

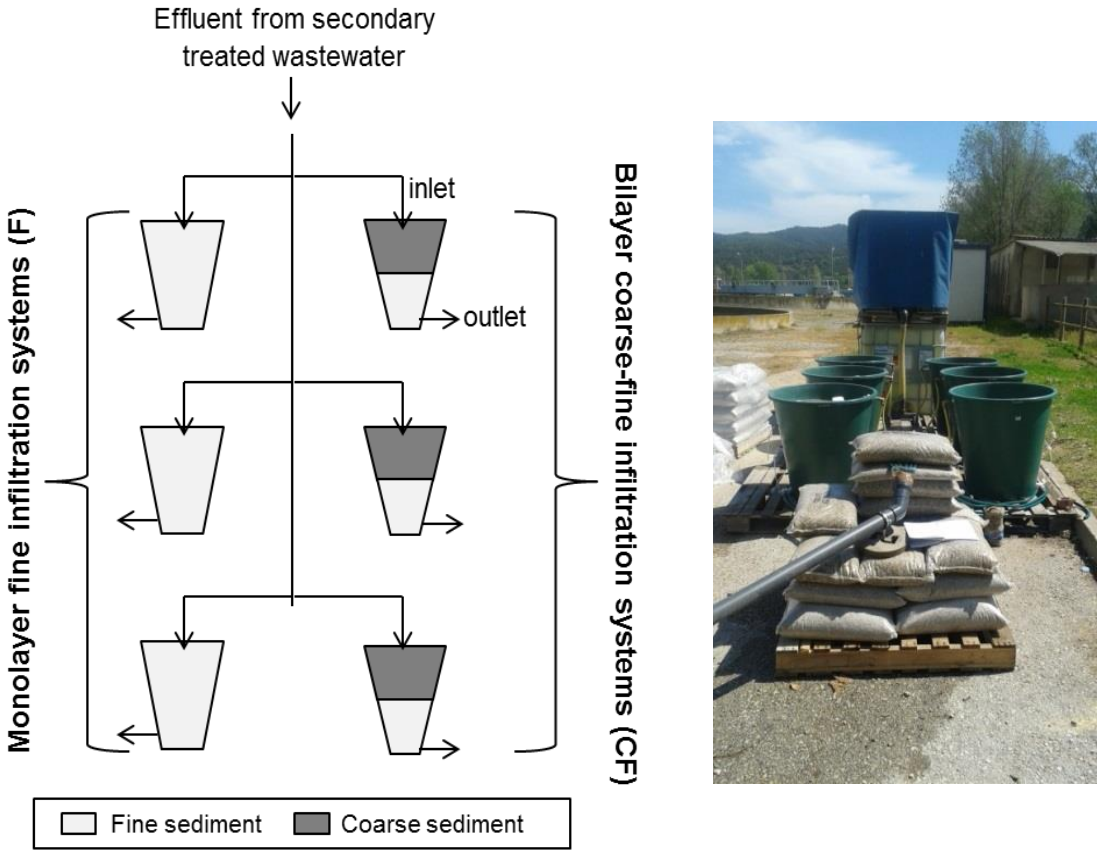

Figure 1 Scheme and photograph of the experimental design

Three water ports were installed in the wall of the tanks; at depths 4, 18 and 38 cm (Fig. 2). The experiment was performed during 104 days from April to July 2016. Outdoor temperature was 21. 6 ºC on average (AEMET) and 234 mm of accumulated rainfall (Meteocat) during the time the experiment ran. Sunlight conditions were allowed only in the surface of the tanks, to mimic real infiltration basins. Since the accumulated rainfall only represented 0.12% and 0.26% of the daily infiltrated water in our systems (CF and F, respectively) we consider that the effect of rainfall was negligible. Hydraulic parameters of each system as well as organic and nutrient loadings are detailed in Table 1.

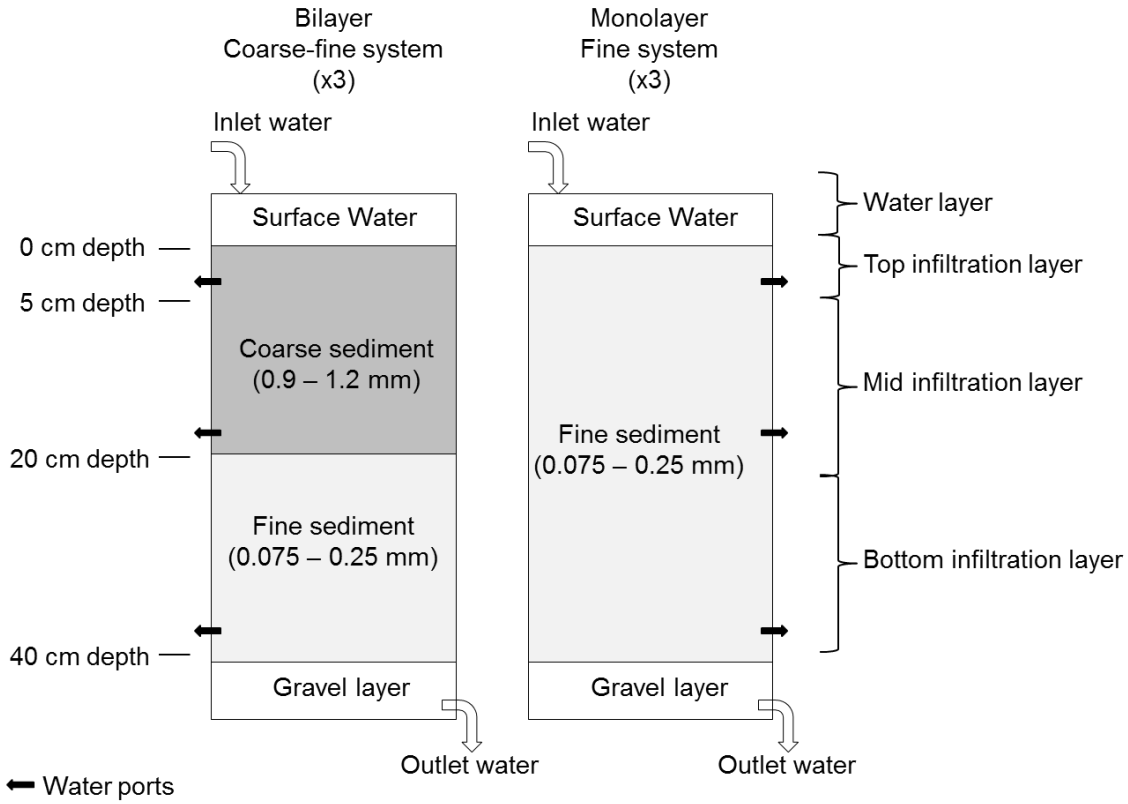

Figure 2 Scheme of the two systems (Bilayer Coarse-Fine –CF- and Monolayer Fine –F-) used in the experiment and the schematic boundaries of the layers used to calculate mass balances (surface water layer and top, mid and bottom infiltration layers). Water ports (black arrows) were placed at 2, 18 and 38 cm depth.

During the performance of the experiment, physicochemical parameters (DO, pH, conductivity and temperature) of the inlet water were measured weekly with specific probes (HQd Field Case, HACH) to ensure homogeneous conditions during all the experiment (Table 1). Hydraulic conductivity for the entire system was also calculated periodically from the difference of hydraulic head between the surface water layer and the water at 40 cm depth for a total of 26 measurements at each sand tank (Table 1). Water and sediments [note that we use the term

"sediment" to refer to the porous media (sand) which is being colonized by biofilm] were sampled weekly at the start and biweekly at the end of the experiment, for a total of 9 sampling campaigns. Samples were collected at about the same time (11 – 12 am), and with consistent weather conditions (sunny, with no registered precipitations 2 days previous to sampling) to minimize variability due to environmental factors. Water samples were collected from the inlet water, the surface water layer and the three water ports installed at each tank. Dissolved nutrient (NO_2^-, NO_3^-, NH_4^+, TDN, DON and TDP) and dissolved organic carbon (DOC) concentrations were analysed for all samples (see *section 3.3 Water parameters, page 21*). DO was also measured from all the water samples.

Table 1 Physicochemical parameters of the inlet water measured during the experiment, hydraulic parameters and input loads of each of the infiltration sand systems used

Inlet water	
DO = 5.42 ± 1.1 mg $O_2 \cdot L^{-1}$	DOC = 8.92 ± 0.6 mg $C \cdot L^{-1}$
pH = 7.63 ± 0.2	TDN = 7 ± 1.1 mg $N \cdot L^{-1}$
Conductivity = 847 ± 105 $\mu s \cdot cm^{-1}$	NH_4 = 0.77 ± 0.7 mg $N \cdot L^{-1}$
Temperature = 21.4 ± 4.3 ºC	NO_x = 3.91 ± 1.9 mg $N \cdot L^{-1}$
	TDP = 0.042 ± 0.01 mg $P \cdot L^{-1}$
Bilayer coarse-fine system (CF)	**Monolayer fine system (F)**
K = 12.28 ± 1.25 $m \cdot day^{-1}$	K = 8.21 ± 1.39 $m \cdot day^{-1}$
Advection time = 2 hours	Advection time = 4 hours
Q = 836 ± 58 $L \cdot day^{-1}$	Q = 378 ± 66 $L \cdot day^{-1}$
Input loads:	**Input loads:**
• 7392 mg C-DOC·day^{-1}	• 3359 mg C-DOC·day^{-1}
• 5840 mg N-TDN·day^{-1}	• 2660 mg N-TDN·day^{-1}
• 498 mg N-NH_4^+·day^{-1}	• 220 mg N-NH_4^+·day^{-1}
• 3661 mg N-NO_x·day^{-1}	• 1666 mg N-NO_x·day^{-1}
• 33.58 mg P-TDP·day^{-1}	• 15.38 mg P-TDP·day^{-1}

Values are the mean ± standard deviation. For the inlet water, n=54; for K values, n=78; for input loadings, n=27.

Sediment sampling was performed using a sediment core sampler (Eijkelkamp 04.23.SA) to a depth of 40 cm and each core was subdivided in three specific depth layers (0 – 4 cm as "surface sediment", 18 – 22 cm as "20 cm depth sediment" and 36-40 cm as "40 cm depth sediment"). Each sediment sample was homogenized, and then subsamples of 1 cm^3 of sediment were collected using an uncapped syringe, and kept frozen (-20 ºC) until analysis to determine nutrient

and carbon content within the sediments (*see section 3.4 Sediment parameters, page 24*). After taking each sediment core, one methacrylate empty column was placed at the same place to avoid the collapse of the surrounding sediment in the tanks, in an attempt to minimize the disruption of the flow field. Table 2 summarizes the sampling design.

Table 2 Sampling design description: measured parameters and sampling periodicity

	Parameters	Periodicity
Inlet water	❖ Physicochemical water parameters (pH, DO, conductivity and temperature)	Once/twice per week (n = 18 x 3)
From surface water to 40 cm water port	❖ Hydraulic conductivity	Twice per week (n = 26 x 3)
Inlet water, surface water and water ports	❖ NO_2^-, NO_3^-,NH_4^+,TDN, DON, TDP, DOC and DO	9 sampling campaigns (n = 9 x 3)
Sediment layers: 0-4, 18-22, 36-40 cm	❖ Carbon, nitrogen, inorganic phosphorus and organic phosphorus contents in sediment	9 sampling campaigns (n = 9 x 3)

5.3.2 Removal rates and efficiencies

Biogeochemical transformation rates were calculated for chemical species measured both in water and in sediment. Data were transformed to homogeneous units to allow the comparison between the rates measured in water and in sediment. Total water nutrient loads were calculated at each sampling depth (surface water layer, 4 cm, 18 cm and 38 cm) for all the period of the experiment, and balances between each two consecutive points were calculated. The results were divided by the total days of the experiment (104 days) and by the spatial volume for each layer. Data from the sediments were calculated separately for each depth (surface, 20 cm and 40 cm), multiplied by the conversion factor (1.45 g DW·cm^{-3}) and divided by 104 days. All values are reported in µg·cm^{-3}·day^{-1}. Negative rates indicate a removal process.

Removal efficiencies were calculated from the nutrient loads following equation 1. Two calculations were performed: 1) from the inlet to the outlet, and 2) from the surface of the sediment to the outlet, this one to exclude processes occurring in the surface water layer and to focus on the processes occurring along the infiltration pathway.

removal efficiency (%) = 100 x (inlet - outlet)/inlet (1)

where, inlet – outlet are the nutrient loads (expressed in $mg \cdot day^{-1}$).

5.3.3 Mass balances

Mass balances were calculated from the removal rates and results are reported for different depth infiltration layers (see Figure 2): top layer (includes water mass balance from surface water to 4 cm depth and the C-N-P contents measured in the surface sediment); mid layer (includes water mass balance from 4 to 18 cm depth and the sediment C-N-P contents measured at 20 cm depth); and finally, the bottom layer (includes water mass balance from 18 to 38 cm depth and the sediment C-N-P contents measured at 40 cm depth). As the potential processes occurring in the layer of surface water include complex biological (photosynthesis, planktonic uptake of nutrients, organic matter transformation) and chemical (photochemical) reactions that were not monitored, mass balances from inlet water to surface water were not assessed.

5.3.3.1 Carbon mass balances

It is assumed that the main carbon removal pathways are depth dependent. In the upper infiltration layer, the main C transformation pathways are C respiration (C_{resp}) and C accumulation in sediments (C_{sed}), and the mass balance can be expressed as:

$$C_{DOC\ inlet} - C_{sed} - C_{resp} = C_{DOC\ outlet} \quad (2)$$

In depth, for the mid and bottom layers, transformation pathways are related to C used in denitrification (C_{denitr}), aside from respiration and accumulation in sediments (Abel et al. 2014). Nonetheless, as the two terms C_{resp} and C_{denitr} were not directly measured in the deeper layers, they were considered as a single term, denoted as $C_{resp/denitr}$, so that the mass balance equation can be written as:

$$C_{DOC\ inlet} - C_{sed} - C_{resp/denitr} = C_{DOC\ outlet} \quad (3)$$

5.3.3.2 Nitrogen mass balances

It is assumed that the main nitrogen transformation pathways are depth dependent: (i) TDN removal pathways in the top infiltration layer are driven by NH_4 volatilization (Reddy et al. 2001) and N accumulation in sediments; (ii) in depth TDN removal pathways consist of denitrification to N gas (Reddy and D'Angelo 1997) and N accumulation in sediments (Bitton 1999). Furthermore, (iii) DON can be mineralized to NH_4 (Ruane et al. 2014); (iv) in depth NO_x can be transformed to DON (Dail et al. 2001). Also, (v) under oxic conditions NH_4 is nitrified to NO_x (Ruane et al. 2014); (vi) in depth NO_x can be denitrified to N_2 (Dong et al. 2009) or reduced to NH_4 (Tiedje 1988).

According to these assumptions, N mass balances are described. TDN mass balances are given by equation 4 for the top infiltration layer and 5 for the mid and bottom ones. The main N removal paths are NH_4 volatilization (denoted in the equations as $TDN_{NH4\ volat}$), N being accumulated in sediments ($TDN_{N\ sed}$), and NO_x denitrification ($TDN_{NOx\ denitr}$).

$$TDN_{inlet} - TDN_{NH4\ volat} - TDN_{N\ sed} = TDN_{outlet} \quad (4)$$

$$TDN_{inlet} - TDN_{N\ sed} - TDN_{NOx\ denitrification} = TDN_{outlet} \quad (5)$$

Ammonium mass balances are given by equation 6 for the top layer and 7 for the mid and bottom ones. Positive contributions on NH_4 mass balances are the DON being mineralized to NH_4 (denoted by $NH_{4\ DON\ mineral}$), and the NO_x being reduced to NH_4 ($NH_{4\ NOx\ reduction}$). Negative contributions on ammonium mass balance are the NH_4 that is being transformed to DON ($NH_{4\ DON\ prod}$), the one that left the system via volatilization ($NH_{4\ volat}$), the one being nitrified to NO_x ($NH_{4\ nitrif}$), and that accumulated in the sediment ($NH_{4\ N\ sed}$).

$$NH_{4\ inlet} + NH_{4\ DON\ mineral} - NH_{4\ volat} - NH_{4\ nitrif} - NH_{4\ N\ sed} = NH_{4\ outlet} \quad (6)$$

$$NH_{4\ inlet} + NH_{4\ NOx\ reduction} - NH_{4\ DON\ prod} - NH_{4\ N\ sed} = NH_{4\ outlet} \quad (7)$$

In parallel, NO_x mass balances are given by equation 8 for the top infiltration layer (where there is a net production) and equation 9 for the mid and bottom ones (with a net reduction). Positive contribution on NO_x mass balances include NH_4 being nitrified to NO_x ($NO_{x\ prod}$). The negative terms in the mass balance equations include the NO_x leaving the system via denitrification (NO_x

$_{denitr}$), that transformed to NH_4 via reduction ($NO_{x\ reduction}$ -in the text named DNRA-), and the NO_x being transformed to DON ($NO_{x\ DON\ prod}$).

$$NO_{x\ inlet} + NO_{x\ prod} = NO_{x\ outlet} \quad (8)$$

$$NO_{x\ inlet} - NO_{x\ denitr} - NO_{x\ reduction} - NO_{x\ DON\ prod} = NO_{x\ outlet} \quad (9)$$

5.3.3.3 Phosphorous mass balances

For the phosphorus mass balances, the assumption is that the TDP removal pathways at any depth are driven by phosphorous content in sediments, $TDP_{\ P\ sed}$ (Brix et al. 2001). Thus, the TDP mass balance equation is written as follows:

$$TDP_{\ inlet} - TDP_{\ P\ sed} = TDP_{\ outlet} \quad (10)$$

Where $TDP_{\ P\ sediment}$ can be also expressed as the sum of phosphorous adsorption in sediments, $TDP_{\ P\ inorg}$ and phosphorous assimilation, $TDP_{\ P\ org}$, resulting in the following mass balance equation:

$$TDP_{\ inlet} - TDP_{\ P\ inorg} - TDP_{\ P\ org} = TDP_{\ outlet} \quad (11)$$

5.3.4 Data analysis

Dissolved nutrient concentrations and DO were analysed by repeated measures ANOVA (factors: depth and system, $p < 0.05$). Data for each system were further analysed separately through Tukey post-hoc analysis to detect significant different groups in depth. The parameters measured in sediments (C, N and P) were analysed by covariance ANCOVA (factors: depth and system, $p < 0.05$) and further analysed using the Bonferroni posthoc test to detect significant different groups in depth and significant differences between systems at each depth. P_{inorg}/P_{org} ratios were also analysed (ANOVA, factor: depth and system, $p < 0.05$) and the Tukey post-hoc analysis was then performed to all systems separately (factor: depth). Removal rates and removal efficiencies were subject to an ANOVA analysis to detect differences between systems at a given depth (factor: system, $p < 0.05$). All statistical analyses have been performed by using R software (R version 3.1.1).

Table 3 Data analysis description

Parameter	Analysis	Factor	Other
DOC, NO_2^-, NO_3^-, NO_x^-, NH_4^+, DON, TDP, DO	ANOVA	Factor: system, depth, system*depth	Tukey's post-hoc
C, N, P_{inorg}, P_{org}, TP in sediment x days	ANCOVA	Factor: system, depth, system*depth	Tukey's post-hoc
Ratio P_{inorg}/P_{org}	ANOVA	Factor: system, depth, system*depth	Tukey's post-hoc
Removal rates/efficiencies	ANOVA	Factor: system	

5.4 Results

5.4.1 Distribution of chemical species in depth

Concentrations of dissolved chemical species measured at each depth are shown in Figures 3-4. Both systems showed an increase in DOC, DON, and DO concentrations in the surface water layer and a slight decrease in the concentrations of NH_4^+, NO_x and TDP in F. These slight changes resulted in higher NO_x and TDP concentrations in the surface water in the CF system; and higher DO concentration in the F one. A decrease in DOC and DON concentrations was observed in the top sediment layer. TDN concentrations gradually decreased in depth, but higher values were measured in CF at 20 cm compared to F. NH_4^+ and NO_x concentration profiles in depth were similar in both systems; NH_4^+ concentration decreased at 5 cm depth but then increased. Oppositely, NO_x concentration increased at 5 cm depth but then decreased. The F system displayed higher NH_4^+ and lower NO_x concentrations at 20 cm than CF. Both systems displayed a similar pattern for the TDP concentration profile, with a decrease from the surface to 5 cm depth and then stabilization. Higher TDP concentrations were reported in the CF system in the surface and at 20 and 40 cm depth than in the F system. DO concentrations decreased with depth, with the lowest values found in the F system at 20 and 40 cm depth.

C, N and P concentrations in sediments (Fig. 5) were higher in the surface than in the deep layers. The CF system showed higher inorganic P concentration in the surface sediment than F, while for total phosphorous no significant differences between systems were detected. At depths 20 and 40 cm, C, N, inorganic P and total P concentrations in sediments were significantly higher in the CF system than in F.

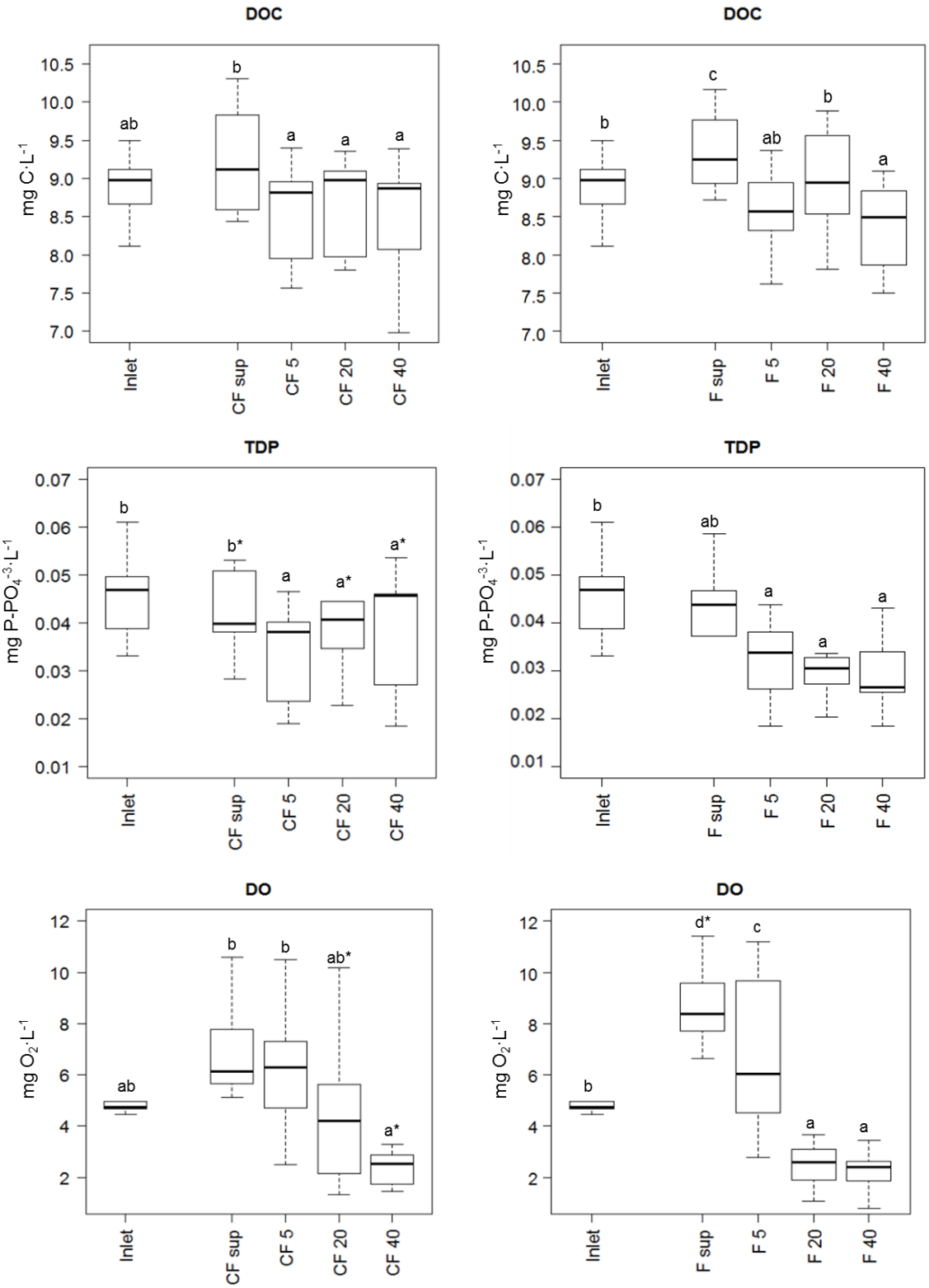

Figure 3 Boxplots of DOC, TDP and DO concentrations measured at each depth and system (CF: bilayer Coarse-Fine system; F: monolayer Fine system), 9 sampling times x 3 replicates, n = 27. Letters next to the boxes indicate different groups determined by Tukey's post-hoc analysis after ANOVA repeated measures (depth, $p < 0.05$). Notation: "inlet" stands for the inlet water, "sup" for the water ponded at the surface, "5 cm depth" for water from -4 cm water port, "20 cm depth" for water from -18 cm water port and "40 cm depth" from water from -38 cm water port. Similar notation regarding systems and depths is used in Figure 4.

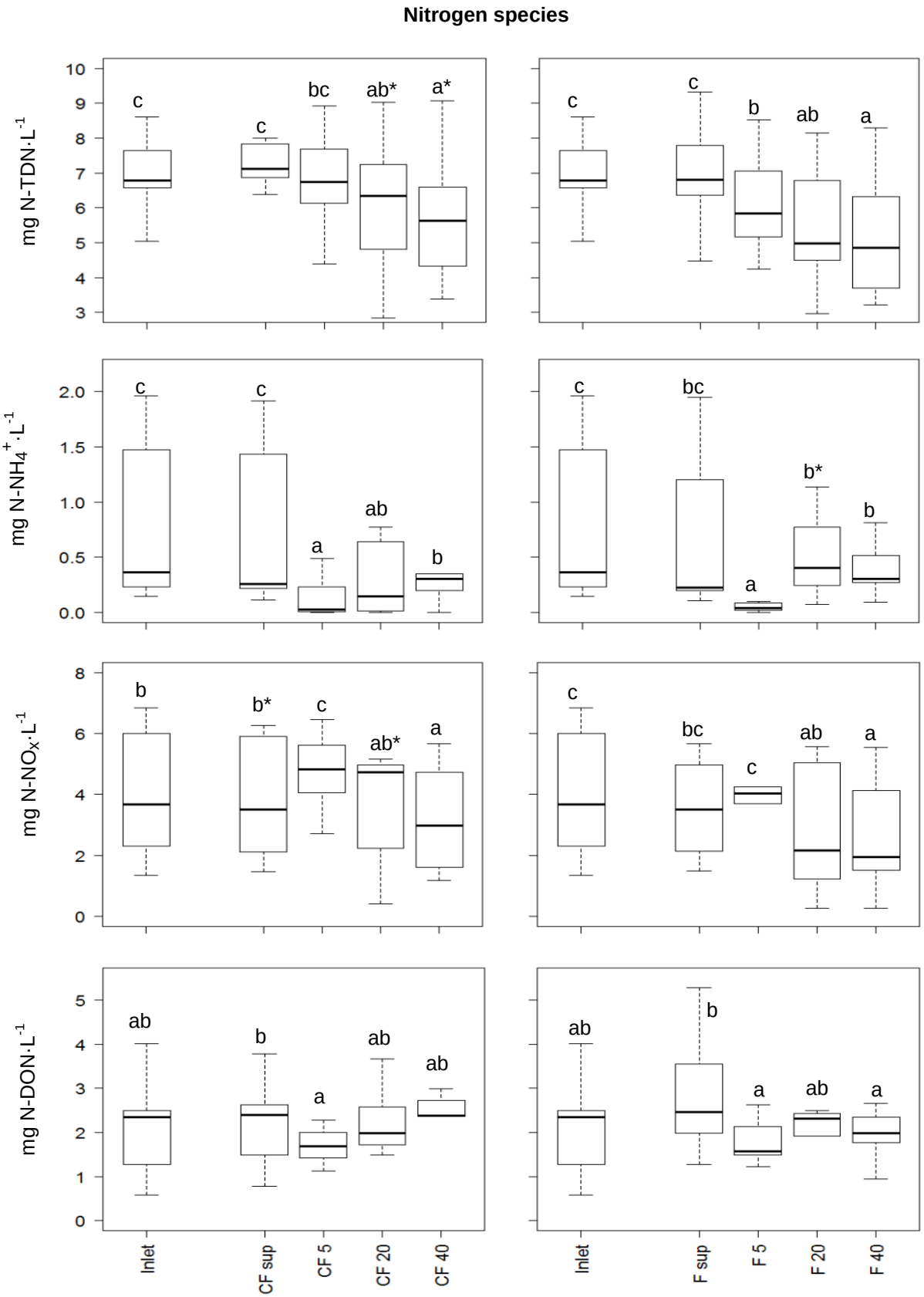

Figure 4 Boxplots of nitrogen-species concentrations measured at each depth and system and Tukey's post-hoc analysis after ANCOVA analysis for depth ($p < 0.05$). Asterisks determine differences between systems at each given depth (ANCOVA, system, $p < 0.05$).

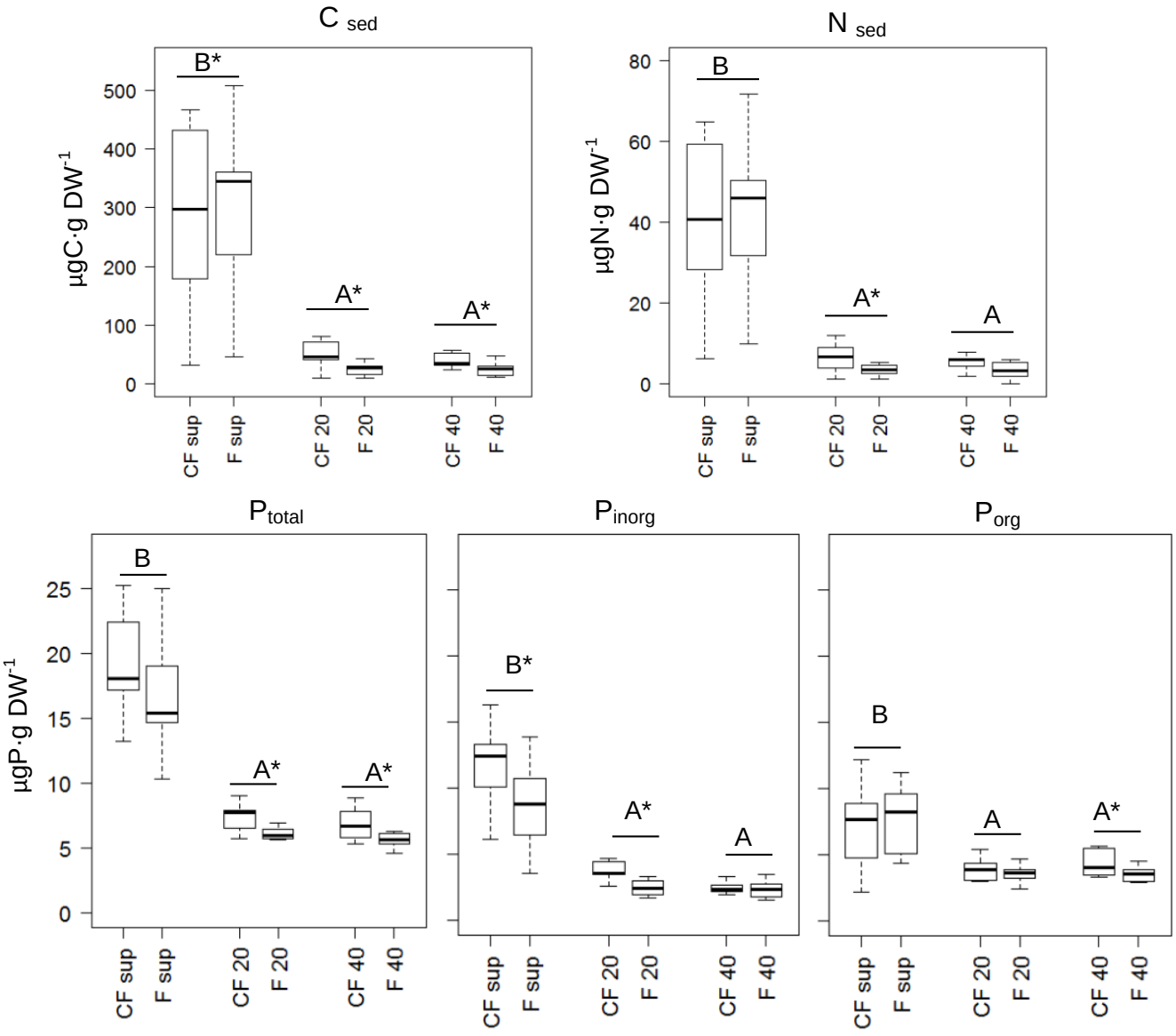

Figure 5 Boxplots for carbon, nitrogen and phosphorous species (total P, inorganic P and organic P) concentrations measured in sediments as a function of depth and GSD and Tukey's post-hoc analysis after ANCOVA analysis for depth ($p < 0.05$). Asterisks determine differences between GSDs at each given depth (ANCOVA, $p < 0.05$).

The ratio P_{inorg}/P_{org} (Table 4) decreased significantly in depth (ANOVA, $p < 0.05$) indicating higher accumulation of organic P than inorganic P in deeper sediments. In the surface, the CF system showed significantly higher P_{inorg}/P_{org} ratio than the F one. Sediment molar ratios are described in Table 5, in the top layer both systems showed similar C:N, $C:P_{org}$ and N:Porg ratios. At 20 cm depth, C:N ratio increased slightly in both systems, and $C:P_{org}$ ratio decreased as well as $N:P_{org}$ ratio. Molar ratios at 40 cm depth are similar than those described at 20 cm depth.

Table 4 Ratios between inorganic and organic P (P_{inorg}/P_{org}) measured at each system and depth

Depth	System	P_{inorg}/P_{org}
Surface[b]	CF	**0.98[b] ± 0.2**
	F	0.70[a] ± 0.06
20 cm depth[a,b]	CF	0.95 ± 0.3
	F	2.3 ± 2
40 cm depth[a]	CF	0.59 ± 0.1
	F	0.79 ± 0.05

Values represent the arithmetic mean and standard deviation for all the sampling days (n = 9). ANOVA analysis detects differences in depth ($p < 0.05$) and also between systems in the surface data ($p < 0.05$).

Table 5 Sediment C:N:P molar ratios measured at each system and depth

Depth	System	C:N molar ratio	$C:P_{org}$ molar ratio	$N:P_{org}$ molar ratio
Surface	CF	7.8 ± 1.2	115.2 ± 58.2	14.7 ± 7.3
	F	7.6 ± 1.6	146.3 ± 86.8	17.7 ± 9.9
20 cm depth	CF	8.3 ± 4.0	35.8 ± 26.5	4.2 ± 2.5
	F	9.0 ± 3.9	22.7 ± 9.9	3.1 ± 1.6
40 cm depth	CF	10.2 ± 6.8	23.9 ± 8.0	2.7 ± 1.2
	F	9.0 ± 3.2	19.2 ± 10.2	4.3 ± 5.4

Values represent the arithmetic mean and standard deviation for all the sampling days (n = 9).

5.4.2 Carbon, nitrogen and phosphorus mass balances

Carbon mass balances per unit volume of sediment at each sediment layer are described in Figure 6. Removal rates decreased in depth in both systems. In the top layer, DOC removal and C respiration rates were largest in CF while C accumulation rates in sediments were similar between GSDs. This resulted in C accumulation in sediments accounting for 25.1 % and 50.3 % of the DOC removal in CF and F, respectively. Thus, respiration resulted in the main C removal path in the CF system (74.9 %), while in the F one an equal contribution of C accumulation and C respiration to the global DOC balance was found (50.3 % and 49.7 %, respectively). In the middle infiltration layer, both systems were estimated to receive unaccounted C inputs as DOC balances were positive; for this reason, we could not estimate the relative contribution of each carbon removal pathway in that layer, however greatest C accumulation rate was found in CF. In the bottom layer (20 to 40 cm depth), greatest C accumulation rate was found in CF but similar C

respiration rates were described in both systems. In this layer, C_{sed} accounted for 19.1 % and 17.3 %, while $C_{resp/denitr}$ accounted for 80.9 % and 82.7 % of the total DOC removed in the CF and F systems, respectively.

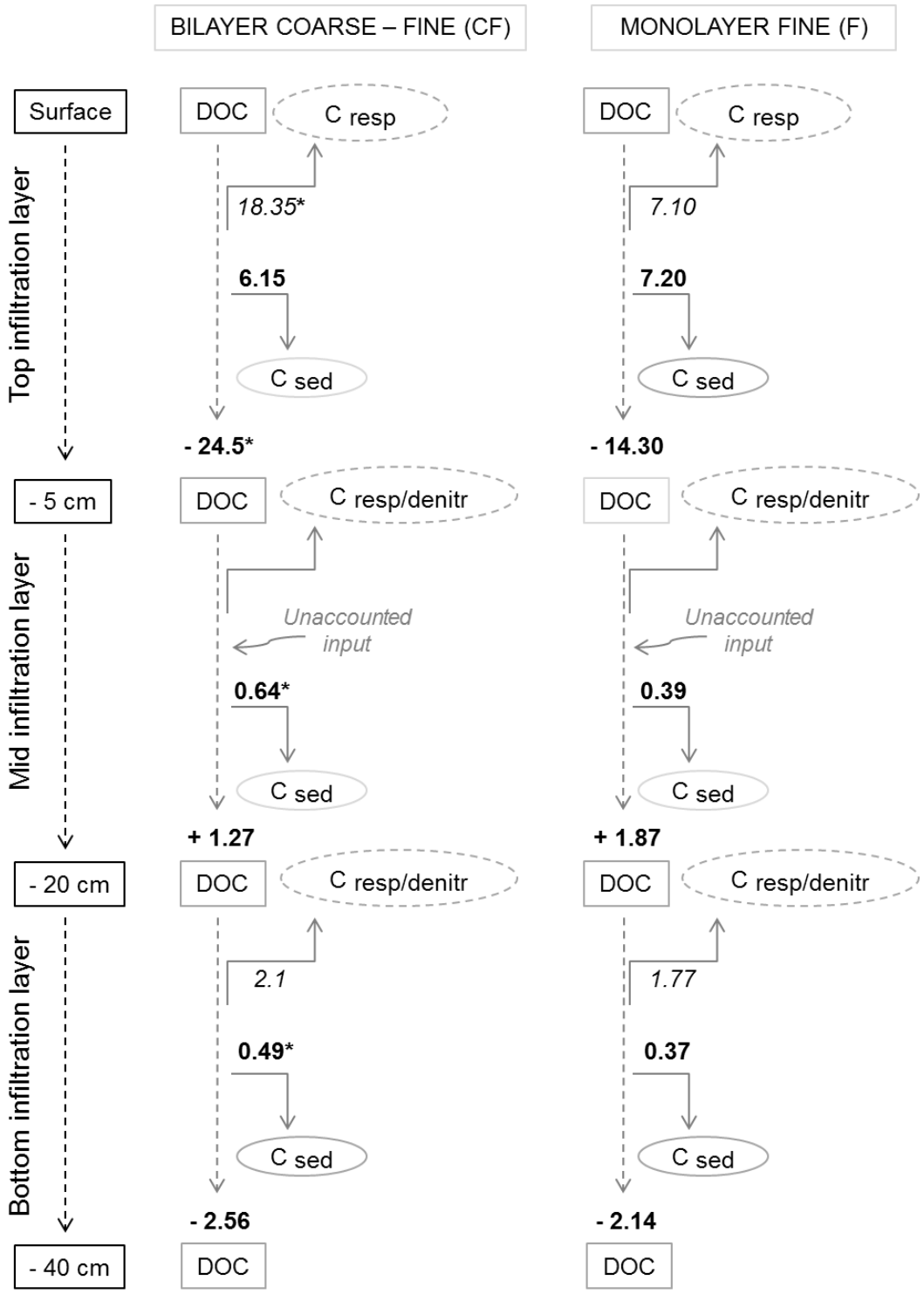

Figure 6 Carbon mass balances for the main C transformation processes and removal paths in the sediment layers. Values in **bold** indicate mass balances calculated from experimental data while values in *italic* are parameters estimated through equations 2 and 3. Asterisk indicates significant difference between systems ($p < 0.05$). Results are expressed as μg $C \cdot cm^{-3} \cdot day^{-1}$.

Nitrogen mass balances per unit volume of sediment are described in Figure 7. Process rates decreased in depth in both systems. In the top infiltration layer, ammonium volatilization was estimated as the main TDN removal path (92.4 % in CF and 90.7 % in F) while N accumulation in the surface sediments accounted for 7.6 % (CF) and 9.3 % (F) of the TDN removal. Notice that only small amounts of N were unaccounted for (3.0 and 0.7 μg $N \cdot cm^{-3} \cdot day^{-1}$ for CF and F, respectively). In the mid and bottom layers, denitrification was estimated to be the main TDN removal pathway in both systems (90 – 95 %) while N accumulation in sediments accounted for only 2 – 10 %. Other N transformation pathways were estimated in the infiltration systems: DON mineralization to NH_4, and NH_4 nitrification to NO_x in the top infiltration layer; DNRA and NO_x transformation to DON in the middle one, and DNRA in the bottom one. The contributions of these processes in the general balance of intermediate species of N (NH_4 and NO_x) vary between GSDs. Thus, in CF we find that with regard to NH_4 transformation in the upper layer, dominates nitrification (65%). Regarding NO_x transformation in this system, in the middle layer dominates the transformation to DON (43%) and denitrification (55%) and in the lower layer dominates DNRA (72%). However, in the F system, in the top layer dominates both nitrification and ammonium volatilization (≈ 50% each), in the middle layer dominates DNRA (43%) and denitrification (60%), and in the bottom layer dominates denitrification (80 %). Mass balance closure discrepancies in the mid and bottom layers were very low (0.17 - 0.25 and 0.41 – 0.44 μg $N \cdot cm^{-3} \cdot day^{-1}$ for CF and F, respectively).

Mass balances of the P species per unit volume of sediment are described in Figure 8. We assumed that all TDP removed was accumulated in the sediment through adsorption or assimilation. However, in some of the mass balance evaluations, TDP removal was lower than P accumulated in sediments, potentially indicating an unaccounted P input. From Total P accumulated in sediments, proportions between organic and inorganic P were calculated; in surface sediments, results suggested similar accumulation of inorganic P (49 %) and organic P (51 %) in CF, while accumulation of organic P (60 %) contributed more than inorganic P (40 %) in F. At 40 cm depth, organic P accumulation accounted for higher proportion (56 – 63 %) compared to inorganic P (37 – 44 %) in both systems. Higher TDP and P accumulation rates were measured in the top infiltration layer. Comparing systems, TDP removal rate was higher in CF in top and bottom layers and P accumulation rate was higher in the CF system in the mid infiltration layer.

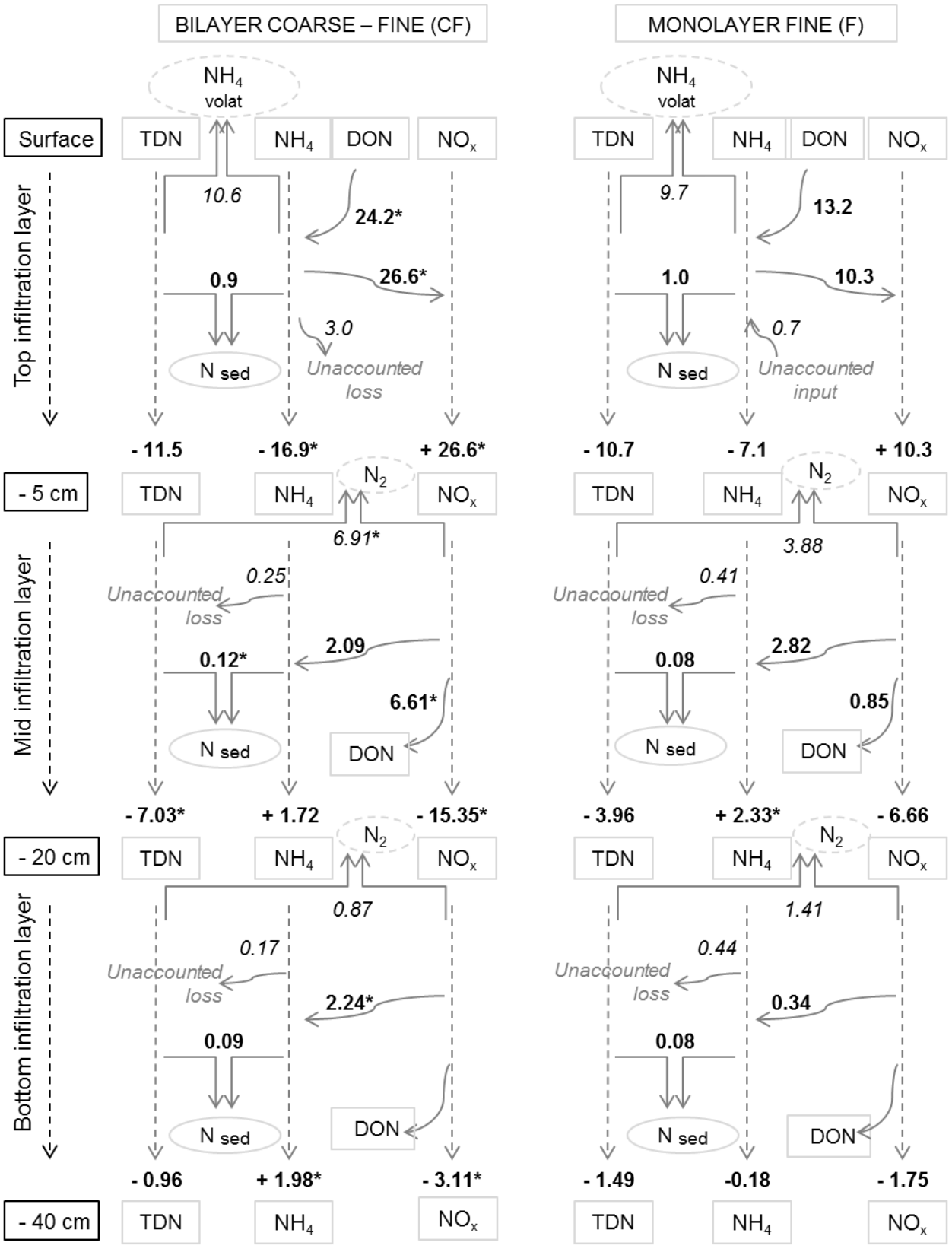

Figure 7 Nitrogen mass balances for the main N transformation processes and removal paths in the sediment layers. Values in **bold** indicate mass balances calculated from experimental data while values in *italic* are parameters estimated through equations 4-9. Asterisk indicates significant difference between systems ($p < 0.05$). Results are expressed as μg $N \cdot cm^{-3} \cdot day^{-1}$. DON balances in the bottom layer resulted in low and highly uncertain values, and so, they were excluded from mass balance calculations.

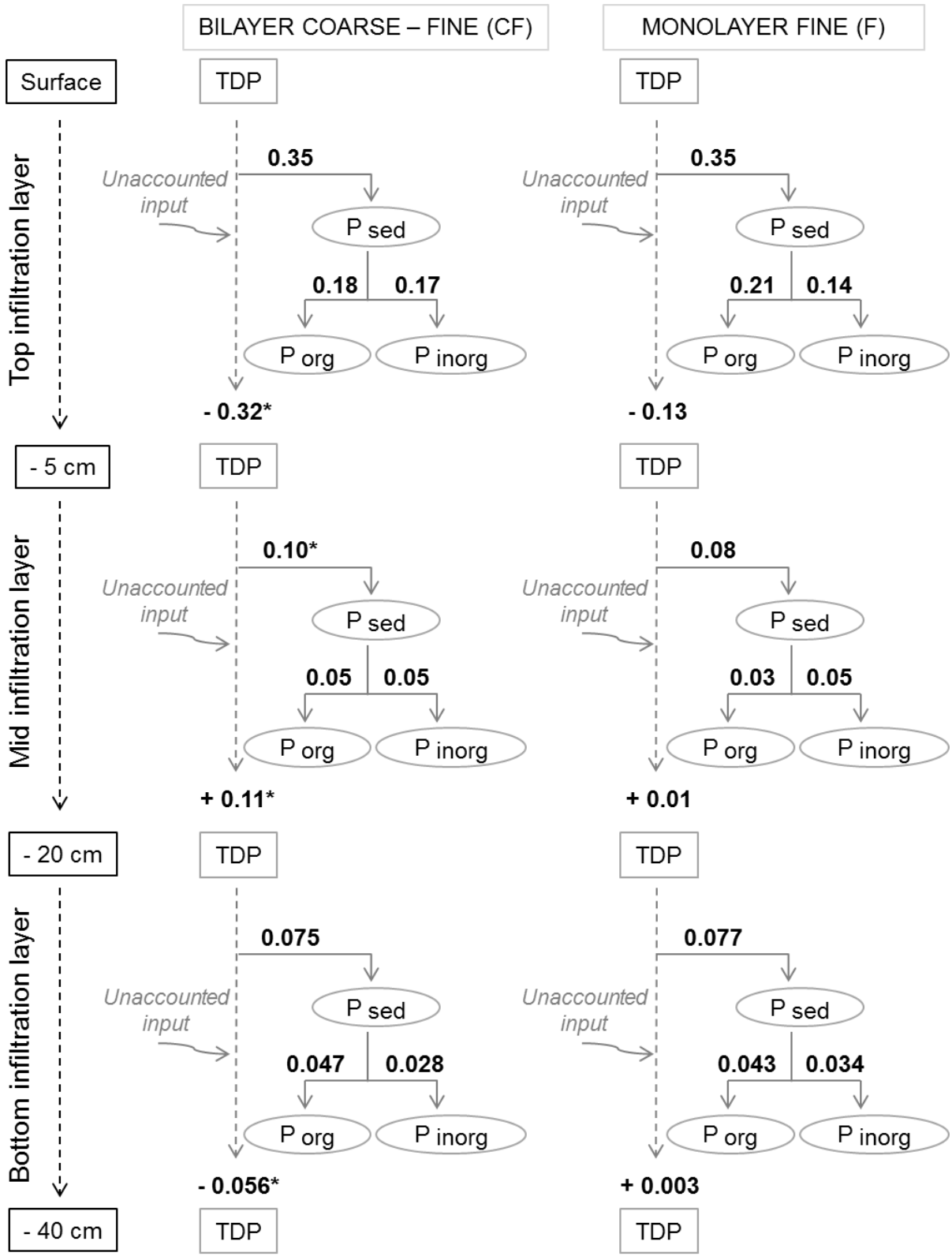

Figure 8 Phosphorous mass balances for the main P transformation processes and removal paths in the sediment layers. Values in **bold** indicate mass balances calculated from experimental data while values in *italic* are parameters estimated through equations 10 and 11. Asterisk indicates significant difference between systems ($p < 0.05$). Results are expressed as $\mu g\ P \cdot cm^{-3} \cdot day^{-1}$.

5.4.3 Removal efficiencies

We report in Table 6 the removal efficiencies of each infiltration system. Considering only the layers that constitute the sediments, both systems showed similar DOC (7 - 11 %), TDN (18 – 23 %) and TDP (14 – 16 %) removal efficiencies, but higher TDN and TDP removal rates were reported in CF as compared to F. Including the processes in the full system (three sediment layers plus the surface water layer), the F system resulted in higher TDP removal efficiency (23 %), compared to the CF (12 %).

Table 6 Removal efficiencies (%) and overall removal rates measured in the infiltration systems

		Surface – 40 cm depth		Inlet – 40 cm depth	
		CF	F	CF	F
DOC	%	7.44 ± *2.7*	11.31 ± *1.8*	5.50 ± *4.5*	6.53 ± *2.0*
	Removal rate	-3.87 ± *1.1*	-2.15 ± *0.4*		
TDN	%	18.45 ± *3.1*	23.03 ± *2.6*	17.23 ± *2.7*	22.75 ± *4.2*
	Removal rate	**-4.55** ± *0.5*	-3.57 ± *0.2*		
TDP	%	13.91 ± *3.0*	16.46 ± *5.4*	11.87 ± *2.6*	**25.67 ±** *4.3*
	Removal rate	**-0.027** ± *0.005*	-0.011 ± *0.002*		

Removal rates are expressed as µg $C \cdot cm^{-3} \cdot day^{-1}$ for DOC, µg $N \cdot cm^{-3} \cdot day^{-1}$ for TDN and µg $P \cdot cm^{-3} \cdot day^{-1}$ for TDP. Considering only the sediment part of the systems (three infiltration layers) correspond to the column "Surface – 40 cm depth", while removal efficiencies for the whole system, including the surface water layer correspond to the column "Inlet – 40 cm depth". Values in bold indicate the system with significant higher value of the specified parameter comparing systems (ANOVA, factor: system, $p < 0.05$).

5.5 Discussion

Our data support that biogeochemical processes of C-N-P species are depth and GSD dependent, both in qualitative (most relevant processes) and in quantitative terms. As expected, the highest rates occurred in the top layer which might be controlled by high nutrient, and DO and electron acceptors availability as well as the higher biomass developed in surface sediments compared to deeper ones (Freixa et al. 2016). Regarding our results, nutrient accumulation in the top layer sediments played a key role on nutrient removal efficiencies, especially for DOC and TDP removals (representing up to 50 % of their respective removal, while N accumulation in sediment represents 10 % of its removal). This removal is suggested to be mainly due to biological processes (assimilation) since the C:N:P elemental molar ratios (calculated from total C and N and organic P in sediments) are close to the known Redfield ratio described for autotrophic biomass (106:16:1, Redfield (1958)). Interestingly, even though we expected higher nutrient accumulation rates in the fine sediment due to higher surface area available in fine compared to coarse sediments (Zhu et al. 2015), both systems showed similar rates. Furthermore, in the case of P, where we distinguished the inorganic to the organic fraction, inorganic P showed greater accumulation in the bilayer coarse-fine system. This contradiction could be due to the fact that difference in sediment texture has mostly been associated with the presence of silts and clays (< 2 μm) (Liu et al. 2015) and in our study the presence of silts and clays was excluded. Furthermore, higher inorganic P accumulation rates measured in the bilayer system could be related to higher TDP concentrations in the surface water layer (Del Bubba et al. 2003) which could enhance physical adsorption of inorganic P. It is also worth noting that we are not comparing coarse and fine sands, but GSDs where the bilayer coarse-fine system does not act like coarse homogeneous sediment since physical characteristics such as K and flow velocity are lower than a coarse sediment (Perujo et al. 2017) and therefore the bilayer coarse-fine and the monolayer fine systems promote the removal of nutrients through the accumulation of these nutrients in the sediments via adsorption and assimilation.

Other significant biogeochemical processes occurring in the top layer of infiltration systems are mostly related to nitrogen (ammonium volatilization and the coupled processes of DON mineralization and nitrification) but also include carbon respiration. As expected, C respiration, nitrification and DON mineralization rates were approximately double in the bilayer system

compared to the monolayer system which would indicate that those rates would be proportional to input loads. Greater attention should be focused on ammonium volatilization as it is the main TDN removal pathway in the aerobic top layer of infiltration systems and it seems to be independent of input loads. Ammonium volatilization is a physicochemical process driven by temperatures higher than 20 ºC and pH ranging 6.6 – 8.0 (Poach et al. 2004), for this reason, showed similar rates in both systems.

In depth, accumulation of nutrients in sediments was less relevant as a removal path to that observed for the top layer. The slight increase in C:N sediment molar ratios as well as the decrease in $C:P_{org}$ and $N:P_{org}$ ratios compared to the top sediment layer could be linked to the fact that the dominant living biomass in depth is microbial biomass which showed a different elemental molar ratio than autotrophic biomass. Cleveland and Liptzin (2007) stated C:N:P = 60:7:1 as the elemental molar ratio for microbial biomass. According to this, sediment molar ratios at 20 and 40 cm depth following the elemental molar ratio described for microbial biomass could be indicative of nutrient assimilation as a main pathway of nutrient accumulation in sediments in depth, but also they could be linked to physical adsorption of microbial biomass that is being transported from upper to lower sediment layers. Specifically, higher accumulation rates in the interface of the bilayer system could be linked to physical entrapment of microbial biomass when reaching the transition from the coarse to the fine sediment layers, as well as retention of carbon, nitrogen and phosphorous species which are then potential to be biologically assimilated or physically adsorbed.

At the same time, the imbalance of the molar ratios to a greater accumulation organic P (low $C:P_{org}$, increase in $N:P_{org}$ ratios) suggests the deposition of dead organic matter and the accumulation and adsorption of P in lower layers where the mineralization processes of this organic matter could possibly be limited by reduced microbial activity and lower DO. We further contend that unaccounted C inputs reported in the experiment at intermediate depths were probably due to the generation of microbial soluble products (Essandoh et al. 2013), or to desorption of organic carbon retained in top sediments (Quanrud et al. 2003). Similarly, unaccounted P inputs in mass balances at intermediate depths could be related to the release of phosphates previously assimilated in upper layers by bacteria and algae following their death and subsequent degradation (Essandoh et al. 2011).

In depth, TDN concentration is the only parameter decreasing in the mid and bottom layers mainly due to anaerobic processes such as denitrification that could take place even in DO concentrations of around 4 mg $O_2 \cdot L^{-1}$ (Gao et al. 2010). Larger loading inputs could explain the larger denitrification rates reported in the bilayer system which resulted in higher TDN removal rates especially in the mid layer as compared to the monolayer fine one. However, sediment GSD in depth modulated N transformation pathways. Specifically, the larger C accumulation in the interface between the coarse and fine layer in CF could favour the conversion of NO_x to DON, most relevant in organic horizons (Dail et al. 2001). NO_x transformation to DON has been mainly attributed to abiotic processes (Rückauf et al. 2004) and specific DON reactions remain unknown. Interestingly, at 40 cm depth, DNRA dominated over denitrification in the CF system, while the opposite happened in the F system. Higher hydraulic conductivity in the former system could have favoured interstitial DO transport in depth (Mueller et al. 2013), driving the high DO concentration measured at 20 and 40 cm depth, and being the reason for DNRA being the dominant pathway in depth compared to denitrification (under oxic conditions the denitrification/DNRA ratio is low, Roberts et al. (2014)). In this study, different contributions of N transformation pathways between the bilayer and the monolayer systems did not affect the overall TDN removal efficiencies, possibly due to the fact that main differences were achieved in mid and bottom layers where N concentrations and transformation rates were far smaller than in the top ones.

To complete the picture, some comments can be made regarding biogeochemical processes occurring in the surface water layer. The observed changes may have implications in the global nutrient balance in infiltration systems. The most significant changes were the increase in DOC and DON concentrations, related to the potential release of soluble microbial products and algal exudates (Czerwionka 2016; Sieckzo et al. 2015), and combined with NH_4^+, NO_x and TDP concentrations decrease, these associated with possible nutrient uptake by planktonic microorganisms and algae (Hein et al. 1995; Kirchman 1994). Photosynthetic activity in the surface water layer might be responsible for DO concentration increase (Drapcho 2000) which, in turn, favours nitrification in the top sediment layer due to high DO concentration in infiltrated water (nitrification has high DO requirements (4.57 g of O_2 per gram of NH_4^+, Tchobanoglous (2003)). Biogeochemical processes occurring in the surface water layer seem to be directly related to the hydraulic retention time (HRT). This should be interpreted carefully since, as large

HRT could favour TDN and TDP removal efficiencies in monolayer fine systems, it could decrease DOC removal efficiency.

Biogeochemical rates - influenced by GSDs - have implications on removal efficiencies in infiltration systems. The main processes related to DOC, TDN and TDP removals are located in the top sediment layer and include C respiration and assimilation, NH_4 volatilitzation, as well as P assimilation and adsorption. On one hand, the bilayer coarse-fine system allows infiltration of a greater volume of water, and so greater input nutrient loads, than the monolayer fine system. This results in greater rates of biogeochemical processes that are dependent on input loads such as C respiration in the bilayer system. Furthermore, in the bilayer coarse-fine system the convergence of characteristics such as grain size distribution and advection times allows to achieve higher TDN and TDP removal rates in the bilayer, as well as similar or even higher (if comparing values in the interface) nutrient accumulation rates in sediments through physical adsorption and biological assimilation, compared to the monolayer system. Overall, the bilayer coarse-fine system allows treatment of a larger volume of water per surface unit achieving similar removal efficiences as the monolayer fine one.

5.6 Conclusions

The present work concludes that infiltration systems can be used as efficient water treatment technologies, so that their design is of great importance. During infiltration through porous media, biogeochemical processes and rates are strongly influenced by the GSD, resulting in different mappings of C-N-P cycles. It should be noted that the effective removal of DOC and TDP occurs mainly in the upper layer of the infiltration systems due to the dominance of aerobic processes while the removal of TDN occurs along the vertical (aerobic and anaerobic processes). Main biogeochemical processes involved are C respiration and assimilation, ammonium volatilization as well as P adsorption and assimilation. In terms of dissolved nutrient removals, sediment plays a key role through the assimilation of C (it can represent up to 50% of DOC removal), the assimilation of P (it can represent up to 50% of TDP removal) and the physical adsorption of P (up to 50% of TDP removal). Accumulation of N (dominated by the assimilation process) only represents up to 10% of the TDN removal. It is worth mentioning that the bilayer coarse-fine GSD enhances nutrient accumulation in the top layer, possibly because K and flow velocity are lower than coarse sand as such resulting in similar accumulation rates than the monolayer fine system. In depth, the bilayer GSD enhances nutrient entrapment in the interface of the coarse and fine sand layers. To sum up, the bilayer coarse-fine system allows treating larger volume of water per surface unit achieving similar removal efficiencies as the monolayer fine system.

6 Chapter III:

Assessing deep clogging in infiltration systems: biofilm depth-dynamics in two grain-size distributions

6.1 Abstract

Biofilms play a key role in organic matter and nutrient processing in infiltration systems, but at the same time, excessive biomass growth is a major problem in such systems due to porous media clogging. Sediment grain size distribution influences the structure of sediment-associated biofilm, as they define the surface area available for colonisation and the interstitial fluxes. An outdoor infiltration experiment was performed during 104 days in sediment tanks (40 cm depth), simulating infiltration systems composed of two different sediment grain size distributions (GSD). The experiment aimed to study the influence of GSD on biomass accumulation, extent and transport in depth, by analysing biofilm structural components and hydraulic conductivity variations in depth. Observations confirmed that structural biofilm components contributed differently to bioclogging depending on both depth and GSD. Moreover, GSD was a controlling factor for biofilm growth dynamics, which could determine the maturity state of biofilms, and therefore influence biomass detachment and further transport in depth (higher in fine sand infiltration systems). Algae bioclogging capacity could decrease when increasing its degradation state. Bacteria as such would not have a direct influence on bioclogging but could boost deep clogging in infiltration systems due to EPS production in deep layers as well as transport downwards dynamics of detached biomass (especially EPS).

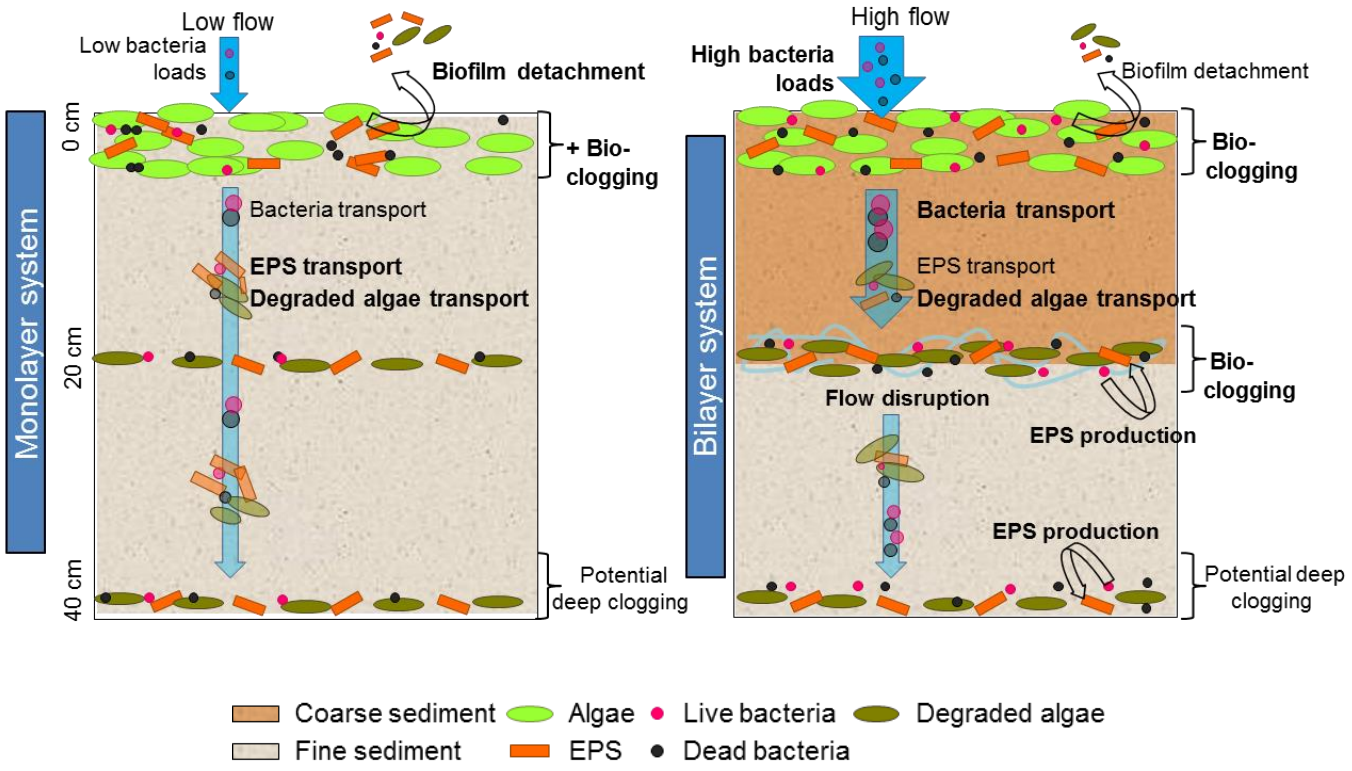

6.2 Introduction

Infiltration systems through a porous medium (acting as filter) are water treatment technologies where the quality of the influent improves progressively during the infiltration path as a consequence of biological, chemical and physical processes (Dillon et al., 2008; Miller et al., 2009). Infiltration basins are used worldwide for groundwater recharge, wastewater treatment, stormwater disposal and/or for setting up hydraulic barriers against the intrusion of undesired water in aquifers (Bardin et al. 2002). Furthermore, they are suitable for the treatment of decentralized sewage (Duan et al. 2015) and have increasingly become a mean of solving water supply stress problems in urban areas (Camprovin et al., 2017) or reducing the degradation of stream water quality (Türkmen et al. 2008). Simplicity and low capital and operating costs are the main advantages of infiltration systems compared to more technologically sophisticated methods of water treatment (Campos et al. 2002). However, research in recent years has revealed that there are still shortcomings in the design and practical applications of subsurface wastewater infiltration systems (Duan et al. 2015; Rodriguez-Escales et al. 2018).

Biofilms are present in many natural and engineered environments (Deng et al. 2013) and are recognized to be the dominant mode of bacterial life (Barai et al. 2016). Natural biofilms are mixtures of autotrophic/heterotrophic assemblages (Gette-Bouvarot et al. 2014), which can be composed of algae (microphytobenthos) and bacteria besides fungi and protozoa embedded in a matrix made of extracellular polymeric substances (EPS) and attached to solid surfaces (Lock et al. 1984). Main producers of EPS are bacteria and algae (Hirst et al. 2003; Malarkey et al. 2015). EPS constitute a fibrous gel-type matrix which can be broken down into different organic molecules such as polysaccharides, proteins, lipids and nucleic acids (Stoodley et al. 2002) and play a crucial role in the initial attachment of cells to solid surfaces, cohesiveness and biofilm thickness (Flemming and Wingender 2010). Polysaccharides have been proved to be the main component of EPS in sediments (Hoffmann and Gunkel 2011; Xia et al. 2016, 2014). Biofilms play a key role in biogeochemical processes (Mermillod-Blondin et al. 2005; Romaní et al. 2004b) by catalysing a number of processes including uptake, storage, and mineralization of dissolved organic matter, as well as assimilation of inorganic nutrients (Findlay et al. 2003).

Sediment grain size shapes the structure and function of sediment-associated biofilm (Santmire and Leff 2007). On one hand, the grain size distribution (GSD) of the sediment defines the

surface area available for colonisation per unit of sediment mass, that increases when decreasing average grain size (Mendoza-Lera et al. 2017). On the other hand, GSD controls hydraulic conductivity (Battin 2000), largest for coarse sands, allowing large supply of solutes in depth (Higashino 2013). Therefore, in fine sands biofilm development will be limited by advective mass transfer in depth, while in coarse sands biofilm development may be limited by the sediment colonisable area (Mendoza-Lera et al. 2017). Perujo et al. (2017) found sediment grain size to modify biomass patterns in depth, and more, they stated that implications of sediment heterogeneity on biofilm biomass and activity were not uniquely characterized by the upper layer of the sediment.

Successful application of infiltration systems generally requires maintaining relatively high hydraulic conductivity values, so that infiltration conveys water efficiently from the surface downwards during periods of system operation (Racz et al. 2012). A major problem in infiltration systems is clogging. Clogging mechanisms are classified into physical, chemical and biological (Baveye et al. 1998). Bioclogging is a main cause of infiltration systems failure (Duan et al. 2015), due to the growth of biofilm that reduces the total volume and the connectivity of the pores accessible to flow (Or et al., 2007b). Bioclogging could trigger deleterious consequences on recharge operation facilities, such as reducing recharge efficiency and increasing operating costs (Xia et al. 2014), limiting the availability of oxidants and nutrients to microorganisms (Thullner et al. 2002), or affecting the quality of infiltrated waters (Dechesne et al. 2004). In short, clogging affects the life cycle of infiltration systems (Duan et al. 2015).

Since a few years ago, several works have studied bioclogging processes focusing on the spatial or temporal evolution of bacteria and/or EPS concentrations (Dupin et al. 2001; Freixa et al. 2016; Vandevivere and Baveye 1992; Xia et al. 2016). In outdoor infiltration systems where biofilms include both phototrophs and heterotrophs the contribution of algae in bioclogging might be relevant (Gette-Bouvarot et al. 2014). Bioclogging might not only be influenced by the biomass growing at the topsoil, but also by that growing in deep layers or being transported vertically from the top sediment layer with the potential to colonize deep sediment.

Advection provides an effective transport mechanism for dissolved and particulate matter through the interstitial space (Huettel et al. 1998) which depends on flow regime, hydraulic conductivity and sediment GSD. Accordingly, Han et al. (2013) studied the retention of bacteria in porous

media in 10 cm sediment columns and Bai et al. (2016) concluded that increasing sand grain size resulted in decreased bacteria retention.

Ehrenhauss et al. (2004) assessed the vertical distribution of algae and the potential role of advective transport processes in sediment cores of size 10 cm. Hoffmann and Gunkel (2011) concluded that biological clogging reached down to a sediment depth of at least 10 cm (median grain diameter of the sediment was about 0.2 mm) and that the clogging process was strongly determined by photoautotrophic and heterotrophic production. However, more studies are needed to gain a better understanding of the complex process of bioclogging; as stated by Benioug et al. (2017), important questions on how the distribution of biomass may affect hydrodynamic properties of porous medium remain to be addressed.

In this work, we performed an outdoor infiltration experiment **with the aim of deepen our knowledge on bioclogging.** Emphasis is placed in **the analysis of the vertical depth-distribution and depth-dynamics of biofilm structural components (algae, EPS, live bacteria and dead bacteria) and the potential role of each biofilm component to hydraulic conductivity variations as a function of depth, time and sediment GSD.**

It is suggested that clogging will be determined mainly by algal biomass on the surface and its influence will decrease in depth. Higher flows in the bilayer coarse-system would enhance biomass transport downwards extending bioclogging in depth, while in the monolayer fine system bioclogging would concentrate in the upper layer.

6.3 Materials & Methods

6.3.1 Experimental design and sampling

The outdoor infiltration experiment used in this chapter is the same as the one used in Chapter II. It consisted in flow-through sediment tanks of two GSDs (three replicates per system): (1) a bilayer system (denoted CF, standing for Coarse-Fine), consisting of a 20 cm layer of coarse sand (0.9 – 1.2 mm) placed on top of a 20 cm layer of fine sand (0.075 – 0.250 mm); and (2) a monolayer system (denoted F, for Fine), consisting of a 40 cm layer of fine sand (0.075 – 0.250 mm). Sunlight conditions were allowed in the surface of the tanks, to resemble real infiltration basins (see *section 5.3.1 Experimental design and sampling*, *page 59* for more details). Three water ports were installed in the wall of each tank, at depths 4, 18 and 38 cm, to allow measuring piezometric head differences as a function of depth (Fig. 1).

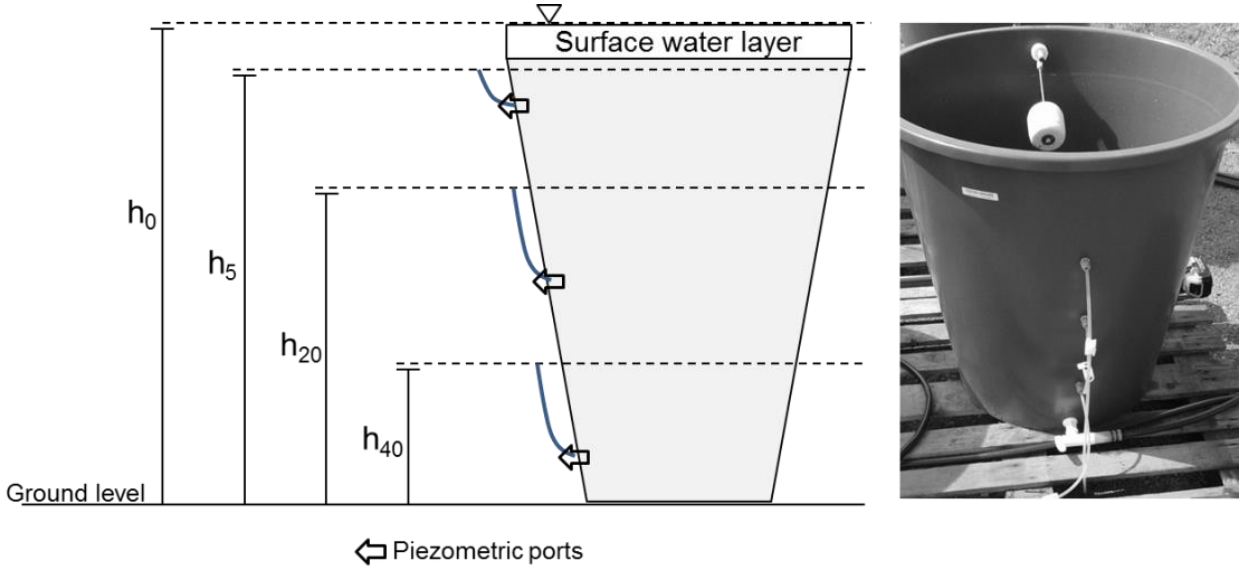

Figure 1 Scheme (left) and photograph (right) of the experimental design used for piezometric head measurements. Water ports (black arrows) were placed at the wall of the tanks at depths 4, 18 and 38 cm depth for measuring piezometric head differences at different depth layers.

Piezometric head measurements were performed from day 19 (earlier values could not be recorded due to technical problems) with 2-4 day intervals, for a total of 26 sampling dates. From these measurements, hydraulic conductivity (K) values were computed corresponding to depth segments limited by contiguous water ports: surface to 5 cm; 5 to 20 cm; 20 to 40 cm, as well as an overall value (surface to 40 cm depth), using Darcy's law. K values were calculated at different time, and the values corresponding to the first sampling time are indicated as K_0 and

reported in Table 1. Values throughout the text are reported normalized by K_0. Sediment samplings were performed periodically for a total of 9 sampling dates. Sampling was performed always at the same time (11 – 12 am), under similar weather conditions.

Table 1 Values of hydraulic conductivity (in $m \cdot d^{-1}$) obtained at day 19 (K_0), for different depth intervals.

Depth	System	K_0 ($m \cdot d^{-1}$)
0-5	CF	8.5
	F	4.1
5-20	CF	65.2
	F	12.6
20-40	CF	10.1
	F	11.3
0-40	CF	14.6
	F	11.2

Sediments were obtained using a sediment core sampler (Eijkelkamp 04.23.SA) and each core was sliced in three depth layers (0-4 cm denoted as "surface sediment", 18-22 cm as "20 cm deep sediment", and 36-40 cm as "40 cm deep sediment"). Each sediment layer was homogenized, and subsamples of 1 cm^3 were collected using an uncapped syringe, and kept frozen (-20 ºC) until analysis to determine algae (chlorophyll-a) and EPS biomass content. For bacterial density and viability determination, samples were kept at 4 ºC during transport to the laboratory to proceed with the analysis on the same day. Specifications of each protocol analysis are detailed in *section 3.4 Sediment parameters, page 24.* After sediment sampling, one methacrylate empty column was placed at each tank to avoid sediment collapse, in an attempt to minimize the disruption of the flow field.

Table 2 Sampling design description: measured parameters and sampling periodicity

	Parameters	**Periodicity**
Piezometric heads in depth segments	❖ Hydraulic conductivity	Twice per week (n = 26 x 3)
Sediment layers: 0-4, 18-22, 36-40 cm	❖ Algae (chl-a concentration), EPS content, live bacteria and dead bacteria densities in sediment	9 sampling campaigns (n = 9 x 3)

6.3.2 Statistical analysis

Biomass data differences in depth was analysed with ANOVA (factor: depth) and further Tukey post-hoc analysis. ANOVA (factor: treatment) was also applied at each depth to determine if there were significant differences between systems. Temporal evolution of biomass data measured at each depth and system was fitted with LOESS curve fitting (n = 27 for data from the top and mid layers, n = 24 for the bottom layer). We generated regular sequences of times for further interpolation at each LOESS curve and obtain continuous data over time (frequency = 7 days). This allowed comparing temporal dynamics between systems and depths by using cross-correlation function estimation. Temporal K/K_0 values were also fitted with LOESS curve fitting to visualize system dynamics (n = 75) at each depth layer. Biofilm and K data were standardized separately for each depth and plotted in a PCA to identify biofilm parameters that contributed most to K variations with depth. All statistical analysis and plots have been performed using R software (version 3.1.1).

6.4 Results & Discussion

Sediment biofilm biomass (algae, EPS, and live and dead bacteria) showed a vertical gradient, with the highest values measured at the top layer, and decreasing in depth (Fig. 2); similar trends have been widely reported elsewhere (Mermillod-Blondin et al. 2005; Gette-Bouvarot et al. 2014; Yan et al. 2017). In the top layer, no differences were observed in biomass between systems except for the highest density of live bacteria in the CF system when the mean values are considered. Again in the top layer, variability was highest for all components in the CF system. In the mid and in the bottom layers similar concentration values were reported (in general at least one order of magnitude smaller than those from the topsoil); algae and bacterial density (both live and dead) were (statistically significantly) higher in the CF system compared to the F one; while EPS concentration showed no significant difference between systems.

In the top layer, positive correlation between systems (R^2 = 0.78-0.81 –algae-; R^2 = 0.57 –EPS-; R^2 = 0.92 –live bacteria-; R^2=0.93 –dead bacteria-) indicated similar colonization dynamics (Figs. 3 and 4). Biofilm structural components showed an increasing trend until day 40, when algal biomass and EPS content were almost stabilized; contrarily, bacterial density reached peaks values at around day 30, followed by a decrease in concentration values. Moreover, algae dynamics showed a slight delay in the CF system compared to F (the exact value could not be given due to the sampling intervals, but it was in the range of 0-7 days). Biofilm formation is a dynamic process characterized by several phases: attachment, adhesion, proliferation, biofilm maturation and release or detachment (Lappin-Scott and Costerton 1989). The initial biofilm formation phases may depend on substratum effects, specifically; attachment appears to increase as shear forces diminished and surface area increases (Donlan 2002) which could explain the slight delay on algal biomass colonization in CF compared to F. On the other hand, the biofilm decay phases (release and detachment) are influenced by decomposition and death rates of algae and bacteria as well as erosion rates of EPS (Romaní et al. 2008; Zhang and Bishop 2003), as well as interactions between biofilm components such as EPS consumption by bacteria (Gerbersdorf and Wieprecht, 2015) which could explain the observed temporal oscillations of algae and EPS in both systems.

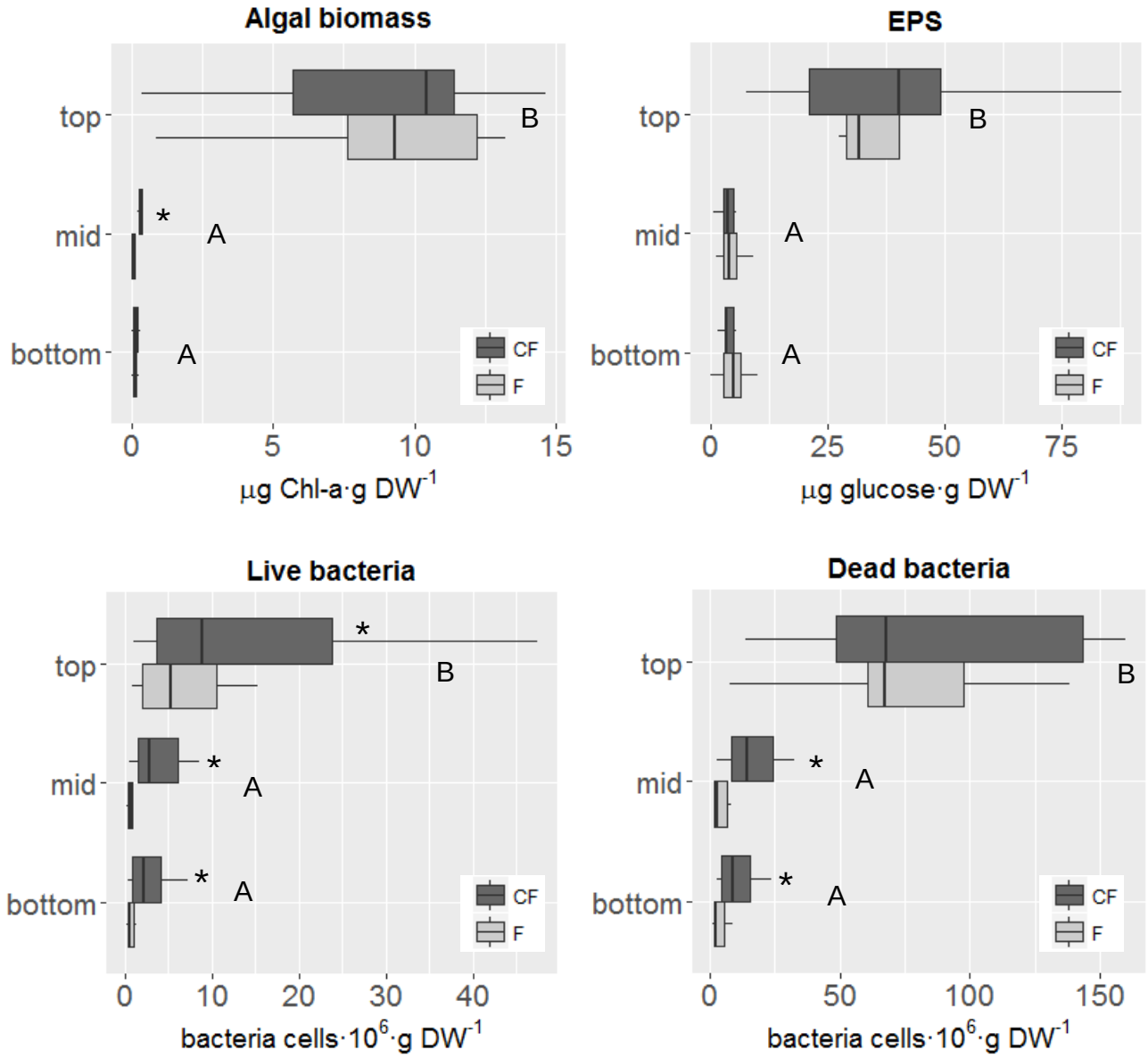

Figure 2 Content of biofilm structural parameters as a function of depth (top and mid depths based on n = 9 data; bottom n = 8) and treatments (CF in dark grey and F in light grey). Capital letters (A, B) indicate that the differences in depth are statistically significant (Tukey post-hoc analysis, $p < 0.05$), asterisks in CF indicate highest biomass (ANOVA, factor: system, $p < 0.05$).

Although differences in biofilm colonization in the top layer between systems were small, the increasing trend in algae, EPS and live bacteria at the end of the experiment in CF suggested that there was still available surface for biomass growth. This surface availability, coupled with high density of live bacteria, could indicate that biofilm in the top sediment layer in CF is still in a growing phase, while biofilm in F could be in a maturity stage.

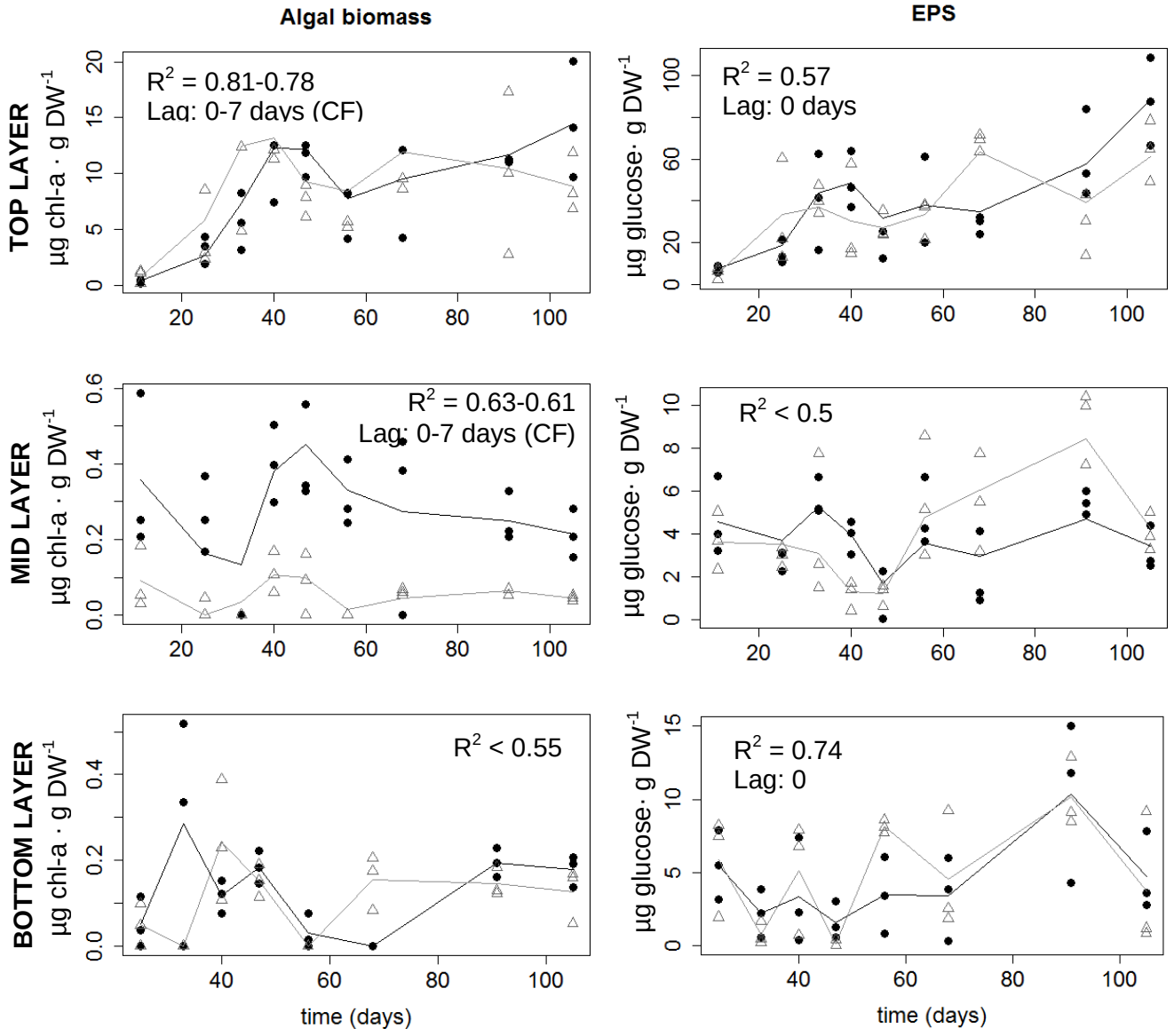

Figure 3 Temporal dynamics of algae and EPS concentrations measured at three depths. Colour lines show LOESS curve fitting (n = 27 in top and mid layers; n = 24 in the bottom layer) for each system (black circle: CF; grey triangle: F). R^2 values indicate temporal dynamics correlation between systems (R^2 critical = 0.5 in top and mid layers; R^2 critical = 0.55 in the bottom layer). Values below the R^2 critical indicate no significant correlation in temporal dynamics between systems.

Biomass accumulation in depth is determined by the combination of biofilm growth and biomass downward transport. Observations suggested that transport is most significant in the monolayer F system. Furthermore, different biofilm detachment ability between systems could in turn be linked to the flow velocities modulated by GSD. According to Laspidou and Rittmann (2002) and Gerbersdorf and Wieprecht (2015), high flow velocities (CF system) result in thin but strong biofilm matrices, while under low-flow conditions (F system), few cohesive biofilms are

observed, favoured by biomass transport in depth. Such effect of depth was analysed by performing time correlations in depth (Table 3). We found that algal biomass accumulation at depth 20 cm showed similar dynamics than those observed at the surface, but with a delay of 7 days (R^2 = 0.5 and R^2 = 0.73 in CF and F, respectively), suggesting the detachment and further vertical downward transport of the autotrophic biomass in both systems. Furthermore, the presence of degraded algae in depth is expected due to the extinction of incident light in depth thus limiting its growth and further is suggested by the increasing values of the Margalef Index (Table 4), indicating the occurrence of chl-a degraded pigments (Margalef 1983).

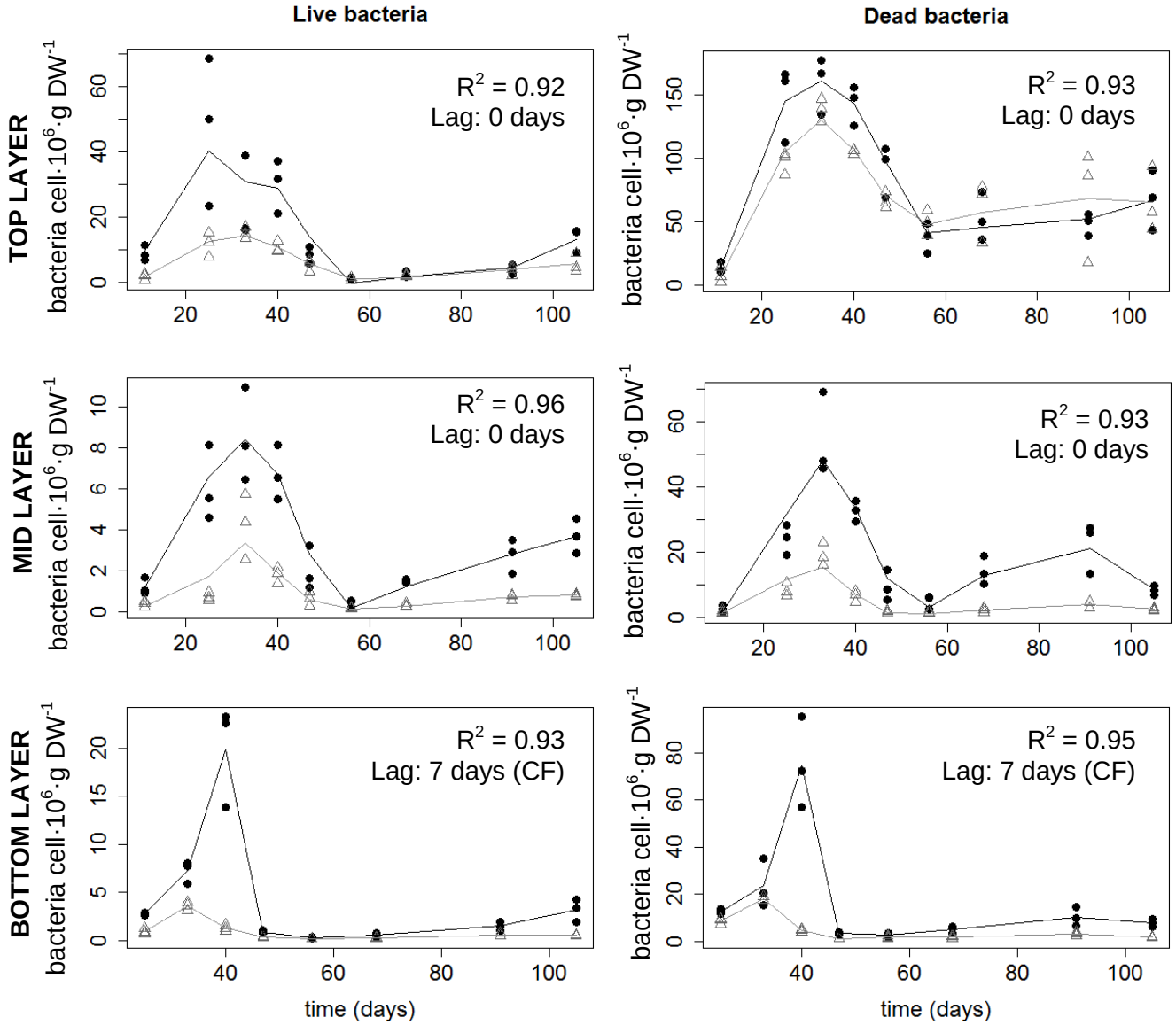

Figure 4 Temporal dynamics of live and dead bacteria densities measured at three depths. Colour lines show LOESS curve fitting (n = 27 in top and mid layers; n = 24 in the bottom layer) for each system (black circle: CF; grey triangle: F). R^2 values indicate temporal dynamics correlation between both systems (R^2 critical = 0.5 in top and mid layers; R^2 critical = 0.55 in the bottom layer).

EPS accumulation in depth is driven both by biomass downward transport and by EPS bacterial production. Our results showed no correlation in EPS dynamics between systems at 20 cm depth (R^2 < 0.5, Fig. 3), probably indicating different mechanisms of EPS accumulation in depth between systems. The low correlation in the CF system between EPS distribution in depth and the highest density of live bacteria at 20 cm depth (Fig. 4) suggest production by bacteria to be the main cause of EPS accumulation. Contrarily, the positive correlation (lag-phase about 0-14 days) between EPS in the top and mid layers in F (Table 3) could be related to EPS detachment and transport in depth. This could be linked to the presence of a degraded biofilm in the top layer of F that would favour biofilm detachment and further transport in depth, as well as low fluxes that could result on less cohesive biofilms in the upper layers, favouring EPS detachment.

Table 3 Time correlations of biofilm parameters in depth. Values in bold indicate significant correlation in depth for each parameter. Lag phase corresponds to the day where the maximum correlation is achieved.

		CF	F
Top →Mid n = 14 critical R^2 = 0.5	Algae	**R^2 = 0.50** Lag: 7 days	**R^2 = 0.73** Lag: 7 days
	EPS	R^2 < 0.5 Lag: -	**R^2 = 0.61** Lag: 0-14 days
	Live Bacteria	**R^2 = 0.87** Lag: 0 days	**R^2 = 0.92** Lag: 0 days
	Dead Bacteria	**R^2 = 0.85** Lag: 0 days	**R^2 = 0.83** Lag: 0 days
Mid →Bottom n = 12 critical R^2 = 0.55	Algae	R^2 < 0.55 Lag: -	**R^2 = 0.72** Lag: 0 days
	EPS	R^2 < 0.55 Lag: -	**R^2 = 0.63** Lag: 0 days
	Live Bacteria	**R^2 = 0.70 -0.75** Lag: 0 - 7 days	**R^2 = 0.95** Lag: 0 days
	Dead Bacteria	**R^2 = 0.60 -0.77** Lag: 0 - 7 days	**R^2 = 0.94** Lag: 0 days

A strong correlation of bacteria in the top and mid layers was found (R^2 values ranging between 0.85 and 0.93, see Table 3). Furthermore, similar dynamics of bacteria accumulation were observed based on the correlation between temporal data in both systems (Fig. 4). Unlike algae, bacteria dynamics at 20 cm depth did not show a lag phase which questions bacteria detachment from the upper sediment layer. Results suggest that bacteria accrual origins from biofilm growth and from bacteria carried in the inlet water that is being transported downwards allowing live and

dead bacterial attachment. This idea is in accordance also to highest bacterial density found in CF, associated with highest bacteria loads driven by downward flow. Although we did not measure bacterial density in the inlet water, other studies showed that WWTPs outflow water can reach values of around 10^8 cells·ml^{-1} (Vivas et al. 2017).

Table 4 Margalef ratio calculated for each system and depth. Letters next to depth categories indicate significant differences in depth (ANOVA, $p < 0.05$), no significant differences were found between systems.

Depth	System	Margalef index
Top[a]	CF	2.18 ± 0.26
	F	2.22 ± 0.11
Mid[b]	CF	3.20 ± 1.04
	F	2.66 ± 1.37
Bottom[b]	CF	3.81 ± 2.23
	F	2.88 ± 0.58

Comparing data at depths 20 and 40 cm, the F system showed a strong correlation in depth for all the parameters studied (algae $R^2 = 0.72$, EPS $R^2 = 0.63$, live bacteria $R^2 = 0.95$ and dead bacteria $R^2 = 0.94$, Table 3), indicating similar accumulation dynamics at both depths. However, the coarse-fine interface in the CF system may act as a filter, trapping algal and bacterial biomass, and hindering advective biomass transport from the interface downwards; this is shown by a lag-phase of 0-7 days on live and dead bacteria dynamics in depth, and by the non-correlation between algae and EPS dynamics from 20 to 40 cm depth (Table 3). These results agree with Zhong et al. (2017), who stated that heterogeneity of pore structure may change the direction and velocity of water flow causing three-dimensional mixing of particles.

The variations of biomass accrual reported in both systems influenced the large temporal oscillations in hydraulic conductivity dynamics (Fig. 5). The highest effect of bioclogging upon K/K_0 reduction was found in the top 5 cm (Fig. 5a), with values ranging from 0.43 – 0.80 (CF) and 0.32 – 0.69 (F), indicating a maximum K decrease of 57 % in CF and 68 % in F. In the top layer, the largest algal biomass developed and the related increase in EPS concentration drove the large reduction observed in hydraulic conductivity in both systems (Fig. 6a). The relation between algae and EPS production is well known, as large fraction of microphytobenthos (unicellular eukaryotic algae and cyanobacteria) primary production is directed into EPS synthesis (De Brouwer and Stal, 2001; Hoffmann and Gunkel 2011). The influence of

phototrophic organisms developed at surface sediments on bioclogging is in accordance to Gunkel and Hoffmann (2005) and Gette-Bouvarot et al. (2014). Densities of live and dead bacteria were not correlated to K variations in the upper layer of the systems studied.

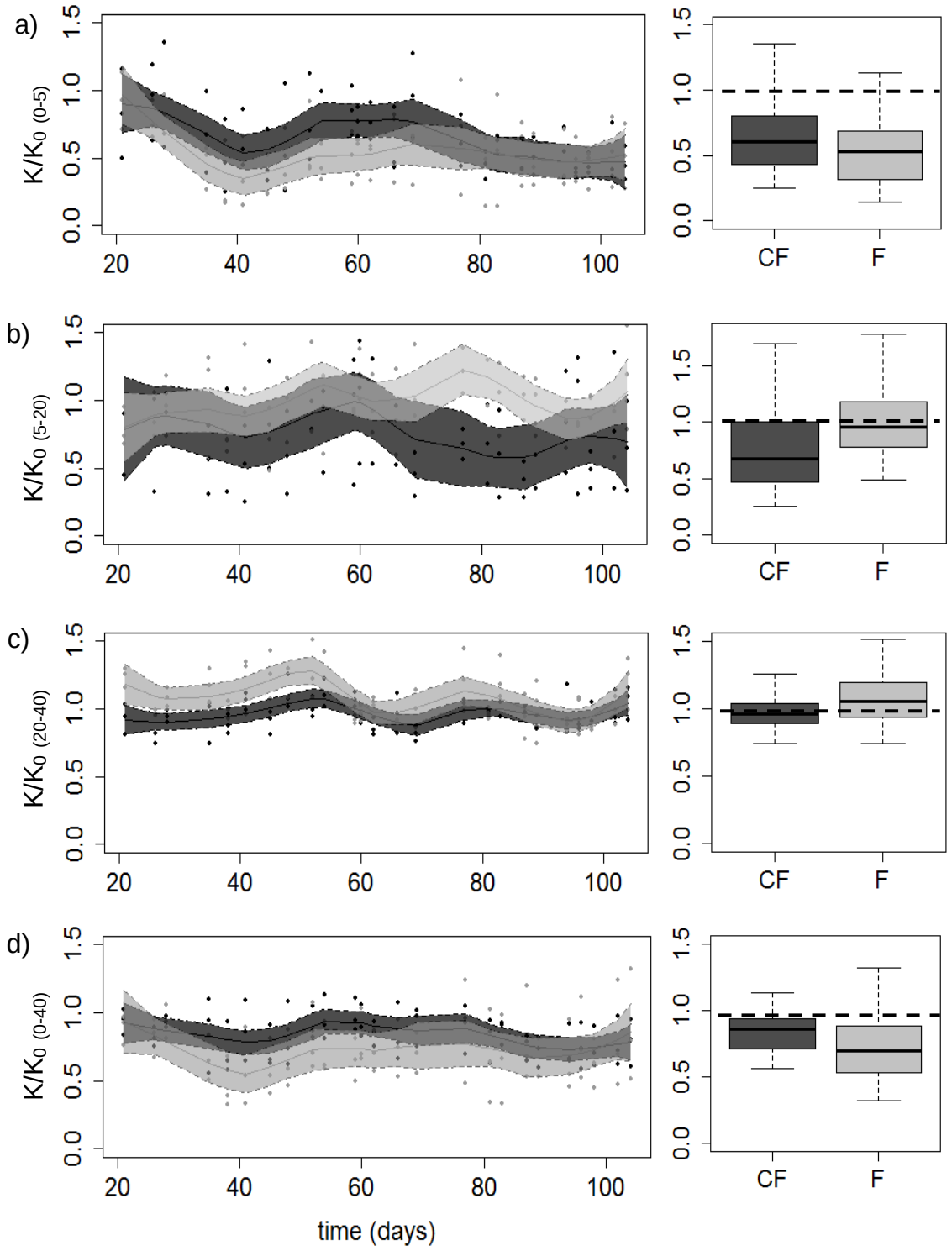

Figure 5 Left: Hydraulic conductivity variations (K/K_0) measured temporally at different depth layers (a: 0 to 5 cm depth, b: 5 to 20 cm, c: 20 to 40 cm and d: 0 to 40 cm) fitted with LOESS curve fitting (n = 75 for each curve) and polygon bounds indicating 95 % of data lying under the normal distribution hypothesis for each curve. The dark curve is for CF while light curve is for F. Right: boxplots of measured data. The $K=K_0$ line is also plotted (dashed line).

From 5 to 20 cm depth (Fig. 5b), K/K_0 ranged from 0.46-1.00 in CF and from 0.77-1.18 in F (maximum K/K_0 reduction of 54 % in CF and 23 % in F). Significant differences were found between systems at 20 cm depth, where the CF system was characterized by higher bacterial and algal biomass and highest reduction of hydraulic conductivity than F (Fig. 6b). At this depth, K reduction was correlated to algal and bacterial biomass, confirming that their accumulation in the interface could have caused bioclogging in the CF system to extend down to 20 cm. Last, from 20 to 40 cm depth (Fig. 5c), K/K_0 values ranged 0.89 – 1.04 in CF and 0.94 – 1.19 in F. Interestingly, these small variations observed in time were strongly correlated with EPS concentration in deep sediments, while bacterial and algal biomass measured at 40 cm depth did not show correlation to K variations (Fig. 6c). Related to this, high EPS concentrations at 40 cm depth (accounting for 15-20 % of the overall carbon biomass in the biofilm) are directly linked to large $K_{20\text{-}40}$ reductions in both systems, which have been also previously reported in Rubol et al. (2014).

Although we could not separate colloidal from bound EPS fractions, microalgal primary production has been related to the presence of labile colloidal EPS fraction, a relation that increasingly decoupled with depth below the photic zone (Gerbersdorf et al. 2009). These authors stated that in deep layers, bacterial densities showed correlations to the more refractory fraction of EPS. Related to this, biomass accumulation in depth could increase over time as a result of bacteria reaching the bottom of the filter and producing EPS. Over time, biomass accumulations could cause deep-clogging, a very difficult problem to mitigate, as opposed to surface clogging which can be mitigated with resting periods or surface scarification (Aronson and Seaburn 1974). Dividing EPS concentrations by live bacteria density, the highest values are found at depth 40 cm, an indication that the EPS production per bacterial cell (and thus, deep clogging) is largest in depth.

Focusing on overall hydraulic conductivity reductions (depth 0-40, Fig. 5d) the F system exhibited higher K reduction (12-47 %) than CF (6-29 %). Accordingly, bioclogging in CF system extended deepest, due to the effect of the coarse-fine sediment interface that promoted biomass accumulation. However, as a whole, the F system showed a highest degree of bioclogging, probably due to the low initial porosity value.

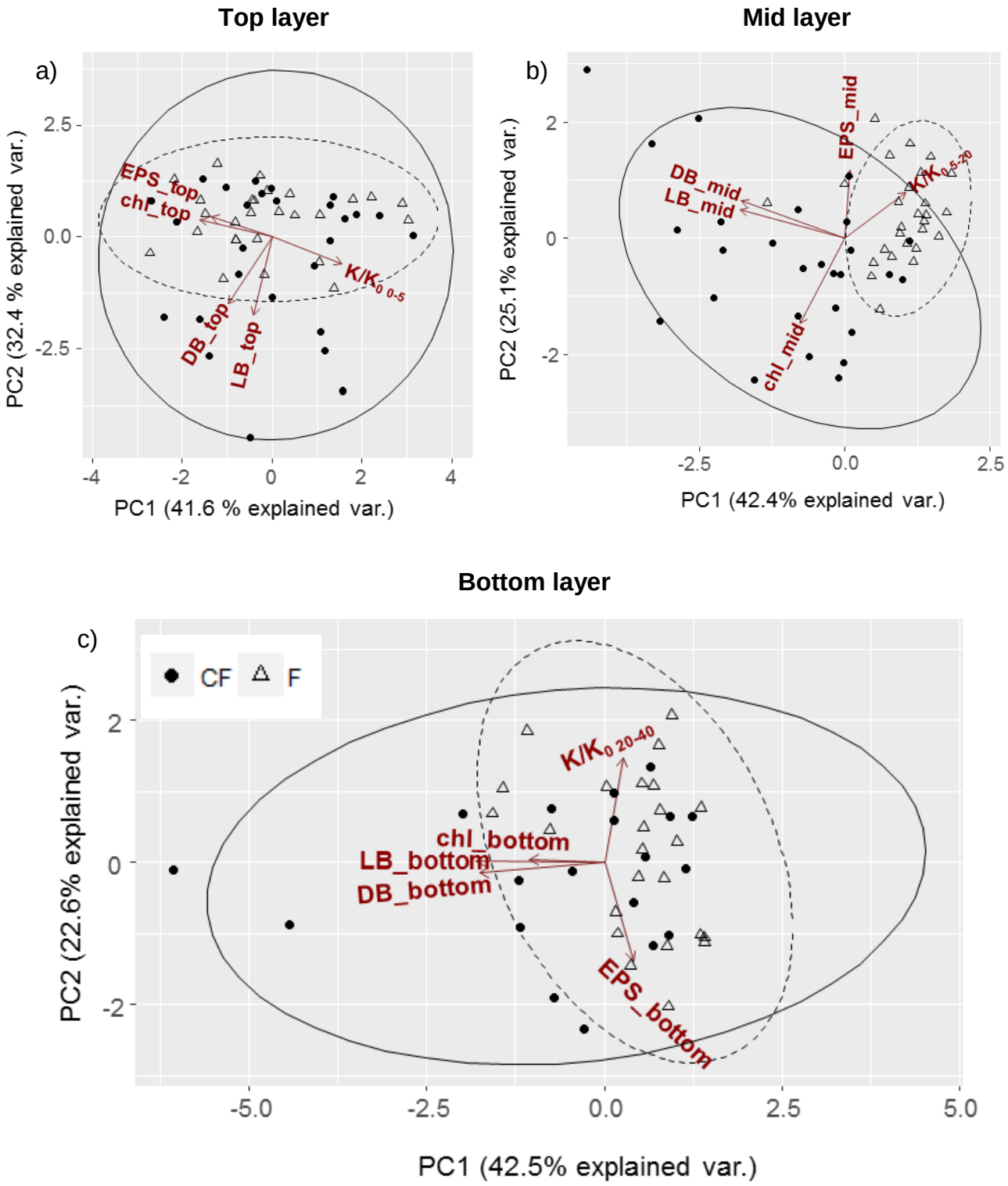

Figure 6 PCA including hydraulic conductivity variations and biofilm structural parameters at each sediment layer analysed. Solid ellipse assumes the multivariate normal distribution of the bilayer coarse-fine samples, dotted ellipse assumes the multivariate normal distribution of the monolayer fine samples.

Analysing organic carbon (OC) contribution of each biofilm component as a function of depth and system (Fig. 7), we found that algae contributed the most to the overall OC measured in sediments; its contribution decreased from the top (≈ 90 % of carbon) to the mid and bottom layers, where it still represented 50 % of OC of the sampled sediments, while the contribution of EPS and live and dead bacteria increased from top to mid and bottom layers in both systems. Although the absolute values of the percentages shown in Fig. 7 can be biased by the use of general conversion factors (i.e. assuming all bacterial cells the same size, all algae the same content of chlorophyll, all EPS made of glucose). It should be noted that although algae at 40 cm depth represented the highest percentage of biofilm C, it had no influence on K variations, while EPS (representing at most 25 % of biofilm carbon) did.

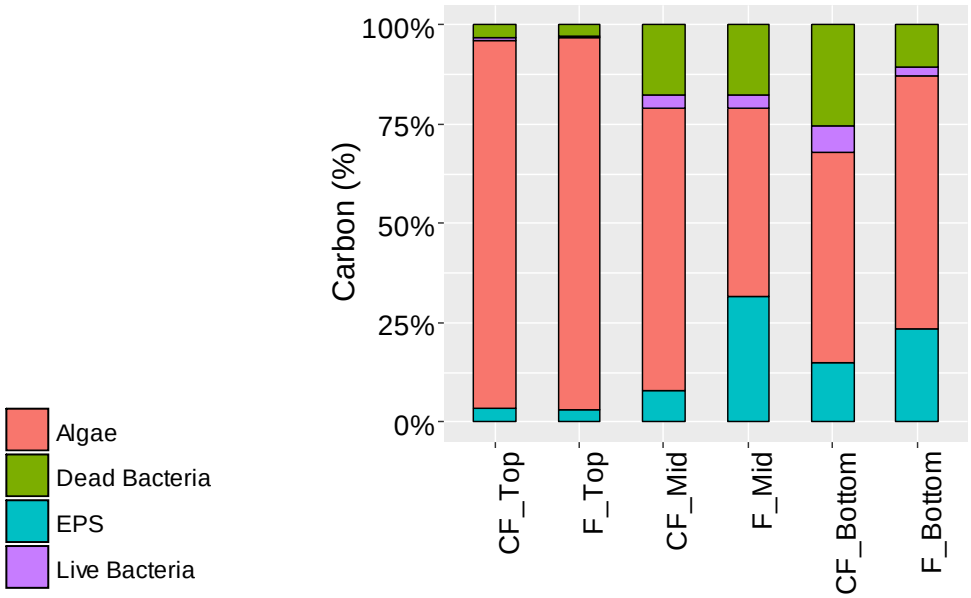

Figure 7 Carbon contributions (as percentage from the total biofilm C) for each of the biofilm components: algae, dead bacteria, EPS and live bacteria as a function of depth and system.

6.5 Conclusions

A 104 day long outdoor infiltration experiment was performed in 40 cm deep sediment tanks, simulating infiltration systems composed of two different sediment grain size distributions. One included a coarse sediment placed on top of a fine one (CF system) and a second one involved a homogeneous fine sand (F system). Observations of four biomass components (algae, EPS, live bacteria and dead bacteria) were recorded at three depths and at different times. Several conclusions can be drawn from this work.

Grain size, and correspondingly pore size are drivers of biofilm formation, due to the higher space availability for colonization in coarse sediments with respect to fine ones which could be related to biofilm reaching a maturity status earlier in the fine sediments. This, together with the low-flow conditions in fine sediments that could propitiate the formation of lower cohesive biofilms, eventually result in enhanced biomass detachment from the top sediment layer.

Algal biomass is the main responsible of bioclogging in the topsoil. Detached algae can reach depths of at least 40 cm in both fine (0.075-0.250 mm) and coarse (0.9 - 1.2 mm) sediments. However, algae in deep sediment layers were found in low concentrations and resulted to be highly degraded and with no direct implications on deep clogging.

The presence of a coarse layer of sediment placed on top of a finer one results in deep bioclogging, mostly accumulating at the interface from coarse to fine sediment; this interface acts as a filter of biomass that is being advected downwards; furthermore, it propitiates the colonization of new biomass. In addition, the interface causes a rupture in the dynamics of transport in depth. However, when the full systems are compared as a whole, overall bioclogging is somewhat similar regardless the vertical distribution of sediment sizes. A reason for this result is that the monolayer fine system results in large overall (non-localized) bioclogging due to lower initial porosity than the bilayer coarse-fine system, thus compensating the effect of interface clogging in the latter system.

Even though EPS was not the main structural component in deep biofilms, it was the main cause of hydraulic conductivity reductions in the bottom sediment layer. Accordingly, inlet water coming from WWTPs can be a relevant source of live and dead bacteria in infiltration systems, and specifically, high densities of live bacteria (main producers of EPS in heterotrophic biofilms)

can be transported to depths of at least 40 cm in fine and coarse sediments and therefore indirectly be potential to cause deep clogging due to EPS release.

GSD was a controlling factor for biofilm growth dynamics, which could determine the maturity state of biofilm, and therefore influence biomass detachment and further transport in depth (higher in fine sands). Early colonization in the monolayer fine system together with lower flow has promoted larger biomass detachment and higher biomass transport downwards compared to the bilayer coarse-fine system.

7 General Discussion

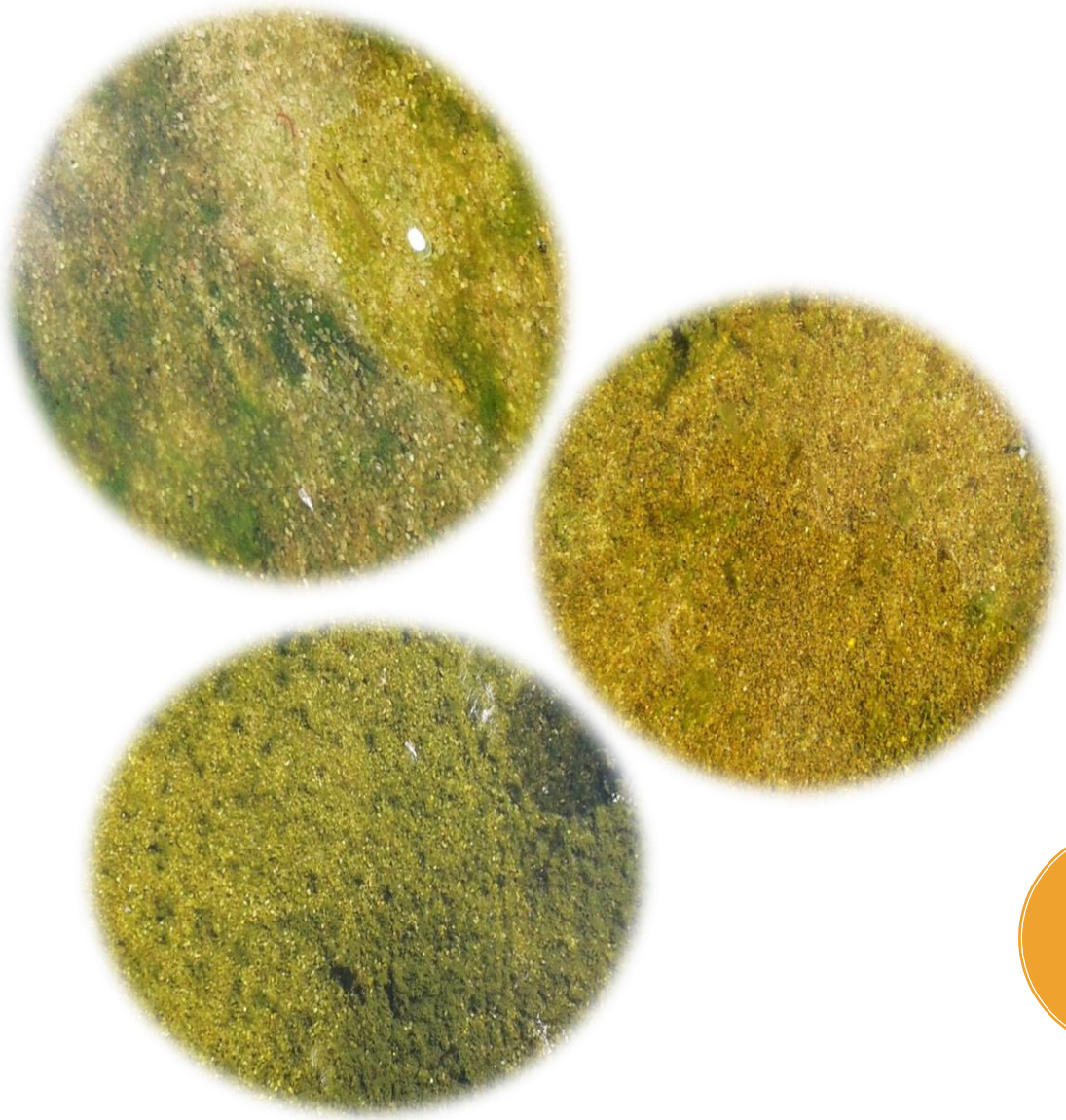

Media characteristics of sand-based treatment systems are among the most important design criteria as they can be the most significant factor affecting costs of sand-infiltration systems (Ball 1997). According to Bekele et al. (2013), there is a critical need for more information about wastewater infiltration designs that are sustainable, cost-effective and meet removal performances. The main objective of this thesis was to study the influence of sediment grain size distribution on biogeochemical processes and on biofilm accumulation in depth in porous media mimicking their use as tertiary water treatment technologies for organic matter and nutrient removals. From this thesis work, it can be stated that biogeochemical processes in infiltration systems were affected by chemical species in the inlet water and sediment GSDs that were responsible for modifications in autotrophic and heterotrophic biomasses, C:N:P molar ratios in sediments, input loads, HRTs, advection times and flow velocities, among others. Physical and biological processes interact each other to define the final porous media performance output. In this general discussion a comparison between the two main experiments (columns versus tank experiments) is performed in order to highlight these interactions and better define pros and cons when defining a GSD in sand-infiltration systems. Data used for the general discussion are grouped in Tables 1-3.

Table 1 Biofilm biomass parameters reported in both experiments

	Columns experiment					Tanks experiment	
	Coarse	**Fine**	**Coarse-fine**	**Fine-coarse**	**Mixture**	**Fine**	**Coarse-fine**
Algae sup (µg Chl·gDW^{-1})	2.8	3.6	3.3	5.1	3.11	**10.4**	**10.8**
Algae 20 cm	0.06	0.05	0.4	0.07	0.1	0.05	0.3
Algae 40 cm	0.08	0.2	0.18	0.08	0.2	0.12	0.14
Live bact sup (cells x 10^{6}·gDW^{-1})	**12.2**	**3.8**	**6.6**	**6.4**	**3.9**	**7.9**	**16.7**
Live bact 20 cm	2.7	0.9	3.7	0.73	0.7	1.1	4.3
Live bact 40 cm	1.2	0.8	1.1	0.77	0.6	1.1	2.2
Dead bact sup (cells x 10^{6}·gDW^{-1})	20.5	38.5	47.3	43	32.7	**87.4**	**83.5**
Dead bact 20 cm	9	3.02	19.4	1.97	3.5	5.4	18.7
Dead bact 40 cm	8.3	2	4.18	1.23	1.6	5.04	9.5
EPS sup (µg glucose·gDW^{-1})	6.0	5	3.7	4.3	5.3	**39.8**	**41**
EPS 20 cm	2.1	2.8	2.4	2.5	1	4.7	3.8
EPS 40 cm	2.7	3	2.8	2.1	1.3	4.9	4.4
Margalef sup	**3.1**	2.1	2.5	2.2	2.5	2.2	2.1
Margalef 20 cm	4.9	5.85	3.1	3.5	3.71	2.7	3.2
Margalef 40 cm	3.8	3.02	2.6	3.1	3.35	2.9	3.8

Table 2 Comparison of physic-chemical parameters in the experiments performed[*γ]

	Columns experiment					Tanks experiment	
	Coarse	**Fine**	**Coarse-fine**	**Fine-coarse**	**Mixture**	**Fine**	**Coarse-fine**
Total volume of sediment (cm^3)	664					186160	
K_0 ($m \cdot d^{-1}$)	8.23	0.62	1.28	1.22	0.63	11.2	14.6
K/K_0	0.17	0.28	0.29	0.18	0.14	0.71	0.81
Advection time (s)	282 - 1757	834 - 3738	714 - 3271	720 – 3379	500 – 3511	12119 - 13920	5965 - 8466
Flow ($cm^3 \cdot s^{-1}$)	0.95 - 0.17	0.25 - 0.07	0.36 - 0.10	0.31 - 0.05	0.42 - 0.06	6.1 - 4.33	11.3 - 9.15
HRT (s)	155	1277	426	976	535	4137	1980
Inlet water C:N:P molar	**23:40:1**					**548:370:1**	
DO sup ($mg\ O_2 \cdot L^{-1}$)	5.46	8.22	5.84	7.75	8.66	7.3	6.5
DO 20 cm	3.86	3.47	2.98	5.43	4.86	2.6	3.9
DO 40 cm	2.92	1.91	2.15	3.44	3.33	2.9	2.9
Ammonium rate ($\mu g\ N \cdot L^{-1} \cdot s^{-1}$)	**-1.7**	-0.52	**-0.75**	-0.36	-0.49		
Nitrate rate ($\mu g\ N \cdot L^{-1} \cdot s^{-1}$)	2.14	0.38	0.63	0.22	0.49		
Ammonium rate ($\mu g\ N \cdot cm\text{-}^{3} \cdot d^{-1}$)						-0.10	**-0.49**
Nitrate rate ($\mu g\ N \cdot cm^{-3} \cdot d^{-1}$)						-2.2	**-4.0**
P rate ($\mu g\ P \cdot cm^{-3} \cdot d^{-1}$)						-0.011	**-0.026**
DOC rate ($\mu g\ C \cdot cm^{-3} \cdot d^{-1}$)						-2.15	**-3.01**

[*] Grain size for the coarse sediment was between 0.9 – 1.2 mm with a surface grain size area between 3 – 4 mm^2. Grain size for the fine sediment was between 0.075 – 0.250 mm with a surface grain size area between 16.32 – 54.4 mm^2. Grain size distributions for each one of the systems are detailed in *Figure , section 4.3.1 Experimental design and sampling, page 35* (columns experiment) and in *Figure 2, section 5.3.1 Experimental design and sampling, page 60* (tanks experiment).

[γ] Grey shaded areas indicate there is no value for that data. It is due to the fact that process rate units were different between experiments. In the columns experiment rates were expressed as $\mu g \cdot L^{-1} \cdot s^{-1}$, while in the tanks experiment rates were expressed as $\mu g \cdot cm^{-3} \cdot d^{-1}$.

Table 3 Enzymatic activity ratios in sediment GSDs and in depth*

	Columns experiment					Tanks experiment	
	Coarse	**Fine**	**Coarse-fine**	**Fine-coarse**	**Mixture**	**Fine**	**Coarse-fine**
GLU:LEU sup	0.98	0.67	0.99	0.64	1.28	**0.21**	**0.20**
GLU:LEU 20	0.47	0.36	0.7	0.2	0.37	*0*	0.02
GLU:LEU 40	0.41	0.37	0.26	0.17	0.43	*0*	*0*
GLU:PHOS sup	0.8	0.55	0.9	0.46	0.68	**0.47**	**0.44**
GLU:PHOS 20	0.56	0.37	0.56	0.20	0.44	*0*	0.06
GLU:PHOS 40	0.60	0.30	0.22	0.18	0.31	*0*	*0*
PHOS:LEU sup	1.21	1.19	1.10	1.41	1.89	**0.45**	**0.45**
PHOS:LEU 20	0.84	1.22	1.22	1.19	0.9	0.4	0.31
PHOS:LEU 40	0.70	1.37	1.14	1.06	1.55	0.4	0.27

*Zeros in the tanks experiment ratios are due to the fact that the values of β-glucosidase activity were below the limit of detection.

7.1 Relevance of GSDs

The ability of biofilms to colonize surfaces has long been related to the sediment grain size. Accordingly, fine sediments (higher surface area) have been linked to larger biomasses than coarse sediments (Bott and Kaplan 1985). However, this statement should be carefully interpreted since our results suggested that **not only colonization surface area determines biofilm establishment and growth in surface sediments but also contact time between sediment and water (determined by advection times)**. In fact, Crites and Tchobanoglous (1998) stated that the GSD is an important design criteria as it influences the retention time of water passing through the media. According to this, in the top sediment layer, the *coarse* system (colonization surface area ≈ 3 - 4 mm^2 and the lowest advection time) showed less biomass (focusing on algae) than the other systems. However, the *coarse-fine* system (same colonization surface area than the coarse one but double advection times) showed similar biomasses than the other GSDs. In depth, the *coarse* system showed higher biomass possibly due to greater interstitial fluxes which determine availability of nutrients, organic matter and electron acceptors in depth (Malard et al. 2002) (Fig. 1).

Inlet water in infiltration systems could carry high bacteria densities that could be retained in the top sediment layer or even to be interstitially transported to bottom sediment layers. Bacteria loads are proportional to input loads in our systems. In this way despite affirming

that the *coarse* system showed less biomass in the top layer, it showed higher live bacteria density (Fig. 1).

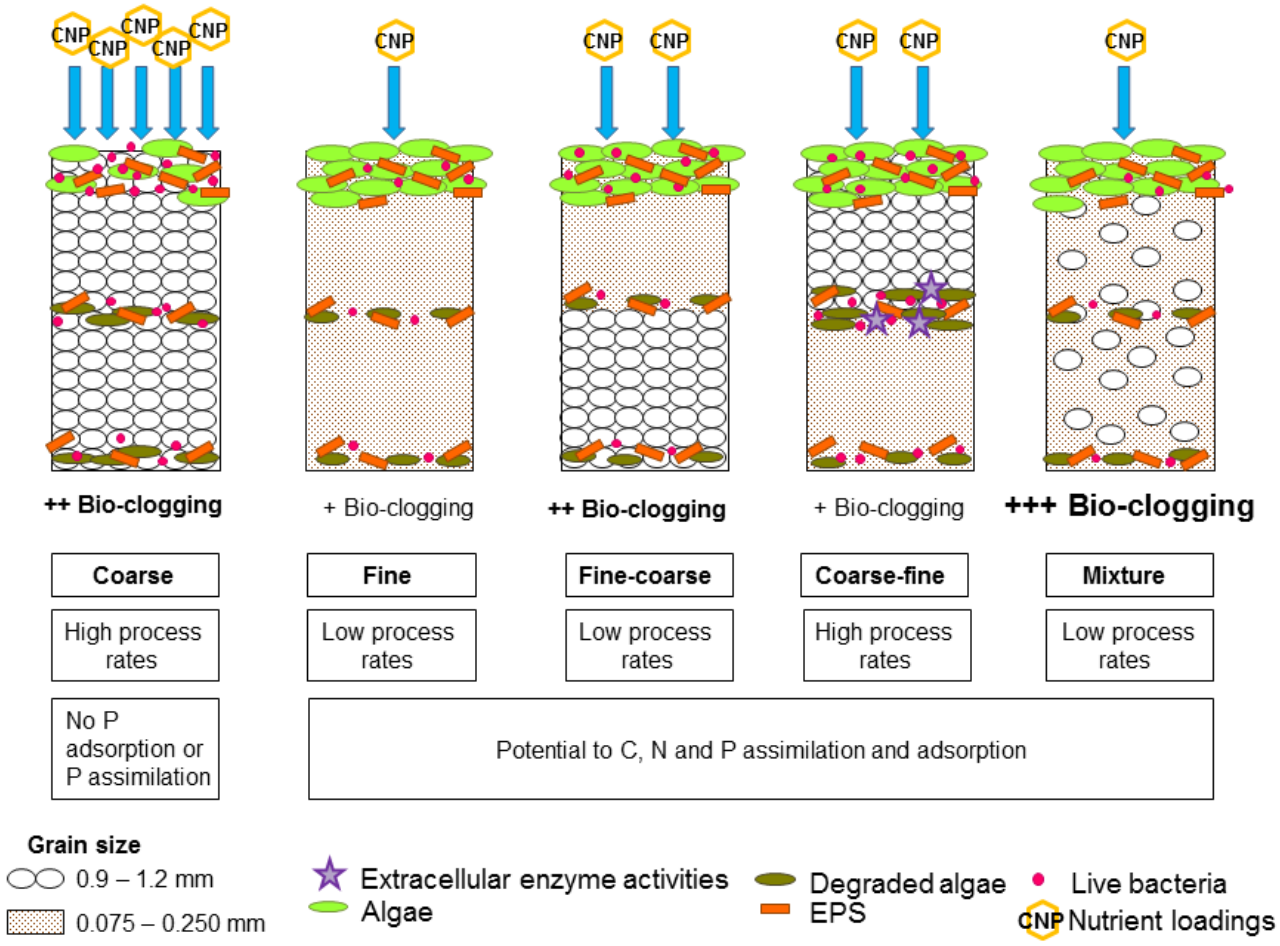

Figure 1 Scheme of biofilm biomass distributions in depth in different GSDs and their implications on hydraulic conductivity reductions, process rates and nutrient accumulation in sediments.

At the same time, high input loads and high live bacteria densities were linked to high biogeochemical process rates (e.g. nitrification) (*coarse* and *coarse-fine* systems), which agrees with Moorhead and Sinsabaugh (2006) who stated the rate of biodegradation to be limited by substrate and by microbial activity. In the *fine-coarse*, rates of biogeochemical processes could be constrained to the upper 20 cm of sediment -due to high flow velocities when reaching the coarse layer as well as low microbial biomass in depth- resulting in 20 cm depth of effective sand filtration while the other systems showed 40 cm depth of effective sand filtration (Fig. 1).

However, rates of physical adsorption and nutrient assimilation in sediments were dependent on more factors. On one hand, physical adsorption of P as well as nutrient

assimilation in sediments is determined by flow rates and time contact between water and sediment (Reddy et al. 1996). Furthermore, assimilation of C, N and P in sediments is determined by the fundamental ratio C:N:P 106:16:1 (Redfield 1958) and fulfilling this ratio, assimilation as it is a biological process is linked to sediment biomass. Given this, **biological assimilation and physical adsorption in sediments were hindered in the *coarse* system possibly due to high flow velocity and low advection times resulting in small contact time between water and sediment as well as slightly low algal biomass on the surface and higher Margalef index** (indicating algal biomass highly degraded which could be less potential to assimilate nutrients) (Fig. 1). The other GSDs, showing higher advection times and similar biomasses between them in the top sediment layer were all potential to remove P from interstitial water. Results from the tank experiment confirm this idea, as **no differences were found in the assimilation rates of C, N and P between the *fine* and the *coarse-fine* systems in the top layer possibly due to similar biomasses and the fact that the *coarse-fine* showed an advection time far higher than the *coarse* and therefore favoured the water-sediment contact time and allowed for both physical adsorption and biological assimilation to occur**.

Comparing both experiments, the greatest bioclogging was observed for all treatments in the columns experiment although showing lower biomass than the tank experiment. From these observations we can conclude that **filter size (total volume of sediment) is a main factor to consider when designing infiltration systems and assessing their clogging potential**. More specifically, one key design criteria is the ratio bed depth divided by the average filter size, the more media grains (more volume of sediment), the greater the effective filtration of water (French 2012). In this sense, infiltration systems with lower input loads but lower volume of sediment have suffered in a shorter time a greater K reduction. Although clogging in the columns experiment occurred more rapidly, from the K/K_0 data measured on the last day of experiment some conclusions about the GSDs and bioclogging can be drawn.

Our results suggested bioclogging to be a conjunction between sediment porosity, sediment biofilm biomass and input loads. The **low coefficient of uniformity of the *mixture* system could be related to higher bioclogging** due to a reduction in the interstitial space (Darby et al. 1996; Crites and Tchobanoglous 1998) despite showing low input loads and low biomass. Surprisingly, the *coarse* system has suffered higher bioclogging, as well as the *fine-coarse*

system. Clogging in the *coarse* system could be due to high input loads and high density of biomass in depth; whereas in the *fine-coarse* system it would be given by the conjunction of high input loads and low initial porosity in the top layer of the filter. In the tank experiment, it has been shown that, despite the fact that both systems (*fine* and *coarse-fine*) showed the same biomass in the surface layer, bioclogging was greater in the *fine* system due to the low porosity of the fine sediment (Fig. 1).

7.2 Chemical characteristics of inlet water

GSDs determine the contact time between water and sediments as well as input loads (these linked to flow rates), and sediment porosity, thus influencing biofilm establishment and growth, rates of biogeochemical processes as well as bioclogging in infiltration systems. However, the achievement of one biogeochemical process or another is also strongly influenced by the chemical characteristics of the inlet water that at the same time may influence removal efficiencies in infiltration systems.

Inhibition of denitrification in the columns experiment could be given by C limitation in the inlet water (C:N = 0.5), while in the tank experiment there was not carbon limitation (C:N = 1.5). Accordingly, Shi et al. (2016) stated that C:N ratio is the main control parameter for denitrification process. In situations of insufficient carbon, nitrate and/or nitrite accumulates, as seen in the column experiment (Table 2). Denitrification has long been linked to low concentrations of DO (Tiedje 1988), however as our experiments showed similar DO concentrations in depth it was suggested that DO conditions were not the limiting factor for denitrification. Comparing experiments, **higher GLU:LEU and GLU:PHOS ratios in the columns experiment (in all treatments) reinforce the idea of a possible limitation in C availability in the inlet water of the columns experiment.** In this way, microbial communities release β-glucosidase enzymes to degrade carbon compounds and to make them assimilable.

The inlet water ratios in the tank experiment (548:370:1) suggests P limitation constraining P assimilation as P deficient growth consistently occurred when TDN:TDP > 50 (Guildford and Hecky 2000). **In situations of nutrient molar equilibrium infiltration systems could be potential to achieve greater P removals due to greater P assimilation in sediments which depends on the fundamental Redfield ratio (C:N:P = 106:16:1)**. As the inlet water in the tanks

experiment showed P limitation (C:P = 548; N:P = 370) we would expected higher phosphatase activity as it is synthesized at low levels of PO_4^{-3} and repressed when P becomes available; therefore being suggested as a P-deficiency index (Caruso 2010). However, low ratios of GLU:LEU, GLU:PHOS and PHOS:LEU in the tank experiment indicated low β-glucosidase and phosphatase activities against the high leucine-aminopeptidase activity.

Leucine-aminopeptidase activity has been linked to DON concentrations (Newman 2011). DON concentration can account for even up to 80 % of the total nitrogen in WWTPs effluent (Chen et al. 2011). According to Hu et al. (2018) the greatest portion of DON is classified as MW < 3 kDa. Forms of DON >1 kDa could be assimilated by microbial populations (algae and bacteria –Liu et al. 2012-) after the use of proteolytic enzymes (e.g. leucine-aminopeptidase) (Berges and Mulholland 2008) and hence can play an important role in N cycling (Vaquer-Sunyer et al. 2015). **The high leucine-aminopeptidase activity in the tank experiment could have limited β-glucosidase activity since DON degradation could provide both C and N to the microbiota** (Chrost 1990, Garcia et al. 2015) **and thus when DON is available bacteria prefer to use this source instead of polysaccharides (providing only C)**.

7.3 Benefits of a bilayer coarse-fine grain-size distribution

This thesis suggests that a bilayer coarse-fine system can provide some advantages compared to the other GSDs studied. **The *coarse-fine* bilayer system achieved higher rates of infiltration which means it requires a smaller area per volume of infiltrated water than monolayer systems of fine sediment**. In addition, the bilayer system is **potential to accumulate similar densities of biomass in the top layer but resulting in lower bioclogging due to the greater porosity of coarse sands** compared to fine ones. Eventually, this increases the longevity of the system, since when an infiltration system significantly reduces its infiltration capacity it must stop and the top sediment layer must be scarified or removed (Hilding 1994), after which sufficient time must be waited for allowing the biofilm to recolonize the sediment (few days). Increasing time between scarification periods increases the performance of these systems. In both experiments **the interface in the *coarse-fine* system accumulated large biomasses** (Table. 1) **and higher assimilation rates possibly due to high density of live bacteria** and the effect of flow disruption when interstitial water reaches the interface. **This interface expressed greater**

extracellular enzymatic activities than the other GSDs acting as a hot spot of microbiological activity (Fig. 1).

However, in GSDs with coarse sediment in the upper layer (*coarse* and *coarse-fine* systems) higher densities of live bacteria were found in the bottom of the filter. Accordingly, these systems could be more potential to start up deep-clogging due to the possible release of microbial EPS at the bottom of the filter. However, there were no differences in EPS concentrations between systems in the bottom layer (Fig. 1). This could indicate that bacteria reaching the bottom in the *fine* system produce higher amounts of EPS per cell, or, as explained in Chapter 3, that in fine systems lower flow and biofilm maturity increases EPS transport downwards.

Overall, the bilayer system is more microbiologically active than the other GSDs. **However, we must bear in mind that the occurrence of biogeochemical processes is strongly dependent on the chemical characteristics of the inlet water.** According to Goren et al. (2014), pilot testing is always necessary when designing slow sand filters as engineers are not able to predict the performance of a sand filter with a specific quality of the inlet water.

8 General conclusions and Future perspectives

8.1 General Conclusions

- Biofilm establishment and growth in surface sediments of fine and coarse sands in infiltration systems has been more influenced by the contact time between sediment and water (determined by the GSD) than by the colonization surface area.
- Inlet water in infiltration systems could carry high bacteria densities that are potential to be retained in the top sediment layer or to be interstitially transported up to the bottom. These bacteria play an important role in infiltration systems being positively linked –together with the input loads- to biogeochemical process rates. However, these bacteria could produce EPS, even in the bottom sediment layer, thus being potential to contribute to deep-clogging.
- Physical adsorption and nutrient assimilation rates mostly depend on biofilm biomass and on hydraulic parameters such as flow velocities, advection times and contact time between sediment and water. For this reason, coarse sands following a homogeneous distribution have not been able to remove phosphorous compounds from water, but a bilayer coarse-fine system has demonstrated to remove phosphorous compounds even in the coarse sediment layer since the advection time in this system is much higher than that of a homogeneous coarse system.
- Bioclogging has been proved to be determined by a set of factors such as sediment porosity, coefficient of uniformity, sediment biofilm biomass, input loads and the total filter size (total volume of sediment).
- Chemical characteristics of the inlet water (specifically C:N:P molar ratios in water) determine biogeochemical processes occurring in infiltration systems. High GLU:LEU and GLU:PHOS ratios in sediments could be indicative of C limitation in the inlet water which could inhibit the denitrification process and TDN removal efficiencies. P limitation could constrain P assimilation in sediments (follows the fundamental Redfield ratio C:N:P = 106:16:1) and therefore P removal efficiencies.
- The *coarse-fine* bilayer system achieved higher rates of infiltration which means it requires a smaller area per volume of infiltrated water than monolayer systems of fine sediment. In addition, it is potential to accumulate similar densities of biomass in the top layer but resulting in lower bioclogging due to the greater porosity of coarse sands. Overall, the bilayer system is more microbiologically active than other GSDs.

8.2 Future perspectives

From the knowledge gained in this PhD thesis several recommendations can be proposed when implementing sand-filtration systems as water treatment technologies. Sand-filtration systems could and should be implemented in WWTP with medium loads and where the availability of surface area for the treatment was feasible, as a natural environmentally friendly and low-cost technology of water quality improvement. In addition, sand-filtration systems would be very beneficial in headwater streams in order to minimize the impact of nutrient loads in the river head as this impact can be cumulative downstream, with overall increasing quality of freshwater resources. They would also be beneficial to apply in areas affected by temporary river flows, and therefore where WWTPs discharge contributes to a high percentage of the river water especially during periods of low flow, when the dilution capacity of the rivers is low. Preliminary studies should be carried out to see which are the potential WWTPs to apply an extra treatment based on sand-filtration systems, and specifically determine which WWTPs do not have a tertiary treatment yet, what surface area would be needed to treat the flow rates of these WWTPs, and which are the critical zones that are more susceptible to suffer from eutrophication due to low dilution capacity of rivers. Where the infiltration system was feasible, it would be good to consider the option of setting a bilayer coarse-fine system since some of the advantages that have been seen with this thesis are that the bilayer system achieves P removal, it deals with higher loads at a smaller surface area due to the higher process rates achieved, and lastly it reduces the bioclogging thus extending the longevity of the system and reducing the periodic maintenance of it (i.e. scarification periods) compared to other GSDs studied.

Further studies should focus on the role of the surface water layer in infiltration systems, specifically the role of algae in infiltration systems. Through this work we have seen that the surface water layer increases removal efficiencies of N and P since algae have a great potential for removal of nitrogen and phosphorus as they use them for their growth; however the surface water layer can decrease the removal efficiency of C in infiltration systems due to algal exudates. Due to photosynthetic activity, the surface water layer is a dynamic environment with strong different patterns during day and night cycles. Further work will be necessary to clarify the effects of day/night cycles in the surface water layer on physic-chemical parameters in infiltration systems and its implications on the system performance. It would be very positive to increase

knowledge on these cycles with the aim of incorporating a surface water layer in infiltration systems in order to achieve economic performance (e.g. biofuel) through algae that would grow in this water layer and which should be harvested periodically to avoid anoxia situations in the top layer of the sediment.

In addition, another future research line could be focused on the presence, origin and characteristics (biodegradability) of the EPS fractions that can be found in deep layers of infiltration systems and which are potential to produce deep-clogging.

9 References

Abel, C.D.T., Sharma, S.K., Mersha, S.A., Kennedy, M.D., 2014. Influence of intermittent infiltration of primary effluent on removal of suspended solids, bulk organic matter, nitrogen and pathogens indicators in a simulated managed aquifer recharge system. Ecol. Eng. 64, 100–107. doi:10.1016/j.ecoleng.2013.12.045.

Achak, M., Mandi, L., Ouazzani, N., 2009. Removal of organic pollutants and nutrients from olive mill wastewater by a sand filter. J. Environ. Manage. 90(8), 2771-2779.

AEMET - State Agency of Meteorology. Ministry of the Environment and Rural and Marine Affairs, Spanish Government. (AEMET - Agencia Estatal de meteorología. Ministerio de Medio Ambiente y Medio Rural y Marino, Gobierno de España). http://www.aemet.es/es/serviciosclimaticos/vigilancia_clima/analisis_estacional (accessed Feb 12, 2017).

Akhavan, M., Imhoff, P. T., Andres, A. S., Finsterle, S., 2013. Model evaluation of denitrification under rapid infiltration basin systems. J. Contam. Hydrol. 152, 18-34.

Allison, S. D., Vitousek, P. M., 2005. Responses of extracellular enzymes to simple and complex nutrient inputs. Soil Biol. Biochem. 37(5), 937-944.

Amalfitano, S., Fazi, S., Puddu, A., 2009. Flow cytometric analysis of benthic prokaryotes attached to sediment particles. J. Microbiol. Methods 79, 246–249. doi:10.1016/j.mimet.2009.09.005.

Amalfitano, S., Fazi, S., 2008. Recovery and quantification of bacterial cells associated with streambed sediments. J. Microbiol. Methods 75, 237–243. doi:10.1016/j.mimet.2008.06.004.

Andersen, J.M., 1976. An Ignition Method for Determination of Total Phosphorus in Lake Sediments. Water Res. 10, 329–331.

Arias, C. A., Del Bubba, M., Brix, H., 2001. Phosphorus removal by sands for use as media in subsurface flow constructed reed beds. Water Res. 35(5), 1159-1168.

Aronson, D. A., Seaburn, G. E., 1974. Appraisal of operating efficiency of recharge basins on Long Island, New York, in 1969. U.S. Govt. Print. Off. Water Supply Paper No. 2001-D.

Aslan, S., Kapdan, I.K., 2006. Batch kinetics of nitrogen and phosphorus removal from synthetic wastewater by algae. Ecol. Eng. 28(1), 64-70.

Aspila, K., Agemian, H., Chau, A.S., 1976. A Semi-automated Method for the Determination of Inorganic, Organic and Total Phosphate in Sediments. Analyst 101, 187–197.

Bai, H., Cochet, N., Pauss, A., Lamy, E., 2016. Bacteria cell properties and grain size impact on bacteria

transport and deposition in porous media. Colloids Surf. B 139, 148–155. doi:10.1016/j.colsurfb.2015.12.016

Baker, M. A., Valett, H. M., Dahm, C. N., 2000. Organic carbon supply and metabolism in a shallow groundwater ecosystem. Ecology 81(11), 3133-3148.

Baker, M.A., Vervier, P., 2004. Hydrological variability, organic matter supply and denitrification in the Garonne River ecosystem. Freshw. Biol. 49, 181–190. doi:10.1046/j.1365-2426.2003.01175.x

Ball, H.L., 1997. Optimizing the Performance of Sand Filters and Packed Bed Filtered Through Media Selection and Dosing Methods. In Proceedings Ninth Northwest On-Site Wastewater Treatment Short Course, College of Engineering, University of Washington, Seattle, WA. pp. 205-213.

Barai, P., Kumar, A., Mukherjee, P.P., 2016. Modeling of mesoscale variability in biofilm shear behavior. PLoS One 11, 1–16. doi:10.1371/journal.pone.0165593

Bardin, J.P., Barraud, S., Alfakih, E., Dechesne, M., 2002. Performance assessment of stormwater infiltration strategies: A multi-indicator approach. In Global Solutions for Urban Drainage. Eds: Strecker, E.W., Huber, W.C. ASCE Book series, pp. 1-14.

Battin, T. J., Kaplan, L.A., Newbold, J.D., Hansen, C.M., 2003. Contributions of microbial biofilms to ecosystem processes in stream mesocosms. Nature 426, 439-442.

Battin, T.J., 2000. Hydrodynamics is a major determinant of streambed biofilm activity: From the sediment to the reach scale. Limnol. Oceanogr. 45, 1308–1319.

Battin, T.J., Sengschmitt, D., 1999. Linking Sediment Biofilms, Hydrodynamics, and River Bed Clogging: Evidence from a Large River. Microb. Ecol. 37, 185–196. doi:10.1007/s002489900142.

Bauer, R.D., Rolle, M., Kürzinger, P., Grathwohl, P., Meckenstock, R.U., Griebler, C., 2009. Two-dimensional flow-through microcosms–versatile test systems to study biodegradation processes in porous aquifers. J. Hydrol. 369(3-4), 284-295.

Baveye, P., Vandevivere, P., Hoyle, B.L., DeLeo, P.C., de Lozada, D.S., 1998. Environmental Impact and Mechanisms of the Biological Clogging of Saturated Soils and Aquifer Materials. Crit. Rev. Environ. Sci. Technol. 28, 123–191. doi:10.1080/10643389891254197

Bayles, K.W., 2007. The biological role of death and lysis in biofilm development. Nat. Rev. Microbiol. 5(9), 721.

Bekele, E., Toze, S., Patterson, B., Fegg, W., Shackleton, M., Higginson, S., 2013. Evaluating two infiltration gallery designs for managed aquifer recharge using secondary treated wastewater. J. Environ. Manage. 117, 115-120.

Bekele, E., Toze, S., Patterson, B., Higginson, S., 2011. Managed aquifer recharge of treated wastewater: Water quality changes resulting from infiltration through the vadose zone. Water Res. 45, 5764–5772. doi:10.1016/j.watres.2011.08.058.

Benioug, M., Golfier, F., Oltéan, C., Buès, M.A., Bahar, T., Cuny, J., 2017. An immersed boundary-lattice Boltzmann model for biofilm growth in porous media. Adv. Water Resour. 107, 65–82. doi:10.1016/j.advwatres.2017.06.009

Berges J.A., Mulholland M., 2008. Enzymes and N cycling. In Nitrogen in the Marine Environment. Eds: Capone, D.G., Bronk, D.A., Mulholland, M., Carpenter, E.J. Academic Press, New York, pp. 1361–1420.

Bitton, G., 1999. Role of microorganisms in biogeochemical cycles. In Wastewater microbiology, Eds: Bitton, G. John Wiley and Sons, New Jersey, pp. 75-105.

Bott, T.L., Kaplan, L.A., 1985. Bacterial biomass, metabolic state, and activity in stream sediments: relation to environmental variables and multiple assay comparisons. Appl. Environ. Microbiol. 50, 508–522.

Boulos, L., Prévost, M., Barbeau, B., Coallier, J., Desjardins, R., 1999. Methods LIVE / DEAD ® Bac Light E : application of a new rapid staining method for direct enumeration of viable and total bacteria in drinking water. J. Microbiol. Methods 37, 77–86.

Boulton, A.J., Findlay, S., Marmonier, P., Stanley, E.H., Valett, H.M., 1998. The Functional Significance of the Hyporheic Zone in Streams and Rivers. Annu. Rev. Ecol. Syst. 29, 59–81. doi:10.1146/annurev.ecolsys.29.1.59.

Bouwer, H., 2002. Artificial recharge of groundwater: hydrogeology and engineering. Hydrogeol. J. 10(1), 121-142.

Bratbak, G., 1985. Bacterial biovolume and biomass estimations. Appl. Environ. Microbiol. 49(6), 1488-1493.

Bratbak, G., Dundas, I., 1984. Bacterial dry matter content and biomass estimations. Appl. Environ. Microbiol. 48(4), 755-757.

Brix, H., Arias, C.A., del Bubba, M., 2001. Media selection for sustainable phosphorus removal in subsurface flow constructed wetlands. Water Sci. Technol. 44, 47 – 54.

Campos, L.C., Su, M.F.J., Graham, N.J.D., Smith, S.R., 2002. Biomass development in slow sand filters. Water Res. 36(18), 4543-4551.

Camprovin, P., Hernández, M., Fernández, S., Martín-Alonso, J., Galofré, B., Mesa, J., 2017. Evaluation of clogging during sand-filtered surface water injection for aquifer storage and recovery (ASR): Pilot experiment in the llobregat delta (Barcelona, Spain). Water 9(4), 263. doi:10.3390/w9040263

Caruso, G., 2010. Leucine aminopeptidase, β-glucosidase and alkaline phosphatase activity rates and their significance in nutrient cycles in some coastal Mediterranean sites. Mar. Drugs 8(4), 916-940.

Chang, N.B., Wanielista, M., Daranpob, A., 2010. Filter media for nutrient removal in natural systems and built environments: II—Design and application challenges. Environ. Eng. Sci. 27(9), 707-720.

Chang, N.B., 2010. Hydrological connections between low-impact development, watershed best management practices, and sustainable development. J. Hydrol. Eng. 15(6), 384-385.

Chow, A.T., Dai, J., Conner, W.H., Hitchcock, D.R., Wang, J.J., 2013. Dissolved organic matter and nutrient dynamics of a coastal freshwater forested wetland in Winyah Bay, South Carolina. Biogeochemistry 112, 571–587. doi:10.1007/s10533-012-9750-z.

Chróst, R. J., Rai, H., 1993. Ectoenzyme activity and bacterial secondary production in nutrient-impoverished and nutrient-enriched freshwater mesocosms. Microb. Ecol. 25(2), 131-150.

Chróst, R. J., 1990. Microbial ectoenzymes in aquatic environments. In Aquatic microbial ecology. Eds: Overbeck, J., Chróst, R.J. Springer, New York, pp. 47.78.

Claret, C., Boulton, A.J., 2009. Integrating hydraulic conductivity with biogeochemical gradients and microbial activity along river–groundwater exchange zones in a subtropical stream. Hydrogeol. J. 17(1), 151.

Cleveland, C.C., Liptzin, D., 2007. C:N:P stoichiometry in soil: is there a "Redfield ratio" for the microbial biomass? Biogeochemistry 85(3), 235-252.

Clinton, S.M., Edwards, R.T., Findlay, S.E., 2010. Exoenzyme activities as indicators of dissolved organic matter composition in the hyporheic zone of a floodplain river. Freshw. Biol. 55(8), 1603-1615.

Cory, R.M., Mcknight, D.M., 2005. Fluorescence Spectroscopy Reveals Ubiquitous Presence of Oxidized and Reduced Quinones in Dissolved Organic Matter Fluorescence Spectroscopy Reveals Ubiquitous Presence of Oxidized and Reduced Quinones in Dissolved Organic Matter. Environ. Sci. Technol. 39, 8142–8149. doi:10.1021/es0506962.

Crites, R., Tchobanoglous, G., 1998. Land treatment systems. In Small and decentralized wastewater management systems. WCB McGraw-Hill, Boston, pp. 703-760.

Cunningham, A.B., Characklis, W.G., Abedeen, F., Crawford, D., 1991. Influence of Biofilm Accumulation on Porous Media Hydrodynamics. Environ. Sci. Technol. 25, 1305–1311.

Czerwionka, K., 2016. Influence of dissolved organic nitrogen on surface waters. Oceanologia 58, 39–45. doi:10.1016/j.oceano.2015.08.002

Dail, D.B., Davidson, E.A., Chorover, J., 2001. Rapid abiotic transformation of nitrate in an acid forest soil. Biogeochemistry 54, 131–146.

Darby, J., Tchobanoglous, G., Nor, M.A., Maciolek, D., 1996. Shallow Intermittent sant filtration: performance evaluation. Small flows journal 2(1), 3-15.

De Brouwer, J., Stal, L., 2001. Short-term dynamics in microphytobenthos distribution and associated extracellular carbohydrates in surface sediments of an intertidal mudflat. Mar. Ecol. Prog. Ser. 218, 33–44. doi:10.3354/meps218033

Dechesne, M., Barraud, S., Bardin, J.P., 2004. Indicators for hydraulic and pollution retention assessment of stormwater infiltration basins. J. Environ. Manage. 71, 371–380. doi:10.1016/j.jenvman.2004.04.005

De Godos, I., Blanco, S., García-Encina, P.A., Becares, E., Muñoz, R., 2009. Long-term operation of high rate algal ponds for the bioremediation of piggery wastewaters at high loading rates. Bioresour. Technol. 100(19), 4332-4339.

Del Bubba, M., Arias, C.A., Brix, H., 2003. Phosphorus adsorption maximum of sands for use as media in subsurface flow constructed reed beds as measured by the Langmuir isotherm. Water Res. 37(14), 3390-3400.

Deng, W., Cardenas, M.B., Kirk, M.F., Altman, S.J., Bennett, P.C., 2013. Effect of permeable biofilm on micro-and macro-scale flow and transport in bioclogged pores. Environ. Sci. Technol. 47, 11092–11098. doi:10.1021/es402596v

Diaz, R.J., Rosenberg, R., 2008. Spreading dead zones and consequences for marine ecosystems. Science 321(5891), 926-929. doi: 10.1126/science.1156401

Dillon, P., Page, D., Vanderzalm, J., Pavelic, P., Toze, S., Bekele, E., Sidhu, J., Prommer, H., Higginson, S., Regel, R., Rinck-Pfeiffer, S., Purdie, M., Pitman, C., Wintgens, T., 2008. A critical evaluation of combined engineered and aquifer treatment systems in water recycling. Water Sci. Technol. 57, 753–762. doi:10.2166/wst.2008.168.

Dodds, W.K., Randel, C.A., Edler, C.C., 1996. Microcosms for aquifer research: application to colonization of various sized particles by ground-water microorganisms. Ground Water 34(4), 756.

Dong, L.F., Smith, C.J., Papaspyrou, S., Stott, A., Osborn, A.M., Nedwell, D.B., 2009. Changes in Benthic Denitrification, Nitrate Ammonification, and Anammox Process Rates and Nitrate and Nitrite Reductase Gene Abundances along an Estuarine Nutrient Gradient (the Colne Estuary , United Kingdom). Appl. Environ. Microbiol. 75, 3171–3179. doi:10.1128/AEM.02511-08

Donlan, R. M., 2002. Biofilms: microbial life on surfaces. Emerg. Infect. Dis. 8(9), 881.

Drapcho, C.M., Brune, D.E., 2000. The partitioned aquaculture system : impact of design and environmental parameters on algal productivity and photosynthetic oxygen production. Aquac. Eng. 21, 151–168.

Duan, Y.L., Ji, X.C., Yu, Y.Y., Li, Y.H., 2015. Clogging of the subsurface infiltration system, in: Architectural, Energy and Information Engineering: Proceedings of the 2015 International Conference on Architectural, Energy and Information Engineering (AEIE 2015), Xiamen, China, May 19-20, 2015. CRC Press, pp. 193.

Dubois, M., Gilles, K.A., Hamilton, J.K., Rebers, P.T., Smith, F., 1956. Colorimetric method for determination of sugars and related substances. Anal. Chem. 28, 350–356. doi:10.1021/ac60111a017

Dupin, H.J., Kitanidis, P.K., Mccarty, P.L., 2001. Pore-scale modeling of biological clogging due to aggregate expansion: A material mechanics approach. Water Resour. Res. 37, 2965–2979.

Ehrenhauss, S., Witte, U., Bühring, S.I., Huettel, M., 2004. Effect of advective pore water transport on distribution and degradation of diatoms in permeable North Sea sediments. Mar. Ecol. Prog. Ser. 271, 99–111. doi:10.3354/meps271099

Eom, H., Borgatti, D., Paerl, H.W., Park, C., 2017. Formation of low-molecular-weight dissolved organic nitrogen in predenitrification biological nutrient removal systems and its impact on eutrophication in coastal waters. Environ. Sci. Technol. 51(7), 3776-3783.

Essandoh, H.M.K., Tizaoui, C., Mohamed, M.H.A., 2013. Removal of dissolved organic carbon and nitrogen during simulated soil aquifer treatment. Water Res. 47, 3559–3572. doi:10.1016/j.watres.2013.04.013.

Essandoh, H.M.K., Tizaoui, C., Mohamed, M.H.A., Amy, G., Brdjanovic, D., 2011. Soil aquifer treatment of artificial wastewater under saturated conditions. Water Res. 45, 4211–4226. doi:10.1016/j.watres.2011.05.017

Falcioni, T., Manti, A., Boi, P., Canonico, B., Balsamo, M., Papa, S., 2006. Comparison of Disruption Procedures for Enumeration of Activated Sludge Floc Bacteria by Flow Cytometry. Cytom. Part B Clin. Cytom. 70B, 149–153. doi:10.1002/cyto.b.20097

Findlay, S., Sinsabaugh, R., 2003. Response of hyporheic biofilm metabolism and community structure to nitrogen amendments. Aquat. Microb. Ecol. 33, 127–136.

Findlay, S.E.G., Sinsabaugh, R.L., Sobczak, W. V, Hoostal, M., 2003. Metabolic and structural response of hyporheic microbial communities to variations in supply of dissolved organic matter. Limnol. Oceanogr. 48, 1608–1617.

Flemming, H., Wingender, J., 2010. The biofilm matrix. Nat. Publ. Gr. 8, 623–633. doi:10.1038/nrmicro2415

Fox, P., 2001. Soil Aquifer Treatment for sustainable water reuse. AWWA Research Foundation and American Water Works Association, Denver, CO.

Francoeur, S. N., Wetzel, R. G., 2003. Regulation of periphytic leucine-aminopeptidase activity. Aquat. Microb. Ecol. 31(3), 249-258.

Freeman, C., Lock, M.A., 1995. The biofilm polysaccharide matrix: A buffer against changing organic substrate supply? Limnol. and Oceanogr. 40(2), 273-278.

Freixa, A., Rubol, S., Carles-Brangarí, A., Fernàndez-Garcia, D., Butturini, A., Sanchez-Vila, X., Romaní, A., 2016. The effects of sediment depth and oxygen concentration on the use of organic matter: An experimental study using an infiltration sediment tank. Sci. Total Environ. 540, 20–31. doi:10.1016/j.scitotenv.2015.04.007.

French, D., 2012. Granular filter media: Evaluating filter bed depth to grain size ratio. Filtration+ Separation 49(5), 34-36.

Fuchs, S., Hahn, H.H., Roddewig, J., Schwarz, M., Turkovic, R., 2004. Biodegradation and Bioclogging in the Unsaturated Porous Soil benath Sewer Leaks. Acta Hydrochim. Hydrobiol. 32, 277-286.

Doi:10.1002/aheh.200400540

Gao, H., Schreiber, F., Collins, G., Jensen, M.M., Kostka, J.E., Lavik, G., de Beer, D., Zhou, H., Kuypers, M.M., 2010. Aerobic denitrification in permeable Wadden Sea sediments. ISME J. 4, 417–426. doi:10.1038/ismej.2010.166

Garcia, J.C., Ketover, R.D., Loh, A.N., Parsons, M.L., Urakawa, H., 2015. Influence of freshwater discharge on the microbial degradation processes of dissolved organic nitrogen in a subtropical estuary. Antonie van Leeuwenhoek 107(2), 613-632.

Gerbersdorf, S.U., Wieprecht, S., 2015. Biostabilization of cohesive sediments: Revisiting the role of abiotic conditions, physiology and diversity of microbes, polymeric secretion, and biofilm architecture. Geobiology 13, 68–97. doi:10.1111/gbi.12115

Gerbersdorf, S.U., Westrich, B., Paterson, D.M., 2009. Microbial extracellular polymeric substances (EPS) in fresh water sediments. Microb. Ecol. 58, 334–349. doi:10.1007/s00248-009-9498-8

Gette-Bouvarot, M., Mermillod-Blondin, F., Angulo-Jaramillo, R., Delolme, C., Lemoine, D., Lassabatere, L., Loizeau, S., Volatier, L., 2014. Coupling hydraulic and biological measurements highlights the key influence of algal biofilm on infiltration basin performance. Ecohydrology 7, 950–964. doi:10.1002/eco.1421

Goren, O., Burg, A., Gavrieli, I., Negev, I., Guttman, J., Kraitzer, T., Kloppmann, W., Lazar, B., 2014. Biogeochemical processes in infiltration basins and their impact on the recharging effluent, the soil aquifer treatment (SAT) system of the Shafdan plant, Israel. Appl. Geochem. 48, 58-69.

Gougoulias, C., Clark, J.M., Shaw, L.J., 2014. The role of soil microbes in the global carbon cycle: tracking the below-ground microbial processing of plant-derived carbon for manipulating carbon dynamics in agricultural systems. J. Sci. Food Agric. 94(12), 2362-2371.

Greskowiak, J., Prommer, H., Massmann, G., Johnston, C.D., Nützmann, G., Pekdeger, A., 2005. The impact of variably saturated conditions on hydrogeochemical changes during artificial recharge of groundwater. Appl. Geochem. 20, 1409–1426. doi:10.1016/j.apgeochem.2005.03.002.

Gücker, B., Brauns, M., Pusch, M.T., 2006. Effects of wastewater treatment plant discharge on ecosystem structure and function of lowland streams. J. N. Amer. Benthol. Soc. 25(2), 313-329.

Guildford, S. J., Hecky, R.E., 2000. Total nitrogen, total phosphorus, and nutrient limitation in lakes and oceans: is there a common relationship?. Limnol. Oceanogr. 45(6), 1213-1223.

Gunkel, G., Hoffmann, A., 2005. Clogging processes in a bank filtration system in the littoral zone of Lake Tegel (Germany). In the Proceedings of 5th International Symposium on Management of Aquifer Recharge, pp. 10-16.

Haglund, A.L., Lantz, P., Törnblom, E., Tranvik, L., 2003. Depth distribution of active bacteria and bacterial activity in lake sediment. FEMS Microbiol. Ecol. 46(1), 31-38.

Haig, S.J., Quince, C., Davies, R.L., Dorea, C.C., Collins, G., 2014. Replicating the microbial community and water quality performance of full-scale slow sand filters in laboratory-scale filters. Water Res. 61, 141-151.

Haig, S.J., Collins, G., Davies, R.L., Dorea, C.C., Quince, C., 2011. Biological aspects of slow sand filtration: past, present and future. Water Sci. Technol. 11(4), 468-472.

Liu, H., Jeong, J., Gray, H., Smith, S., Sedlak, D.L., 2012. Algal Uptake of Hydrophobic and Hydrophilic Dissolved Organic Nitrogen in Effluent from Biological Nutrient Removal Municipal Wastewater Treatment Systems. Environ. Sci. Technol. 46(2), 713-721. doi: 10.1021/es203085y

Lorenzen, C.J., 1968. Carbon/chlorophyll relationships in an upwelling area. Limnology and Oceanography 13(1), 202-204.

Hall, E.K., Besemer, K., Kohl, L., Preiler, C., Riedel, K., Schneider, T., Wanek, W., Battin, T.J., 2012. Effects of resource chemistry on the composition and function of stream hyporheic biofilms. Front. Microbiol. 3, 1–14. doi:10.3389/fmicb.2012.00035.

Han, P., Shen, X., Yang, H., Kim, H., Tong, M., 2013. Influence of nutrient conditions on the transport of bacteria in saturated porous media. Colloids Surf. B Biointerfaces 102, 752–758. doi:10.1016/j.colsurfb.2012.08.053

Hand, V.L., Lloyd, J.R., Vaughan, D.J., Wilkins, M.J., Boult, S., 2008. Experimental studies of the influence of grain size, oxygen availability and organic carbon availability on bioclogging in porous media. Environ. Sci. Technol. 42(5), 1485-1491.

Hein, M., Pedersen, M.F., Sand-Jensen, K., 1995. Size-dependent nitrogen uptake in micro- and macroalgae. Mar. Ecol. Prog. Ser. 118, 247–253.

Helms, J.R., Stubbins, A., Ritchie, J.D., Minor, E.C., Kieber, D.J., Mopper, K., 2008. Absorption spectral slopes and slope ratios as indicators of molecular weight, source, and photobleaching of chromophoric dissolved organic matter. Limonol. Oceanogr. 53, 955–969. doi:10.4319/lo.2008.53.3.0955.

Henderson, C., Greenway, M., Phillips, I., 2007. Removal of dissolved nitrogen, phosphorus and carbon from stormwater by biofiltration mesocosms. Water Sci. Technol. 55(4), 183-191.

Higashino, M., 2013. Quantifying a significance of sediment particle size to hyporheic sedimentary oxygen demand with a permeable stream bed. Environ. Fluid Mech. 13(3), 227-241.

Hilding, K., 1994. Longevity of infiltration basins assessed in Puget Sound. Watershed Protection Techniques. Water 1(3), 3.

Hill, A.R., 1996. Nitrate removal in stream riparian zones. J. Environ. Qual. 25(4), 743-755.

Hirst, C.N., Cyr, H., Jordan, I.A., 2003. Distribution of exopolymeric substances in the littoral sediments of an oligotrophic lake. Microb. Ecol. 46, 22–32. doi:10.1007/s00248-002-1064-6

Hoffman, F., Ronen, D., Pearl, Z., 1996. Evaluation of flow characteristics of a sand column using magnetic resonance imaging. J. Contam. Hydrol. 22(1-2), 95-107.

Hoffmann, A., Gunkel, G., 2011. Bank filtration in the sandy littoral zone of Lake Tegel (Berlin): Structure and dynamics of the biological active filter zone and clogging processes. Limnologica 41, 10–19. doi:10.1016/j.limno.2009.12.003

Hoffmann, J. P., 1998. Wastewater treatment with suspended and nonsuspended algae. J. Phycol. 34(5), 757-763.

Hoppe-Jones, C., Oldham, G., Drewes, J.E., 2010. Attenuation of total organic carbon and unregulated trace organic chemicals in US riverbank filtration systems. Water Res. 44(15), 4643-4659.

Hu, H., Liao, K., Geng, J., Xu, K., Huang, H., Wang, J., Ren, H., 2018. Removal Characteristics of Dissolved Organic Nitrogen and Its Bioavailable Portion in a Postdenitrifying Biofilter: Effect of the C/N Ratio. Environ. Sci. Technol. 52(2), 757-764.

Hu, C., Zhang, T.C., Huang, Y.H., Dahab, M.F., Surampalli, R., 2005. Effects of long-term wastewater application on chemical properties and phosphorus adsorption capacity in soils of a wastewater land treatment system. Environ. Sci. Technol. 39(18), 7240-7245.

Huang, X., Liu, C., Wang, Z., Gao, C., Zhu, G., Liu, L., 2013. The Effects of Different Substrates on Ammonium Removal in Constructed Wetlands: A Comparison of Their Physicochemical Characteristics and Ammonium-Oxidizing Prokaryotic Communities. Clean Soil Air Water 41, 283–290.

Huettel, M., Ziebis, W., Forster, S., Luther Iii, G. W., 1998. Advective transport affecting metal and nutrient distributions and interfacial fluxes in permeable sediments. Geochim. Cosmochim. Acta 62(4), 613-631.

Huguet, A., Vacher, L., Relexans, S., Saubusse, S., Froidefond, J.M., Parlanti, E., 2009. Properties of fluorescent dissolved organic matter in the Gironde Estuary. Org. Geochem. 40, 706–719. doi:10.1016/j.orggeochem.2009.03.002.

Hunter, K. S., Wang, Y., Van Cappellen, P., 1998. Kinetic modeling of microbially-driven redox chemistry of subsurface environments: coupling transport, microbial metabolism and geochemistry. J. Hydrol. 209(1-4), 53-80.

Jansson, M., Olsson, H., Pettersson, K., 1988. Phosphatases; origin, characteristics and function in lakes. In Phosphorus in Freshwater Ecosystems. Eds: Persson, G., Jansson, M. Springer, Dordrecht, pp. 157-175.

Jardine, P.M., Mayes, M.A., Mulholland, P.J., Hanson, P.J., Tarver, J.R., Luxmoore, R.J., McCarthy, J.F., Wilson, G.V., 2006. Vadose zone flow and transport of dissolved organic carbon at multiple scales in humid regimes. Vadose Zone J. 5(1), 140-152.

Jarvie, H.P., Smith, D.R., Norton, L.R., Edwards, F.K., Bowes, M.J., King, S.M., Scarlett, P., Davies, S., Dils, R.M., Bachiller-Jareno, N., 2018. Phosphorus and nitrogen limitation and impairment of headwater streams relative to rivers in Great Britain: A national perspective on eutrophication. Sci. Total Environ. 621, 849-862.

Jarvie, H.P., Neal, C., Warwick, A., White, J., Neal, M., Wickham, H.D., Hill, L.K., Andrews, M.C., 2002. Phosphorus uptake into algal biofilms in a lowland chalk river. Sci. Total Environ. 282, 353-373.

Jeffrey, S.W., Humphrey, G.F., 1975. New spectrophotometric equations for determining chlorophylls a, b, c1 and c2 in higher plants, algae and natural phytoplankton. Biochemie und Physiologie der Pflanzen 167, 191-194.

Jenkinson, H.F., Lappin-Scott, H.M., 2001. Biofilms adhere to stay. Trends Microbiol. 9(1), 9-10.

Jones, J.B., Holmes, R.M., 1996. Surface-subsurface interactions in stream ecosystems. Trends Ecol. Evol. 11(6), 239-242.

Jones, S.E., Lock, M.A., 1993. Seasonal determinations of extracellular hydrolytic activities in heterotrophic and mixed heterotrophic/autotrophic biofilms from two contrasting rivers. Hydrobiologia 257(1), 1-16.

Pretty, J.N., Mason, C.F., Nedwell, D.B., Hine, R.E., Leaf, S., Dils, R., 2003. Environmental Costs of Freshwater Eutrophication in England and Wales. Environ. Sci. Technol. 37 (2), 201-208 DOI: 10.1021/es020793k

Kauppinen, A., Martikainen, K., Matikka, V., Veijalainen, A.M., Pitkänen, T., Heinonen-Tanski, H., Miettinen, I.T., 2014. Sand filters for removal of microbes and nutrients from wastewater during a one-year pilot study in a cold temperate climate. J. Environ. Manage. 133, 206-213.

Kemp, M.J., Dodds, W.K., 2002. The influence of ammonium, nitrate, and dissolved oxygen concentrations on uptake, nitrification, and denitrification rates associated with prairie stream substrata. Limnol. Oceanogr. 47(5), 1380-1393.

Kirchman, D.L., 1994. The uptake of inorganic nutrients by heterotrophic bacteria. Microb. Ecol. 28, 255–271. doi:10.1007/BF00166816

Koroleff, F., 1983. Simultaneous oxidation of nitrogen and phosphorus compounds by persulfate. Methods Seawater Analysis 2, 205–206.

Lappin-Scott, H.M., Costerton, J.W., 1989. Bacterial biofilms and surface fouling. Biofouling 1(4), 323-342.

Laspidou, C.S., Rittmann, B.E., 2002. A unified theory for extracellular polymeric substances , soluble microbial products , and active and inert biomass. Water Res. 36(11), 2711–2720.

Latrach, L., Ouazzani, N., Masunaga, T., Heijaj, A., Bouhoum, K., Mahi, M., Mandi, L., 2016. Domestic wastewater disinfection by combined treatment using multi-soil-layering system and sand filters (MSL-SF): A laboratory pilot study. Ecol. Eng. 91, 294-301.

Leaf, S., 2018. Taking the P out of pollution: an English perspective on phosphorus stewardship and the Water Framework Directive. Water Environ. J. 32, 4–8.

Li, D., Sharp, J.O., Saikaly, P.E., Ali, S., Alidina, M., Alarawi, M.S., Keller, S., Hoppe-Jones, C., Drewes, J.E., 2012. Dissolved organic carbon influences microbial community composition and diversity in managed aquifer recharge systems. Appl. Environ. Microbiol. 78(19), 6819-6828.

Liu, Q., Liu, S., Zhao, H., Deng, L., Wang, C., Zhao, Q., Dong, S., 2015. The phosphorus speciations in

the sediments up-and down-stream of cascade dams along the middle Lancang River. Chemosphere 120, 653-659.

Lock, M.A., Wallace, R.R., Costerton, J.W., Ventullo, R.M., Charlton, S.E., 1984. River epilithon: toward a structural-functional model. Oikos 10-22.

Macdonald, M.J., Minor, E.C., 2013. Photochemical degradation of dissolved organic matter from streams in the western Lake Superior watershed. Aquat. Sci. 75, 509–522. doi:10.1007/s00027-013-0296-5.

Magurran, A.E., 1988. Diversity indices and species abundance models. In: Ecological Diversity and Its measurement. Eds: Magurran, A.E. Springer, Netherlands, pp. 7-45.

Malard, F., Tockner, K., Dole-Olivier, M.J., Ward, J.V., 2002. A landscape perspective of surface-subsurface hydrological exchanges in river corridors. Freshw. Biol. 47, 621–640. doi:10.1046/j.1365-2427.2002.00906.x.

Malarkey, J., Baas, J.H., Hope, J.A., Aspden, R.J., Parsons, D.R., Peakall, J., Paterson, D.M., Schindler, R.J., Ye, L., Lichtman, I.D., Bass, S.J., Davies, A.G., Manning, A.J., Thorne, P.D., 2015. The pervasive role of biological cohesion in bedform development. Nat. Commun. 6, 1–6. doi:10.1038/ncomms7257

Margalef, R., 1983. Limnología. Ed: Margalef, R. Editorial Omega, Barcelona.

Marti, E., Riera, J.L., Sabater, F., 2009. Effects of wastewater treatment plants on stream nutrient dynamics under water scarcity conditions. In Water Scarcity in the mediterranean; Sabater, S., Barceló, D., Eds.; Springer: Berlin, Heidelberg, pp 173-195.

Marti, E., Aumatell, J., Godé, L., Poch, M., Sabater, F., 2004. Nutrient retention efficiency in streams receiving inputs from wastewater treatment plants. J. Environ. Qual. 33(1), 285-293.

Martienssen, M., Schöps, R., 1997. Biological treatment of leachate from solid waste landfill sites—alterations in the bacterial community during the denitrification process. Water Res. 31(5), 1164-1170.

Marxsen, J., Witzel, K.P., 1990. Measurement of exoenzymatic activity in streambed sediments using methylumbelliferyl-substrates. Archiv für Hydrobiologie/Fundam. Appl. Limnol. 34, 21-28.

McCrackin, M.L., Jones, H.P., Jones, P.C., Moreno-Mateos, D., 2017. Recovery of lakes and coastal marine ecosystems from eutrophication: A global meta-analysis. Limnol. Oceanogr. 62(2), 507-518.

Mendoza-Lera, C., Frossard, A., Knie, M., Federlein, L.L., Gessner, M.O., Mutz, M., 2017. Importance of

advective mass transfer and sediment surface area for streambed microbial communities. Freshw. Biol. 62(1) 133–145. doi:10.1111/fwb.12856

Meng, J., Yao, Q., Yu, Z., 2014. Particulate phosphorus speciation and phosphate adsorption characteristics associated with sediment grain size. Ecol. Eng. 70, 140–145. doi:10.1016/j.ecoleng.2014.05.007

Mermillod-Blondin, F., Mauclaire, L., Montuelle, B., 2005. Use of slow filtration columns to assess oxygen respiration, consumption of dissolved organic carbon, nitrogen transformations, and microbial parameters in hyporheic sediments. Water Res. 39, 1687–1698. doi:10.1016/j.watres.2005.02.003.

Meteocat - Meteorological Service of Catalonia. Department of Territory and Sustainability, Government of Catalonia. (Meteocat - Servei meteorològic de Catalunya. Departament de Territori i Sostenibilitat, Generalitat de Catalunya). http://www.meteo.cat/wpweb/serveis/ peticions-de-dades/peticio-dinformes-meteorologics (accessed Feb 12, 2017).

Miller, J.H., Ela, W.P., Lansey, K.E., Chipello, P.L., Arnold, R.G., 2009. Nitrogen Transformations during Soil–Aquifer Treatment of Wastewater Effluent—Oxygen Effects in Field Studies. J. Environ. Eng. 132, 1298–1306. doi:10.1061/ASCE0733-93722006132:101298.

Minero, C., Lauri, V., Falletti, G., Maurino, V., Pelizzetti, E., Vione, D., 2007. Spectrophotometric characterisation of surface lakewater samples: implications for the quantification of nitrate and the properties of dissolved organic matter. Ann. Chim. 97, 1107–1116.

Moorhead, D.L., Sinsabaugh, R.L., 2006. A theoretical model of litter decay and microbial interaction. Ecol. Monogr. 76(2), 151-174.

Mousavinezhad, M., Rezazadeh, M., Golbabayee, F., Sadati, E., 2015. Land treatment Methods A review on available methods and its ability to remove pollutants. Oriental Journal of Chemistry 31(2), 957-966.

Mueller, M., Pander, J., Wild, R., Lueders, T., Geist, J., 2013. The effects of stream substratum texture on interstitial conditions and bacterial biofilms : Methodological strategies. Limnologica 43, 106–113. doi:10.1016/j.limno.2012.08.002

Murphy, J., Riley, J., 1962. A modified single solution method for the determination of phosphate in natural waters. Analytica chimica acta 27, 31-36.

Navel, S., Sauvage, S., Delmotte, S., Gerino, M., Marmonier, P., Mermillod-Blondin, F., 2012. A modelling approach to quantify the influence of fine sediment deposition on biogeochemical processes

occurring in the hyporheic zone. Annales de Limnologie-International Journal of Limnology 48(3), 279-287.

Nogaro, G., Datry, T., Mermillod-Blondin, F., Descloux, S., Montuelle, B., 2010. Influence of streambed sediment clogging on microbial processes in the hyporheic zone. Freshw. Biol. 55, 1288–1302. doi:10.1111/j.1365-2427.2009.02352.x.

Nogaro, G., Datry, T., Mermillod-Blondin, F., Foulquier, A., Montuelle, B., 2013. Influence of hyporheic zone characteristics on the structure and activity of microbial assemblages. Freshw. Biol. 58, 2567–2583. doi:10.1111/fwb.12233.

Okubo, T., Matsumoto, J.,1979. Effect of infiltration rate on biological clogging and water quality changes during artificial recharge. Water Resour. Res. 15(6), 1536-1542.

Or, D., Smets, B.F., Wraith, J.M., Dechesne, A., Friedman, S.P., 2007a. Physical constraints affecting bacterial habitats and activity in unsaturated porous media – a review. Adv. Water Resour. 30, 1505–1527. doi:10.1016/j.advwatres.2006.05.025.

Or, D., Phutane, S., Dechesne, A., 2007b. Extracellular Polymeric Substances Affecting Pore-Scale Hydrologic Conditions for Bacterial Activity in Unsaturated Soils. Vadose Zo. J. 6, 298–305.

Pai, H., Villamizar, S. R., Harmon, T. C., 2017. Synoptic Sampling to Determine Distributed Groundwater-Surface Water Nitrate Loading and Removal Potential Along a Lowland River. Water Resour. Res. 53(11), 9479-9495. doi:10.1002/2017WR020677

Pavelic, P., Dillon, P.J., Mucha, M., Nakai, T., Barry, K.E., Bestland, E., 2011. Laboratory assessment of factors affecting soil clogging of soil aquifer treatment systems. Water Res. 45(10), 3153-3163. doi:10.1016/j.watres.2011.03.027.

Pedretti, D., Barahona-Palomo, M., Bolster, D., Sanchez-Vila, X., Fernàndez-Garcia, D., 2012. A quick and inexpensive method to quantify spatially variable infiltration capacity for artificial recharge ponds using photographic images. J. Hydrol. 430, 118-126.

Perujo, N., Sanchez-Vila, X., Proia, L., Romaní, A.M., 2017. Interaction between Physical Heterogeneity and Microbial Processes in Subsurface Sediments : A Laboratory-Scale Column Experiment. Environ. Sci. Technol. 51, 6110–6119. doi:10.1021/acs.est.6b06506

Perujo, N., Freixa, A., Vivas, Z., Gallegos, A. M., Butturini, A., Romaní, A.M., 2016. Fluvial biofilms from upper and lower river reaches respond differently to wastewater treatment plant inputs. Hydrobiologia 765(1), 169-183.

Phanikumar, M.S., Hyndman, D.W., Zhao, X., Dybas, M.J., 2005. A three-dimensional model of microbial transport and biodegradation at the Schoolcraft, Michigan, site. Water Resour. Res. 41(5), 1-17.

Poach, M.., Hunt, P., Reddy, G., Stone, K., Matheny, T., Johnson, M.H., Sadler, E.J., 2004. Ammonia Volatilization from Marsh-Pond-Marsh Constructed Wetlands. J. Environ. Qual. 33, 844–851.

Pusch, M., Fiebig, D., Brettar, I., Eisenmann, H., Ellis, B.K., Kaplan, L.A., Lock, M.A., Naegeli, M.W., Traunspurger, W., 1998. The role of micro-organisms in the ecological connectivity of running waters. Freshw. Biol. 40(3), 453-495.

Quanrud, D.M., Hafer, J., Karpiscak, M.M., Zhang, J., Lansey, K.E., Arnold, R.G., 2003. Fate of organics during soil-aquifer treatment: sustainability of removals in the field. Water Res. 37, 3401–3411.

Quéric, N.V., Soltwedel, T., Arntz, W.E., 2004. Application of a rapid direct viable count method to deep-sea sediment bacteria. J. Microbiol. Methods 57, 351–367. doi:10.1016/j.mimet.2004.02.005.

Racz, A.J., Fisher, A.T., Schmidt, C.M., Lockwood, B.S., Huertos, M.L., 2012. Spatial and Temporal Infiltration Dynamics During Managed Aquifer Recharge Introduction and Project Motivation. Ground Water 50, 562–570. doi:10.1111/j.1745-6584.2011.00875.x

Rauch-Williams, T., Drewes, J.E., 2006. Using soil biomass as an indicator for the biological removal of effluent-derived organic carbon during soil infiltration. Water Res. 40, 961–968. doi:10.1016/j.watres.2006.01.007.

Reardon, J., Foreman, J.A., Searcy, R.L., 1966. New reactants for the colorimetric determination of ammonia. Clin. Chim. Acta 14, 403–405. doi:http://dx.doi.org/10.1016/0009-8981(66)90120-3

Reddy, G.B., Hunt, P.G., Phillips, R., Stone, K., Grubbs, A., 2001. Treatment of swine wastewater in marsh-pond-marsh constructed wetlands. Water Sci. Technol. 44, 545 – 550.

Reddy, K.R., D'Angelo, E.M., 1997. Biogeochemical indicators to evaluate pollutant removal efficiency in constructed wetlands. Water Sci. Technol. 35, 1–10. doi:http://dx.doi.org/10.1016/S0273-1223(97)00046-2

Reddy, K.R., Flaig, E., Scinto, L.J., Diaz, O., DeBusk, T.A., 1996. Phosphorus assimilation in a stream system of the Lake Okeechobee Basin. JAWRA Journal of the American Water Resources Association 32(5), 901-915.

Redfield, A.C., 1958. The biological control of chemical factors in the environment. American scientist 46(3), 230A-221.

Ren, Y.X., Zhang, H., Wang, C., Yang, Y.Z., Qin, Z., Ma, Y., 2011. Effects of the substrate depth on purification performance of a hybrid constructed wetland treating domestic sewage. J. Environ. Sci. Heath A 46, 777-782.

Ricart, M., Barceló, D., Geiszinger, A., Guasch, H., de Alda, M.L., Romaní, A.M., Vidal, G., Villagrasa, M., Sabater, S., 2009. Effects of low concentrations of the phenylurea herbicide diuron on biofilm algae and bacteria. Chemosphere 76(10), 1392-1401.

Riemann, B., Simonsen, P., Stensgaard, L., 1989. The carbon and chlorophyll content of phytoplankton from various nutrient regimes. J. Plankton Res. 11(5), 1037-1045.

Rinck-Pfeiffer, S., Ragusa, S., Sztajnbok, P., Vandevelde, T., 2000. Interrelationships between biological, chemical, and physical processes as an analog to clogging in aquifer storage and recovery (ASR) wells. Water Res. 34, 2110–2118. doi:10.1016/S0043-1354(99)00356

Roberts, K.L., Kessler, A.J., Grace, M.R., Cook, P.L.M., 2014. Increased rates of dissimilatory nitrate reduction to ammonium (DNRA) under oxic conditions in a periodically hypoxic estuary. Geochim. Cosmochim. Acta 133, 313–324. doi:10.1016/j.gca.2014.02.042

Rodríguez-Escales, P., Sanchez-Vila, X., 2016. Fate of sulfamethoxazole in groundwater: Conceptualizing and modeling metabolite formation under different redox conditions. Water Res. 105, 540-550. doi: 10.1016/j.watres.2016.09.034.

Rodríguez-Escales, P., Folch, A., van Breukelen, B.M., Vidal-Gavilan, G., Sanchez-Vila, X., 2016. Modeling long term Enhanced in situ Biodenitrification and induced heterogeneity in column experiments under different feeding strategies. J. Hydrol. 538, 127–137. doi: 10.1016/j.jhydrol.2016.04.012.

Rodríguez-Escales, P., Canelles, A., Sanchez-Vila, X., Folch, A., Kurtzman, D., Sapiano, M., Fernández-Escalante, E., Rossetto, R., Lobo-Ferreira, J.P., San Sebastian, J., Schüth, C., 2018. A risk assessment methodology to evaluate the risk failure of Managed Aquifer Recharge in Mediterranean basin. Hydrology and Earth System Sciences, doi:10.5194/hess-2018-8

Rogers, H.J., 1961. The dissimilation of high molecular weight organic substrates. In The Bacteria, Vol.2. Eds: Gunsalus, I.C., Stanier, R.Y. Academic Press, New York, pp. 261–318.

Romaní, A.M., Artigas, J., Ylla, I., 2012. Extracellular Enzymes in Aquatic Biofilms: Microbial Interactions versus Water Quality Effects in the Use of Organic Matter. In Microbial Biofilms. Eds: Lear, G., Lewis, G. Caister Academic Press, UK, pp. 153–174.

Romaní, A.M., Fund, K., Artigas, J., Schwartz, T., Sabater, S., Obst, U., 2008. Relevance of Polymeric Matrix Enzymes During Biofilm Formation. Microb. Ecol. 56(3), 427–436. doi:10.1007/s00248-007-9361-8

Romaní, A.M., Guasch, H., Muñoz, I., Ruana, J., Vilalta, E., Schwartz, T., Emtiazi, F., Sabater, S., 2004a. Biofilm Structure and Function and Possible Implications for Riverine DOC Dynamics. Microb. Ecol. 47, 316–328. doi:10.1007/s00248-003-2019-2

Romaní, A.M., Giorgi, A., Acuña, V., Sabater, S., 2004b. The influence of substratum type and nutrient supply on biofilm organic matter utilization in streams. Limnol. Oceanogr. 49, 1713–1721.

Romaní, A.M., Sabater, S., 2000. Influence of Algal Biomass on Extracellular Enzyme Activity in River Biofilms. Microb. Ecol. 41, 16–24. doi:10.1007/s002480000041.

Romaní, A. M., 2000. Characterization of extracellular enzyme kinetics in two Mediterranean streams. Archiv für Hydrobiologie 148(1), 99-117. doi: 10.1127/archiv-hydrobiol/148/2000/99.

Ruane, E.M., Murphy, P.N.C., French, P., Healy, M.G., 2014. Comparison of a Stratified and a Single-Layer Laboratory Sand Filter to Treat Dairy Soiled Water from a Farm-Scale Woodchip Filter. Water. Air. Soil Pollut. 225, 1–10. doi:10.1007/s11270-014-1915-z

Rubol, S., Freixa, A., Carles-Brangarí, A., Fernàndez-Garcia, D., Romaní, A.M., Sanchez-Vila, X., 2014. Connecting bacterial colonization to physical and biochemical changes in a sand box infiltration experiment. J. Hydrol. 517, 317-327. doi:10.1016/j.jhydrol.2014.05.041.

Rückauf, U., Augustin, J., Russow, R., Merbach, W., 2004. Nitrate removal from drained and reflooded fen soils affected by soil N transformation processes and plant uptake. Soil Biol. Biochem. 36, 77–90. doi:10.1016/j.soilbio.2003.08.021

Rulík, M., Spáčil, R., 2004. Extracellular enzyme activity within hyporheic sediments of a small lowland stream. Soil Biol. Biochem. 36(10), 1653-1662.

Rusch A. Huettel M., 2000. Advective particle transport into permeable sediments-evidence from experiments in an intertidal sandflat. Limnol. Oceanogr. 45, 525–533.

Sabater, S., and Romaní, A.M., 1996. Metabolic changes associated with biofilm formation in an undisturbed Mediterranean stream. Hydrobiologia 335(2), 107-113.

Santmire, J.A., Leff, L.G., 2007. The influence of stream sediment particle size on bacterial abundance and community composition. Aquatic Ecology 41(2), 153-160.

Schmidt, C.M., Fisher, A.T., Racz, A., Wheat, C.G., Los Huertos, M., Lockwood, B., 2012. Rapid nutrient load reduction during infiltration of managed aquifer recharge in an agricultural groundwater basin: Pajaro Valley, California. Hydrological Processes 26(15), 2235-2247.

Schnurr, P.J., Allen, D.G., 2015. Factors affecting algae biofilm growth and lipid production: a review. Renewable and Sustainable Energy Reviews 52, 418-429.

Seifert, D., Engesgaard, P., 2007. Use of tracer tests to investigate changes in flow and transport properties due to bioclogging of porous media. J. Contam. Hydrol. 93(1-4), 58-71.

Servais, P., Anzil, A., Ventresque, C., 1989. Simple Method for Determination of Biodegradable Dissolved Organic Carbon in Water. Appl. Environ. Microbiol. 55, 2732–2734. doi:0099-2240/89/102732-03.

Shi, Y., Wei, N., Wu, G., 2016. Tertiary denitrification of the secondary effluent in biofilters packed with composite carriers under different carbon to nitrogen ratios. Environmental Engineering Research 21(3), 311-317.

Sieczko, A., Maschek, M., Peduzzi, P., 2015. Algal extracellular release in river-floodplain dissolved organic matter: Response of extracellular enzymatic activity during a post-flood period. Front. Microbiol. 6, 1–15. doi:10.3389/fmicb.2015.00080

Sinsabaugh, R.L., Lauber, C.L., Weintraub, M.N., Ahmed, B., Allison, S.D., Crenshaw, C., Contosta, A.R., Cusack, D., Frey, S., Gallo, M.E., Gartner, T.B., Hobbie, S.E., Holland, K., Keeler, B.L., Powers, J.S., Stursova, M., Takacs-Vesbach, C., Waldrop, M.P., Wallenstein, M.B., Zak, D.R., Zeglin, L.H., 2008. Stoichiometry of soil enzyme activity at global scale. Ecology letters 11(11), 1252-1264.

Smith, V. H., 2003. Eutrophication of freshwater and coastal marine ecosystems a global problem. Environmental Science and Pollution Research 10(2), 126-139.

Søndergaard, M., Jensen, J.P., Jeppesen, E., 2003. Role of sediment and internal loading of phosphorus in shallow lakes. Hydrobiologia 506(1-3), 135-145.

Søndergaard, M., Theil-Nielsen, J., Christoffersen, K., Schlüter, L., Jeppesen, E., 1998. Bacterioplankton and carbon turnover in a dense macrophyte canopy. In The structuring role of submerged macrophytes in lakes. Eds: Jeppesen, E., Sondergaard, M., Christoffersen, K. Springer, New York, NY, pp. 250-261.

Stoodley, P., Sauer, K., Davies, D.G., Costerton, J.W., 2002. Biofilms as complex differentiated

communities. Annu. Rev. Microbiol. 56, 187–209. doi:10.1146/annurev.micro.56.012302.160705

Sutherland, I.W.,1985. Biosynthesis and composition of gram-negative bacterial extracellular and wall polysaccharides. Annual Reviews in Microbiology 39(1), 243-270.

Tchobanoglous, G., 2003. Fundamentals of biological treatment. In Wastewater Engineering : Treatment and Reuse. Eds: Tchobanoglous, G., Burton, F.L., Stensel, H.D. Metcalf & Eddy, pp. 611–635.

Thullner, M., 2010. Comparison of bioclogging effects in saturated porous media within one-and two-dimensional flow systems. Ecol. Eng. 36(2), 176-196.

Thullner, M., Zeyer, J., Kinzelbach, W., 2002. Influence of Microbial Growth on Hydraulic Properties of Pore Networks. Transp. Porous Media 49, 99–122.

Tiedje, J.M., 1988. Ecology of denitrification and dissimilatory nitrate reduction to ammonium. In Environmental Microbiology of Anaerobes. Eds: Zehnder, A.J.B. John Wiley and Sons, pp. 179–244.

Türkmen, M., Walther, E.F., Andres, A.S., Chirnside, A.A.E., Ritter, W.F., 2008. Evaluation of rapid infiltration basin systems (RIBS) for wastewater disposal: Phase I. Delaware Geol. Surv.

Turley, C.M., Mackie, P.J., 1994. Biogeochemical significance of attached and free-living bacteria and the flux of particles in the NE Atlantic Ocean. Marine Ecology Progress Series 115, 191-203.

Vanderzalm, J.L., Page, D.W., Barry, K.E., Dillon, P.J., 2010. A comparison of the geochemical response to different managed aquifer recharge operations for injection of urban stormwater in a carbonate aquifer. Applied Geochemistry 25(9), 1350-1360.

Vandevivere, P., Baveye, P., 1992. Effect of bacterial extracellular polymers on the saturated hydraulic conductivity of sand Effect of Bacterial Extracellular Polymers on the Saturated Hydraulic Conductivity of Sand Columns. Appl. Envirnomental Microbiol. 58, 1690–1698.

Vaquer-Sunyer, R., Conley, D.J., Muthusamy, S., Lindh, M.V., Pinhassi, J., Kritzberg, E.S., 2015. Dissolved organic nitrogen inputs from wastewater treatment plant effluents increase responses of planktonic metabolic rates to warming. Environ. Sci. Tech. 49(19), 11411-11420.

Vivas, Z., Perujo, N., Freixa, A., Romaní, A.M., 2017. Changes in bacterioplankton density and viability in the Tordera river due to the input of ef fl uents from waste water treatment plants. Limnetica 36, 461–475. doi:10.23818/limn.36.15

Von Schiller, D., Marti, E., Riera, J.L., 2009. Nitrate retention and removal in Mediterranean streams bordered by contrasting land uses: a 15 N tracer study. Biogeosciences 6(2), 181-196.

Vu, B., Chen, M., Crawford, R.J., Ivanova, E.P., 2009. Bacterial extracellular polysaccharides involved in biofilm formation. Molecules 14(7), 2535-2554.

Wakelin, S.A., Colloff, M.J., Kookana, R.S., 2008. Effect of wastewater treatment plant effluent on microbial function and community structure in the sediment of a freshwater stream with variable seasonal flow. Appl. Environ. Microbiol. 74(9), 2659-2668.

Wang, S.Y., Sudduth, E.B., Wallenstein, M.D., Wright, J.P., Bernhardt, E.S., 2011. Watershed urbanization alters the composition and function of stream bacterial communities. PLoS One 6, 1–9. doi:10.1371/journal.pone.0022972.

Wathugala, A.G., Suzuki, T., Kurihara, Y., 1987. Removal of nitrogen, phosphorus and COD from waste water using sand filtration system with Phragmites australis. Water Res. 21(10), 1217-1224.

Wentworth, C.K., 1922. A scale of grade and class terms for clastic sediments. The journal of geology 30(5), 377-392.

Wu, H.M., Zhang, J., Ngo, H.H., Guo, W.S., Hu, Z., Liang, S., Fan, J.L., Liu, H., 2015. A review on the sustainability of constructed wetlands for wastewater treatment: design and operation. Bioresour. Technol. 175, 594-601.

Xia, L., Zheng, X., Shao, H., Xin, J., Sun, Z., Wang, L., 2016. Effects of bacterial cells and two types of extracellular polymers on bioclogging of sand columns. J. Hydrol. 535, 293–300. doi:10.1016/j.jhydrol.2016.01.075

Xia, L., Zheng, X., Shao, H., Xin, J., Peng, T., 2014. Influences of environmental factors on bacterial extracellular polymeric substances production in porous media. J. Hydrol. 519, 3153–3162. doi:10.1016/j.jhydrol.2014.10.045

Yacobi, Y. Z., Zohary, T., 2010. Carbon: chlorophyll a ratio, assimilation numbers and turnover times of Lake Kinneret phytoplankton. Hydrobiologia 639(1), 185-196.

Yan, Z., Liu, C., Liu, Y., Bailey, V.L., 2017. Multiscale Investigation on Biofilm Distribution and Its Impact on Macroscopic Biogeochemical Reaction Rates. Water Resour. Res. 53, 8698–8714. doi:10.1002/2017WR020570

Ylla, I., Romaní, A.M., Sabater, S., 2012. Labile and recalcitrant organic matter utilization by river

biofilm under increasing water temperature. Microb. Ecol. 64(3), 593-604.

Zhang, L.Y., Ye, Y.B., Wang, L.J., Xi, B.D., Wang, H. Q., Li, Y., 2015. Nitrogen removal processes in deep subsurface wastewater infiltration systems. Ecol. Eng. 77, 275-283.

Zhang, J., Huang, X., Liu, C., Shi, H., Hu, H., 2005. Nitrogen removal enhanced by intermittent operation in a subsurface wastewater infiltration system. Ecol. Eng. 25(4), 419-428.

Zhang, X., Bishop, P.L., 2003. Biodegradability of biofilm extracellular polymeric substances. Chemosphere 50, 63–69. doi:10.1016/S0045-6535(02)00319-3

Zhao, Z., Chang, J., Han, W., Wang, M., Ma, D., Du, Y., Qu, Z., Chang, S.X., Ge., Y., 2016. Effects of plant diversity and sand particle size on methane emission and nitrogen removal in microcosms of constructed wetlands. Ecol. Eng. 95, 390-398.

Zhong, H., Liu, G., Jiang, Y., Yang, J., Liu, Y., Yang, X., Liu, Z., Zeng, G., 2017. Transport of bacteria in porous media and its enhancement by surfactants for bioaugmentation: A review. Biotechnol. Adv. 35, 490–504. doi:10.1016/j.biotechadv.2017.03.009

Zhu, H., Wang, D., Cheng, P., Fan, J., Zhong, B., 2015. Effects of sediment physical properties on the phosphorus release in aquatic environment. Science China Physics, Mechanics & Astronomy 58(2), 1-8.